Alma Mater Studiorum – Università di Bologna

DOTTORATO DI RICERCA IN

INGEGNERIA ELETTRONICA, INFORMATICA E DELLE TELECOMUNICAZIONI

Ciclo XXVII

Settore Concorsuale di afferenza: 09/E3 – ELETTRONICA

Settore Scientifico disciplinare: ING-INF/01 ELETTRONICA

ULTRA-LOW POWER AND NON-INTRUSIVE WIRELESS MONITORING FOR SMART BUILDINGS

Presentata da: DOMENICO BALSAMO

Coordinatore Dottorato	**Relatore**
PROF. VANELLI CORALLI	**PROF. LUCA BENINI**

Esame finale anno 2015

Ultra-low Power and Non-intrusive Wireless Monitoring for Smart Buildings

Domenico Balsamo

Abstract

Wireless Sensor Networks (WSNs) offer a new solution for distributed monitoring, processing and communication. WSNs are implemented in a wide range of distributed sensing applications and offer numerous challenges due to their peculiarities. First of all, the stringent energy constraints to which sensing nodes are typically subjected. WSNs are often battery powered and placed where it is not possible to recharge or replace batteries. Energy can be harvested from the external environment but it is a limited resource that must be used efficiently. Energy efficiency is a key requirement for a credible WSNs design. From the power source's perspective, aggressive energy management techniques remain the most effective way to prolong the lifetime of a WSN. A new adaptive algorithm will be presented, which minimizes the consumption of wireless sensor nodes in sleep mode, when the power source has to be regulated using DC-DC converters.

Another important aspect addressed is the time synchronisation in WSNs. WSNs are used for real-world applications where physical time plays an important role. An innovative low-overhead synchronisation approach will be presented, based on a Temperature Compensation Algorithm (TCA).

The last aspect addressed is related to self-powered WSNs with Energy Harvesting (EH) solutions. Wireless sensor nodes with EH require some form of energy storage, which enables systems to continue operating during periods of insufficient environmental energy. However, the size of the energy storage strongly restricts the use of WSNs with EH in real-world applications. The main challenge for self-powered WSNs is to run programs under transient power conditions without using any external energy storage. A new approach will be presented, which enables computation to be sustained during intermittent power supply.

The discussed approaches (power management, time synchronisation and self-powered solutions) will be used for real-world WSN applications. The first pre-

sented scenario is related to the experience gathered during an European Project (3ENCULT Project - Efficient Energy for EU Cultural Heritage), regarding the design and implementation of an innovative network for monitoring heritage buildings. The second scenario is related to the experience gathered during the project in collaboration with Telecom Italia s.p.a., regarding the design of smart energy meters for monitoring the usage of household's appliances.

Contents

List of Figures

LIST OF FIGURES

LIST OF FIGURES

List of Tables

Chapter 1

Introduction

1.1 Wireless Sensor Networks architecture

Wireless Sensor Networks (WSNs) consist of small devices with limited capabilities, named wireless sensor nodes, which collect information from the environment, process data and communicate with other nodes using wireless communication [18].

Wireless sensor nodes are usually equipped with one or more sensors, a microcontroller, a power unit, a radio transceiver and may also contain one or more actuators. They send data to a gateway, which makes information available as part of Internet of Things (IoT). IoT is the interconnection of embedded systems, such as WSNs, within the existing Internet infrastructure [1].

In Fig. 1.1 is shown a typical multi-hop wireless sensor network architecture while in Fig. 1.2 a typical wireless sensor node architecture.

The deployment of a WSN provides a non-intrusive approach and a remarkable degree of granularity in data acquisition. WSNs are implemented in a wide range of distributed sensing applications. Environmental and energy monitoring, medical applications, structural health monitoring, agriculture, production and delivery, military networks are only a few examples of distributed sensing applications with WSNs.

Moreover, they offer numerous challenges due to their peculiarities [2]: pri-

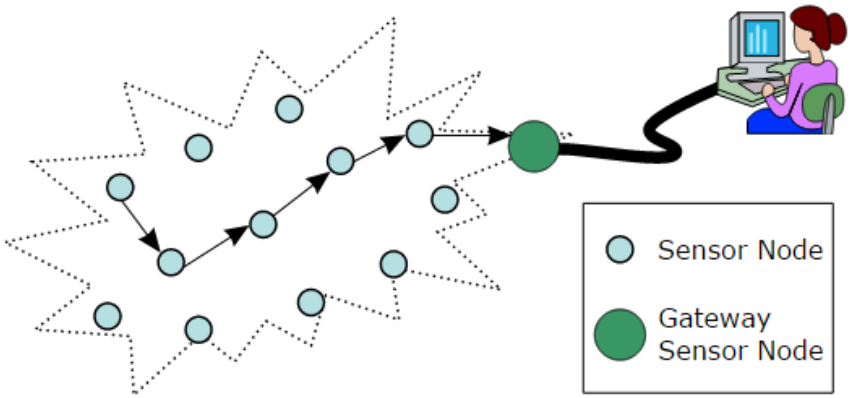

Figure 1.1: Typical multi-hop wireless sensor network architecture

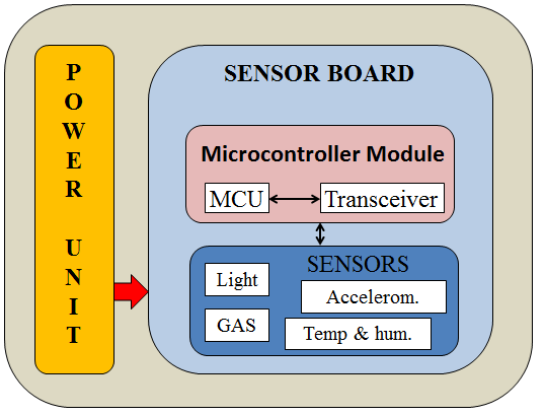

Figure 1.2: Typical wireless sensor node architecture

marily, the stringent energy constraints to which sensing nodes are typically subjected; secondarily, the constrains for the time synchronisation to which real-world WSNs applications are often subjected; and finally, the issues related to the WSNs with Energy Harvesting (EH) solutions.

The main aim of this dissertation is to address the presented issues by introducing innovative solutions and by implementing these novelties in two real-world WSNs applications: environmental monitoring of historical buildings and self-powered wireless energy meters. In particular, the first application strongly require a power management technique to extend the lifetime of its battery-powered nodes. Moreover, it requires a local clock synchronisation strategy for reducing the effects of the temperature changes, without using any extra network

messages. The second application also requires a power management technique in order to properly use the energy harvested for the self-powered nodes and a local time synchronization strategy.

1.1.1 Power Management in WSNs

Energy consumption is the key parameter in determining the lifetime of distributed systems such as WSNs. Lifetime is extremely critical for most of real-world applications and it largely depends on the consumption at each wireless sensor node.

WSNs are often battery powered, with a limited lifetime, and placed where the batteries can not be replaced. Additional energy can be harvested from the external environment, but it is a limited resource that must be used efficiently. Moreover, despite the well-known advantages of energy harvesting solutions, there are several scenarios where the absence of batteries is not a possible option. For instance, applications which need of extra power for energy-hungry sensors and macro-scale actuation are becoming quite common in the last few years[34].

The alternative is to extend the lifetime of primary batteries as much as possible. Aggressive power management techniques, which combine hardware and software solutions, remain the most effective way to prolong the lifetime of WSNs.

In the Chapter 2, a new approach aimed at minimising the sensor node's power consumption in sleep mode is presented, when the nodes are equipped with energy-hungry sensors and the power source has to be regulated using switching converters (DC-DC converter) [15].

This new approach is based on an adaptive low-level algorithm, which modulates the DC-DC converter activation for minimising the quiescent current consumption. This algorithm allows a discontinuous usage of the DC-DC converter during the sleep time, without requiring any modification in the user's main program, by powering the system only with the internal DC-DC converter capacitor and without using any other additional capacitors as energy buffer. Moreover, the algorithm dynamically computes the maximum interval between consecutive

wake-ups, for the capacitor recharge, by taking into account both the global leakage and the temperature-dependent variations.

1.1.2 Time Synchronisation in WSNs

Another critical aspect for WSNs is the time synchronization, which is fundamental for coordinating activities performed by multiple wireless sensor nodes [16]. Multi-sensor data fusion, network protocols, task scheduling and distributed power management require an accurate knowledge of time, to minimize communication overhead and maximize the sleep time. However, some intrinsic properties of WSNs, primarily the limited energy resources, make traditional synchronization methods unsuitable for this kind of networks. The main aim for the WSNs is to maintain the nodes synchronized and, at the same time, to minimize power consumption.

In the Chapter 3, an innovative low-overhead clock synchronisation approach is presented, based on a Temperature Compensation Algorithm (TCA) [79]. The proposed TCA is local and it uses a temperature sensor to remove the effects of environmental changes, and increase the time between synchronisation intervals. Using this TCA, the 32 KHz clock achieves a drift of less than few ppm over a wide range of operating temperatures, which is a significant improvement compared to the drift obtained without any temperature compensation.

1.1.3 Self-powered WSNs with Energy Harvesting

The last aspect addressed in the first part of this dissertation is related to self-powered WSNs with Energy Harvesting (EH) solutions. Wireless Sensor Nodes with EH require some form of energy storage, which enables systems to also continue operating during periods of insufficient environmental energy. However, the size and the weight of energy storage strongly restricts the use of self-powered WSNs in real world applications. The main challenge for these systems is to run programs with a discontinuous power supply, that is often generated, without using any external energy storage. We propose a new approach (Chapter 4), named

Hibernus, which enables computation to be sustained during an intermittent supply [17]. This approach has a low energy and time overhead, which is achieved by reactively hibernating: saving system state only once when power is about to be lost, and then sleeping until the supply recovers. We validate this approach experimentally on a microcontroller with FRAM non-volatile memory, allowing it to reactively hibernate using only energy stored in its decoupling capacitance. When compared to recently proposed techniques, our approach significantly reduces processor time and energy overheads.

1.2 Wireless sensor networks applications

The second part of this thesis (Chapter 5 and Chapter 6) considers the introduced approaches (power management, time synchronisation and self-powered solutions) in real-world WSNs applications.

1.2.1 Environmental Monitoring of Heritage Buildings

The first scenario (Chapter 5) is related to the experience gathered during an European Project (3ENCULT Project - Efficient Energy for EU Cultural Heritage), regarding the design and implementation of an innovative network for monitoring heritage buildings [19, 20].

Structural health and the local climate monitoring of historical heritage buildings is a hard task for civil engineers, due to the lack of a pre-existing monitoring model and difficult installation constrains. An innovative hardware and software solution will be presented to efficiently satisfy the requirements for long-term monitoring of a historical building, called Palazzina della Viola, located in the centre of Bologna, Italy. The presented system provides real-time feedback to civil engineers, which can retrieve sensed data using remote interfaces. Based on 7 months of operation, the proposed solution, compared with other standard monitoring systems, is an effective low-cost alternative testing tool for assessing the environmental monitoring in heritage buildings.

1.2.2 Self-powered Wireless Energy Meters

The second scenario (Chapter 6) is related to the experience gathered during the project in collaboration with Telecom Italia s.p.a., regarding the design of smart energy meters for monitoring the power usage of appliances [21, 22, 82].

Energy saving in smart buildings is one of the main aim in sustainability strategies for the next future. Energy saving policies should gradually improve in the next few years, but the rate of improvement is not increasing rapidly enough to meet the EU (and worldwide) 2020 objectives of zero energy buildings.

The building sector is responsible for the 40% of the overall energy consumptions, which are divided in air conditioning (heating, cooling and ventilation) and electrical (appliances) consumption. In the last years, air conditioning and electric consumption are getting more and more integrated. In the EU Member States the electric consumption of residential sector increased by 17.4% during the period between 1999 and 2004. In the USA the annual power consumption has tripled during the past two decades. Furthermore, it has been estimated that 30% of that energy consumption is wasted. The scientific community suggests that the increment of energy consumption is due to the user's lack of energy usage awareness.

However, smart meters can provide useful feedback and therefore reduce the amount of wasted energy. In this way, energy efficiency in smart buildings is oriented to distributed sensor applications, which monitor the power consumption of appliances in industrial, commercial and domestic environments.

The analysis of current and voltage waveforms is fundamental for analysing the power quality and reducing the amount of wasted power. Moreover, it enables Non-intrusive Load Monitoring (NILM), which is the process of disaggregating a household's total electricity consumption into its contributing appliances, by analysing the voltage and current changes [23].

An innovative Non-intrusive Wireless Energy Meter (NIWEM) will be presented to measure the current, the voltage and the power factor. As a key feature, this smart meter is completely non-invasive and it can self-sustain its operations by harvesting energy from the monitored load. In particular, an im-

portant section of this dissertation will be dedicated for introducing the innovative non-invasive approach used for measuring the voltage waveform, which exploits capacitive-coupling elements.

1.3 Thesis Outline

The remainder of this thesis is structured as follows.

Chapter 2 describes a new strategy for minimising the power consumption in sleep mode in a WSN, when the nodes are equipped with energy-hungry sensors and the power source has to be regulated using switching converters.

Chapter 3 describes an innovative low-overhead and local clock synchronisation approach based on a Temperature Compensation Algorithm (TCA).

Chapter 4 describes a new approach, named Hibernus, which enables computation to be sustained during an intermittent supply.

Chapter 5 describes the first scenario regarding the design of an innovative network for monitoring heritage buildings. In particular, this application deploys the technologies presented in Chapter 2 and Chapter 3.

Chapter 6 describes the second scenario regarding the design of smart energy meters for monitoring the power usage of appliances. In particular, an innovative non-invasive approach will be introduced, for measuring the voltage waveform.

Chapter 2

Sleep Power Minimization in WSNs with Adaptive Usage of DC-DC Converter

Aggressive power management techniques, which combine hardware and software solutions, are fundamental for embedded computing platforms, especially if they are battery operated.

In this Chapter an innovative adaptive low-level algorithm is presented, which modulates the DC-DC converter activation for minimizing quiescent current consumption. This algorithm allows a discontinuous usage of the DC-DC converter during the sleep time, without requiring any modification in the user's main program and by only powering the system with the internal DC-DC converter capacitor.

The algorithm computes the maximum interval between consecutive wake-ups, for the capacitor recharging, at run-time. Intervals are decided by taking into account both the global leakage and the temperature-dependent variations of the capacitor. This solution significantly enhances the lifetime of applications with a low-activity rate, such as Wireless Sensor Networks (WSNs), while still guaranteeing efficient power delivery for high-current demand intervals.

2.1 Introduction

Power consumption is a key parameter in determining the lifetime of battery-operated systems, standalone or distributed such as WSNs. Despite innovations in battery technologies, increasing the system power efficiency remains the most effective way to prolong battery lifetime during intensive computing activities and with the system is in sleep mode [24, 25]. Specific low-power applications, such as military networks [26], factory automation [27], distributed monitoring and process control [28, 29, 30], are characterized by low activity rates and long intervals with the system in sleep mode, where the RAM and registers remain active to preserve the stored data [31]. In these cases, global average power consumption approximates the consumption in sleep mode because of the large intervals of sleep time.

Battery-operated IEEE 802.15.4 sensor nodes are usually in sleep mode for almost 99% of the time when used in typical WSNs applications, waking up periodically for a few *ms* for checking sensors or polling the radio interface [32]. Unfortunately, sleep power cannot be reduced to zero, by switching OFF the power supply, without state loss or expensive copies into non-volatile memory. Sleep mode power optimization is a crucial challenge for improving energy efficiency.

However, aggressive reduction of current consumption of low-power nodes, in sleep mode, is not trivial. Power-hungry blocks, such as microcontrollers(MCUs) and radio transceivers, are often OFF during sleep mode. However, sleep mode consumption usually includes the contribution of components which must be kept ON, such as power-supply circuitry and data retention memories (e.g. DC-DC converters and low drop-out linear regulators (LDOs), RAM memories and sleep timers) [33, 35].

WSNs are normally powered by primary batteries. Batteries are characterized by non-linear voltage drops during discharge. A sensor node directly powered by batteries can exhibit progressive reduction of functionality over time due to voltage degradation. To maintain the required quality of service and predictable operation, the voltage has to be regulated using DC-DC converters or LDOs that

guarantee a stable output reference. Due to the lower efficiency of LDOs, DC-DC converters are the common choice to generate the desired output from a variable input source in power-sensitive applications. However, the most serious impact of a DC-DC converters, on low-power embedded systems, is the reduction of battery lifetime due to the quiescent current (I_Q), which causes a limited efficiency with low-output current.

The main aim of this adaptive low-level algorithm is to minimize the losses, due to the quiescent current, of the DC-DC converter with the system in sleep mode. DC-DC converters are usually equipped with an output capacitor, which plays an important role in their functionality. We named it *Intermediate Buffer Capacitor (IBC)* and this is also used as an energy buffer for the system.

IBC can significantly influence the performance and the stability of a DC-DC converter and its regulator feedback loop. The proposed solution uses capacitances which fit the range recommended by DC-DC converter manufacturers, without introducing any design modification. Moreover, the proposed approach is general and larger capacitors can be applied to systems, which are not constrained by strict design recommendations.

In the next sections, the *low-level Dynamic DC-DC Management* (D3M) algorithm is described, which activates the DC-DC converter at small intervals, minimizing the quiescent current consumption. In sleep time, the system is only powered by the *IBC*, without using any other energy buffer.

Discontinuous and intermittent DC-DC converter wake-ups are needed to recharge the *IBC*. The algorithm computes the maximum interval between two forced wake-ups taking into account both the total leakage and its variations with the temperature. During the main user's application, the D3M is not used and the DC-DC converter is permanently switched ON to provide the required power.

The contribution of this research is twofold:

1. to characterize the temperature-dependent time interval with the node only powered with *IBC*;

2. to develop a controllable power-supply unit with an adaptive algorithm to modulate the DC-DC converter usage.

2.2 Overview of power supply architectures

The use of WSNs to monitor complex phenomena has highlighted the need of having power supply units able to support high amount of current consumption, for different scenarios. WSNs can be typically used with energy-hungry sensors (i.e. gas sensors), along with traditional ones such as temperature, air pressure and humidity sensors, and with actuators, which consume large quantities of current [34]. For instance, the authors in [36] present a WSN to detect gas pollution, which uses Metal Oxide Semiconductor MOX sensors. These sensors must be heated up to 400^oC and they need hundreds of mW. The authors in [37] analyse the energy requirements of a set of sensors typically used in WSNs for long-term structural monitoring. This analysis also includes displacement transducers, which need $500ms$ of warm-up and about 14 times the power needed for a packet transmission over IEEE 802.15.4. For this kind of sensors, DC-DC converters, with high current output, are necessary to support WSNs in real-world applications.

The power unit, for low-power wireless sensor nodes equipped with energy-hungry sensors, usually consists of both primary batteries and a DC-DC converter, which provides high-current output when needed. An example of an ultra-low power wireless sensor module, which uses a DC-DC converter is the BTnode [38]. BTnode is a versatile, autonomous wireless communication and computing platform based on Bluetooth radio. It serves as a demonstration and prototyping platform for research in mobile and ad-hoc connected networks (MANETs) and distributed sensor networks. The standard power supply of BTnode consists of two batteries and a primary LTC3429 boost converter with an input range of $0.5-3.3V_DC$. Another example of wireless platform for embedded networks is Mica [39] developed by UC Berkeley to enable WSN research as a foundation for the emerging possibilities. The Mica platform runs the TinyOS operating system and supports the self-configuring multi-hop wireless network as well as sensing, communication and I/O capabilities. A DC-DC converter, which provides a constant $3.3V$ supply, is used because of its small form factor and high efficiency.

DC-DC converters guarantee a clean and stable voltage source for the whole system. However, the main problem of a DC-DC converter is its quiescent current consumption, which causes a lower efficiency in the case of low output current (i.e. during the sleep phases).

Many kinds of DC-DC converters have been presented in literature and are available on the market [40, 41, 42, 43], but the efficiency is usually limited in case of low-output current. This main drawback is due to the quiescent current that the DC-DC converter consumes with the system in sleep mode, which strongly reduces the lifetime of battery-powered systems. For instance, the commercial Boost Regulator MCP1640 developed by Microchip [44] has an efficiency of $60 - 70\%$, when the nominal voltage is within $1.2 - 2.3V$ and with an output current lower than $0.1mA$. Similar considerations apply to DC-DC converters series developed by other manufacturers [45, 46].

The novelty of the proposed approach consists of a discontinuous and intermittent usage of the DC-DC converter during the sleep time. When the system is only powered by *IBC*, the quiescent current is absent because the DC-DC converter is not connected. This solution is synergistic with traditional power management approaches and can be also applied to commercial, high-efficiency DC-DC converters, providing an alternative adaptive management.

2.3 Related works

The lifetime of a WSN largely depends on the power consumption of each sensor node and an efficient power management can improve the network lifetime. Several solutions proposed in the literature focus on reducing consumption when the node is in active mode while neglecting consumption in sleep mode.

Several solutions proposed in the literature are focused on reducing power consumption when the nodes are in active mode, neglecting consumption in sleep mode. For instance, many power management schemes are targeted at minimizing data transmission [3, 4, 5, 10]. Other energy-efficient techniques act at the unit, cluster and network levels, by considering compressive sampling techniques [6],

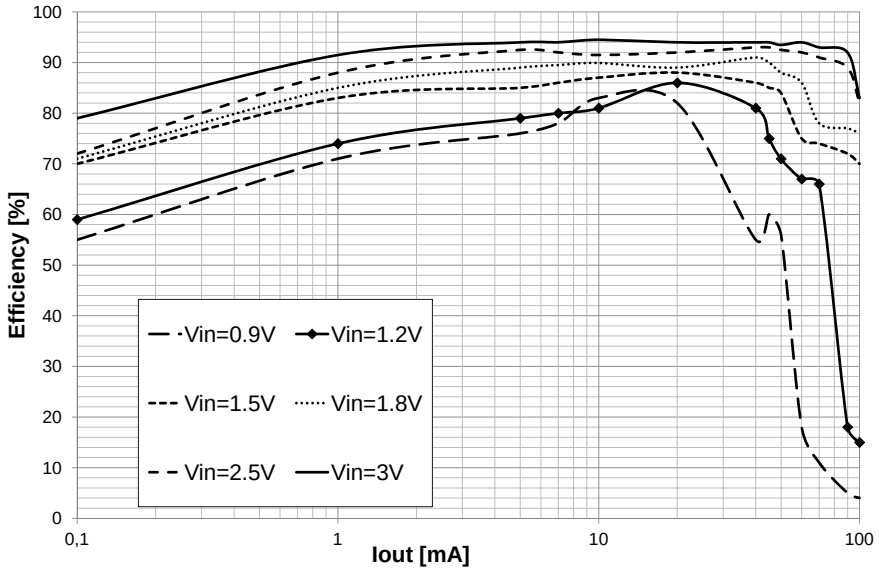

Figure 2.1: Output current vs. efficiency of our test-bed DC-DC converter.

data aggregation [7], adaptive sampling [8] or by reducing the number of data acquisitions at sensor level [9]. Other works are focused on adaptive power management approaches, with energy harvesting systems, based on duty-cycle decreasing or increasing as a function of the harvested energy [11, 12, 13, 14]. However, WSNs spend almost 99% of the time in sleep mode in typical WSN applications. In this context, effective energy management strategies should include policies for power consumption reduction when the nodes are in sleep mode, which is the main aim of this work.

2.4 Problem statement

In WSNs applications, the battery lifetime mainly depends on the power consumption in sleep time. DC-DC converter efficiency is usually very low with a small output current (e.g. when the node is in sleep mode) and the quiescent current of the DC-DC converter is considerable compared to the current needed for the other sub-blocks.

We have considered different kinds DC-DC converters with low quiescent current that are commercially available and we have evaluated how the quiescent

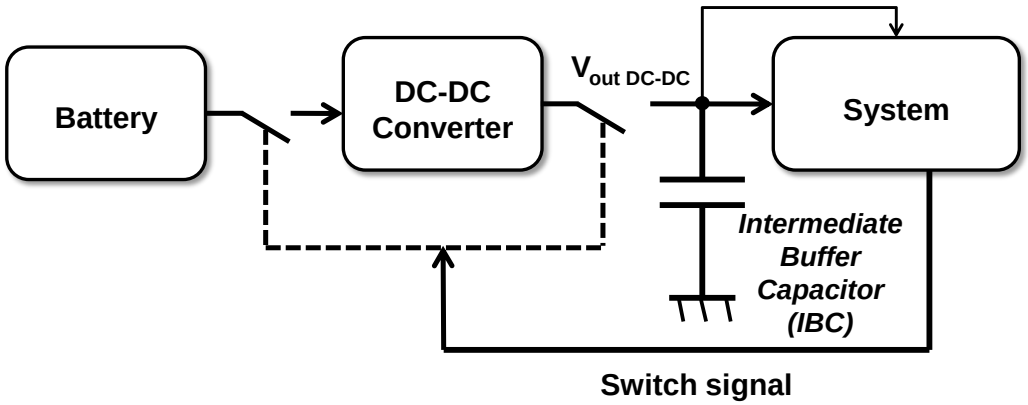

Figure 2.2: Power supply of a wireless node.

current I_Q significantly impacts the lifetime of these systems.

For this purpose, we have also considered the innovative low-input voltage synchronous boost converter (e.g. TPS61097 from Texas Instruments), which is an ultra-low power (ULP) DC-DC converter with a low quiescent current of less than $10\mu A$.

Fig. 2.1 shows the measured efficiency of the TPS61097 as a function of the output current with a nominal voltage between $0.9-3V$, which rapidly decreases for low output current. We will demonstrate that, even in this specific, the proposed algorithm is useful because it improves the lifetime of each wireless sensor node of 10%. Higher performance are achieved with other DC-DC converters.

As shown in Fig. 2.2, the power supply architecture consists of a battery, a DC-DC converter and the system unit. When a WSN node implements the D3M algorithm, the DC-DC converter is directly controlled by the system, providing a stable voltage when the system is in active mode. When the system is in sleep mode, the DC-DC converter is periodically connected for charging *IBC*.

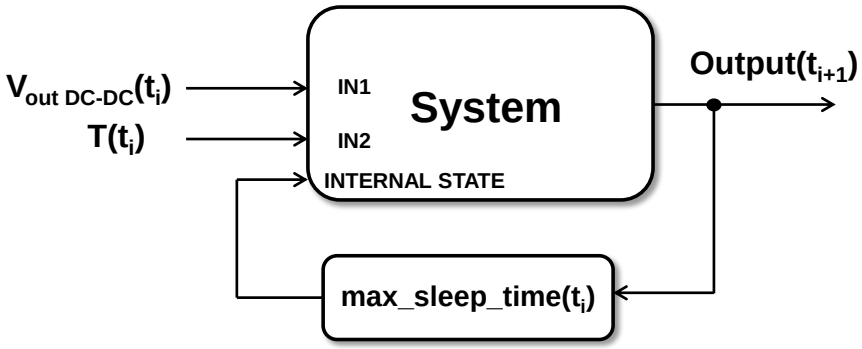

Figure 2.3: Dynamic System used to model the algorithm.

2.5 Adaptive Control Algorithm

2.5.1 High Level Description

The low-level D3M algorithm minimizes the use of the DC-DC converter by only supplying the node with the *IBC* for the most of the time during the sleep mode. Short wake-ups to recharge *IBC* are required due to leakage current. The key idea of the algorithm is to dynamically compute, at each wake-up, the maximum interval with the DC-DC converter OFF, for the next sleep time, taking into account both the global leakage and its variations with the temperature.

We refer to a simple dynamic system with memory, shown in Fig. 2.3, where the output, at each wake-up (t_{i+1}), depends on the inputs and the internal state. In this specific case, $T(t_i)$ is the internal temperature, and $Vout\_DC\text{-}DC(t_i)$ is the voltage across *IBC*.

The internal state is the current value of $max\_sleep\_time(t_i)$, which describes the maximum time before a forced wake up for charging *IBC*.

When the WSN node starts up, depending on the application, the user can set the total sleep time *tot_sleep_time* between two active phases. The algorithm does not modify the user's main program. However, during the sleep time it is necessary to wake up the system a few times for charging the *IBC*. As a result, the parameter *sleep_time_remaining*, which indicates the remaining sleep time between forced wakes-up, is updated at each forced wake-up (Fig. 2.4).

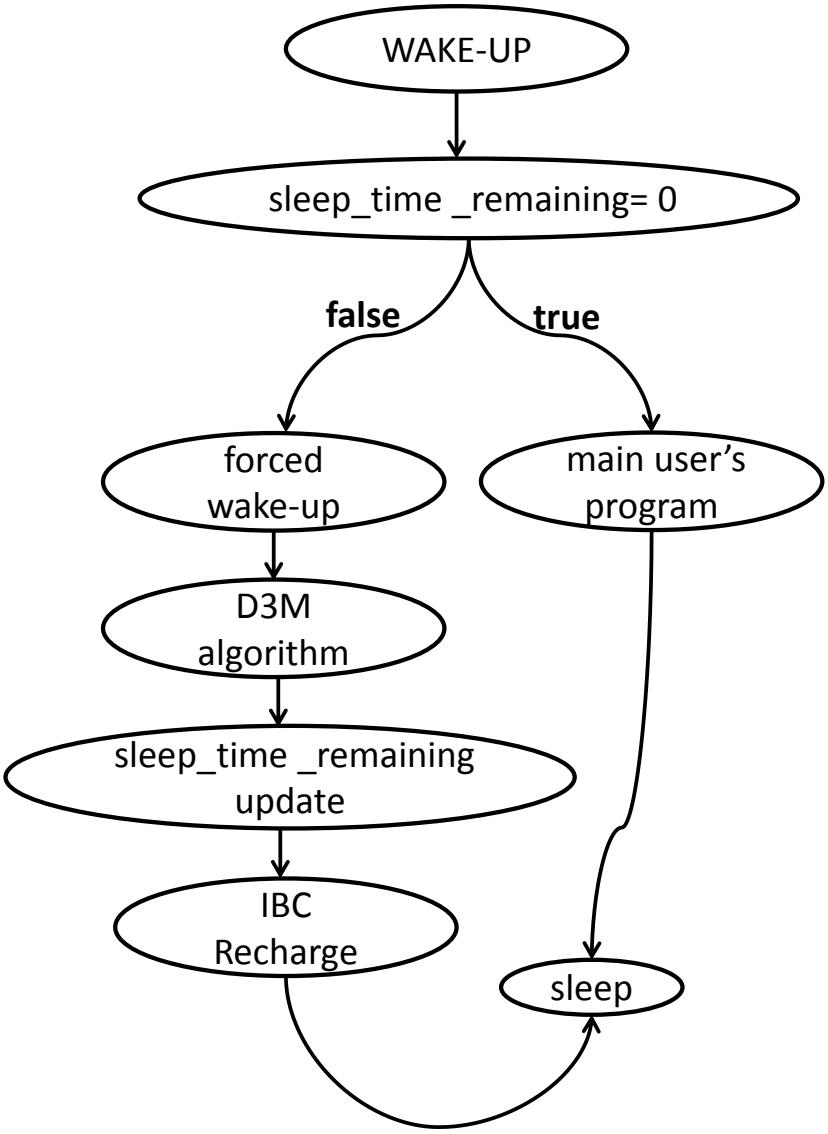

Figure 2.4: *sleep_time_remaining* updating

The main idea of the algorithm is to check the internal temperature $T(t_i)$ and the voltage across *IBC* $Vout\_DC\text{-}DC(t_i)$ at each forced wake-up. If the temperature is above a certain threshold $Tmax$, it means that the leakage is too high and the voltage across *IBC* quickly decreases below the minimum operating voltage. In this case, the DC-DC converter is kept ON ($output(t_{i+1})$ is DC-DC-ON) instead of using the *IBC*, for the next sleep period. However, in normal operat-

ing conditions, the temperature is lower than *Tmax* and the algorithm defines a new value of *max_sleep_time(t_{i+1})* for the next sleep period. This interval is computed according to *Vout_DC-DC(t_i)* and *max_sleep_time(t_i)*. Then, the algorithm switches the DC-DC OFF until the following wakeup.

2.5.2 D3M algorithm energy consumption

The algorithm increases the *max_sleep_time(t_{i+1})* if *Vout_DC-DC(t_i)* is greater than expected (i.e. greater than a given threshold). This means that *IBC* has a slow discharge process and the time needed for the following forced wake-up can be extended. Conversely, if the voltage across *IBC* is lower than expected (i.e. lower than a fixed threshold), the algorithm reduces this time for the following forced wake-up.

The initial values of the parameters must guarantee the robustness of the algorithm. For this reason, *max_sleep_time* is initialized, at boot time, with a small value (i.e. $1s$) because the initial temperature and leakage current are unknown.

The algorithm saves energy with every kind of the DC-DC converter and it is more efficient than keeping DC-DC converter always active.

In the case of DC-DC always active, the energy $E_{DCDC-ON}$ absorbed by the system, for a given value of *tot_sleep_time*, is:

$$E_{DCDC-ON} = tot\_sleep\_time \cdot \frac{P_{system}}{\eta_1} \tag{2.1}$$

where P_{system} is the power used to supply the entire system in sleep mode and η_1 is the DC-DC converter efficiency with the system in sleep mode. The energy used between two wake-ups is:

$$E_{D3M} = charging\_time \cdot \frac{P_{IBC\_charging}}{\eta_2} \tag{2.2}$$

where $P_{IBC\_charging}$ is the power used to charge *IBC* and then supply the system for the next interval, η_2 the DC-DC converter efficiency with the system in active

mode and *charging_time* the time needed to charge the *IBC*, as follows:

$$P_{IBC\_charging} = \frac{tot\_sleep\_time}{charging\_time} \cdot P_{system} \tag{2.3}$$

Since $P_{IBC\_charging}$ is greater than P_{system}, the efficiency of the DC-DC will be greater (i.e. $\eta_2 > \eta_1$) and therefore $E_{D3M} < E_{DCDC-ON}$.

Energy savings *Es* can be described as:

$$E_S = E_{DCDC-ON} - E_{D3M} \tag{2.4}$$

The break-even point is reached when E_S is equal to the overhead needed by the algorithm for measuring the energy in *IBC* and computing a new *tot_sleep_time*.

2.5.3 D3M algorithm following wake-up and consumption during sleep time

At each wake-up, the algorithm checks the temperature *Ti* and, if it is below then *Tmax*, the algorithm will set the next sleep time with the DC-DC converter in OFF mode (*output*(t_{i+1}) is DC-DC OFF).

Since it is not possible to accurately determine the relationship between the temperature and the leakage current, due to the components variability, the algorithm measures the *IBC* voltage *Vout_DC-DC* to detect the discharge level of the capacitor. In this way, it is then possible to indirectly assess the leakage.

Fig. 2.5 shows an example of voltage discharge with an *IBC* of $100\mu F$, which is typically used as the nominal value for DC-DC converters. The graph shows the discharge curves at different temperature values (25^oC and 50^oC) during sleep time, when the DC-DC converter is OFF and the node is only supplied by the capacitor. The discharge time depends on the leakage using the following equation:

$$i(T) = KT^2 \tag{2.5}$$

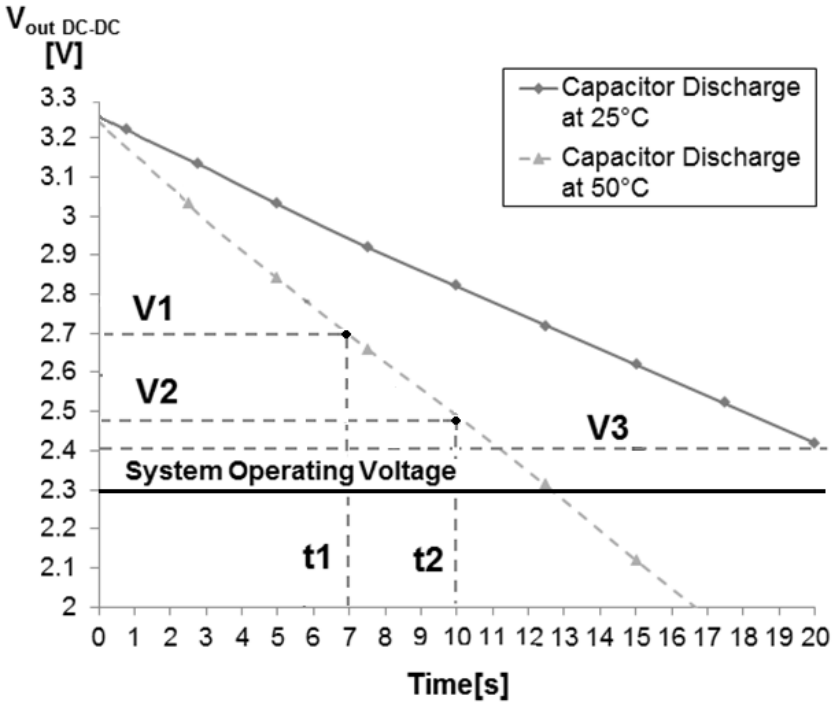

Figure 2.5: Discharge of *Intermediate Buffer Capacitor (IBC)*.

where K is a constant value, T the temperature and the voltage *Vout_DC-DC(t)* is defined as:

$$V_{out\_DC-DC}(t) = V_0 - \frac{i(T)\,t}{C} \tag{2.6}$$

where V_0 is the initial voltage value of the charged capacitor, t is the time and C is the capacitance.

The curve related to the voltage discharge with temperature equal to 50^oC (worst case in our test-bed), the equation (5) and the minimum operating voltage, are utilized to define the parameters V1, V2 and V3, which are used for setting the minimum value of *max_sleep_time* while the values t1 and t2 are defined to guarantee the time necessary to put the system in a safe state, even in case of a rapid decreasing in the voltage, due to the temperature.

The algorithm finds an equilibrium condition as a function of the temperature. When the temperature increases it puts the system into a safe state. Furthermore, the algorithm overhead and the energy used to charge *IBC* is much less than

the energy needed to keep the DC-DC converter always ON. For example, in the presented test-bed, where the supply voltage is 3.3V and a $100\mu F$ of *IBC* is used, the discharging phase in about *20s* while the time required for recharging is about $3ms$. During the recharge, the microcontroller is busy executing the algorithm but, with the exception of the ADC module and the DC-DC converter, the other sub-blocks are OFF. In this case, the energy used by the D3M algorithm is less than 50μJ. If the system keeps the DC-DC converter always ON (without D3M), the energy used in the same intervals is about 660μJ, when very low quiescent current DC-DCs are used, such as the TPS61097 DC-DC.

These results highlight the advantage of switching OFF the DC-DC converter, regardless the type of the DC-DC converter on-board.

2.5.4 D3M algorithm max_sleep_time setting

Depending on the temperature and the *IBC* voltage, the state of the DC-DC converter will dynamically change. Thus, the D3M algorithm will set the DC-DC state (ON, OFF) and the sleep time length *max_sleep_time*(t_{i+1}) for the next sleep period.

Therefore, to ensure the correct operation of the node even in extreme cases (i.e. high temperature) we take the following condition into consideration: if the microcontrollers internal temperature is greater than *Tmax*, the DC-DC converter will stay ON during the next sleep phase because current leakage is high and rapidly discharges the *IBC* below the minimum system operating voltage.

The algorithm uses the voltage discharge curve at $Tmax$=50^oC of the *IBC* and the equation (5) for setting *max_sleep_time* to its minimum value. This choice is based on the input voltage *Vout_DC-DC*(t_i) and the previous *max_sleep_time*(t_i) value.

We have considered a series of cases where *max_sleep_time*(t_{i+1}) is set to its minimum value to assure safe working:

- if *Vout_DC-DC*(t_i) is less than V1 and *max_sleep_time*(t_i) is less than t1 seconds;

- if *Vout_DC-DC(t_i)* is less than V2 and *max_sleep_time(t_i)* is between t1 and t2 seconds;

- if *Vout_DC-DC(t_i)* is less than V3 and *max_sleep_time(t_i)* is greater than t2 seconds;

This happens to indirectly counteract the increase of leakage current with the temperature. The values of the parameters V1, V2, V3 are selected considering the worst voltage discharge curve of the *IBC*, Equation (5) and the minimum operating voltage. The time t1 and t2 are chosen to ensure a reactive response of the system in the case of a rapidly increase of the temperature.

At each wake up, the algorithm checks the value of the *sleep_time_remaining*. If this value is equal to zero it means that the node has completed its sleep phase. The algorithm executes the user's main program (i.e. sample sensors and transmit data over the network) and, finally, the node goes to sleep (*sleep_time_remaining* is set again with the *tot_sleep_time* value). If *sleep_time_remaining* is different from zero, it means that the node has not completed the total sleep phase yet, and there is a forced wake-up.

At every forced wake-up, if *max_sleep_time(t_{i+1})* is not already set to the minimum value, as described above, *max_sleep_time(t_{i+1})* is augmented by one or two seconds:

- if *Vout_DC-DC(t_i)* is greater than V5 and *max_sleep_time(t_i)* is less than t3 seconds *max_sleep_time(t_{i+1})* = *max_sleep_time(t_i)* +1;

- if *Vout_DC-DC(t_i)* is greater than V4 and *max_sleep_time(t_i)* is greater than t3 *max_sleep_time(t_{i+1})* = *max_sleep_time(t_i)* + 2;

The values of the parameters V4 and V5 are chosen for increasing the value of *max_sleep_time* slower when *max_sleep_time* is near its minimum value (only +1) and quicker when *max_sleep_time* is far enough from its minimum value (+2). These two values (+1 and +2) are chosen, after the experimental calibration, to gradually increase *max_sleep_time*.

The value of t3 is defined as:

$$t3 = t1 + \frac{t2 - t1}{2} \tag{2.7}$$

In Fig. 2.6, the block diagram of the algorithm used for setting *max_sleep_time* is shown.

2.5.5 IBC Recharge

If *sleep_time_remaining* is different from zero, the node has a forced wake-up that allows the recharging of the *IBC*. In this condition, the node will remain active as long enough as to execute the D3M algorithm and check the *IBC* voltage for the recharge phase. During the recharge phase, the DC-DC converter is turned ON and, using an internal ADC of the MCU, the voltage of the *IBC* is checked. When it exceeds a threshold value, the node enters in sleep mode and DC-DC is turned OFF again.

2.5.6 D3M algorithm summary

The algorithm uses the voltage discharge curve at *Tmax* to set *max_sleep_time* to completely exploit the *IBC* energy from V_{DD} to the lowest operating voltage for any value of temperature.

Fig. 2.7 schematically shows how the next value of *max_sleep_time* is selected using the D3M algorithm. If the previous value of *max_sleep_time*(t_i) and the measured input voltage *Vout_DC-DC*(t_i) are such as to identify a point in the R1 region, the *max_sleep_time*(t_{i+1}) value will be set to the minimum value.

If the combination of *max_sleep_time*(t_i) and *Vout_DC-DC*(t_i) is in the R2 region, *max_sleep_time*(t_{i+1}) will hold the same value as the previous period, because the maximum benefit from the *IBC* has already been exploited.

Finally, if a point is identified in the R3 or R4 regions, *max_sleep_time*(t_{i+1}) will be increased by one second or two seconds compared to the previous value.

The R3 and R4 regions are chosen to increase the value of *max_sleep_time* slower when *max_sleep_time* is close to its minimum value and more quickly when

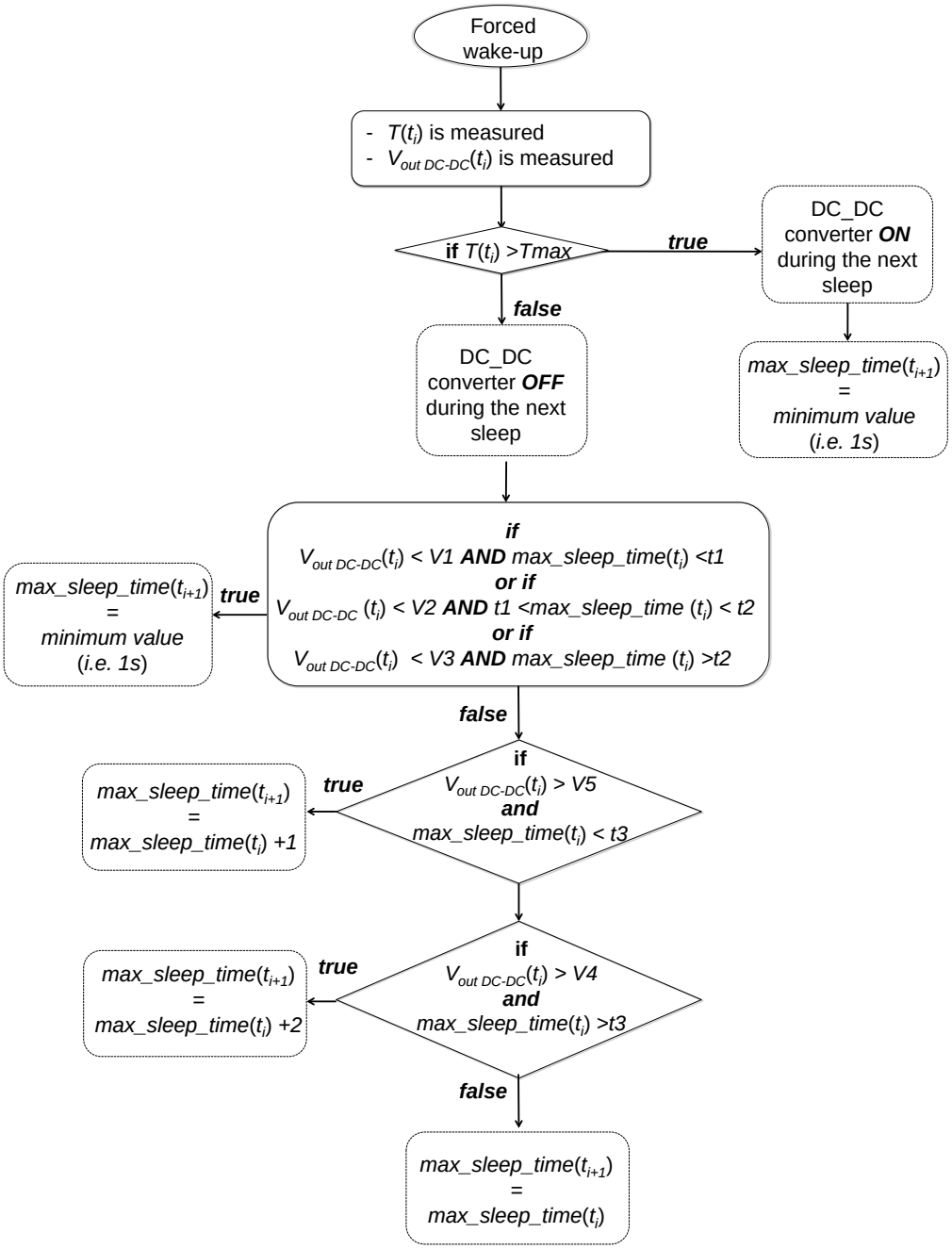

Figure 2.6: Block diagram of the D3M algorithm used for setting *max_sleep_time*.

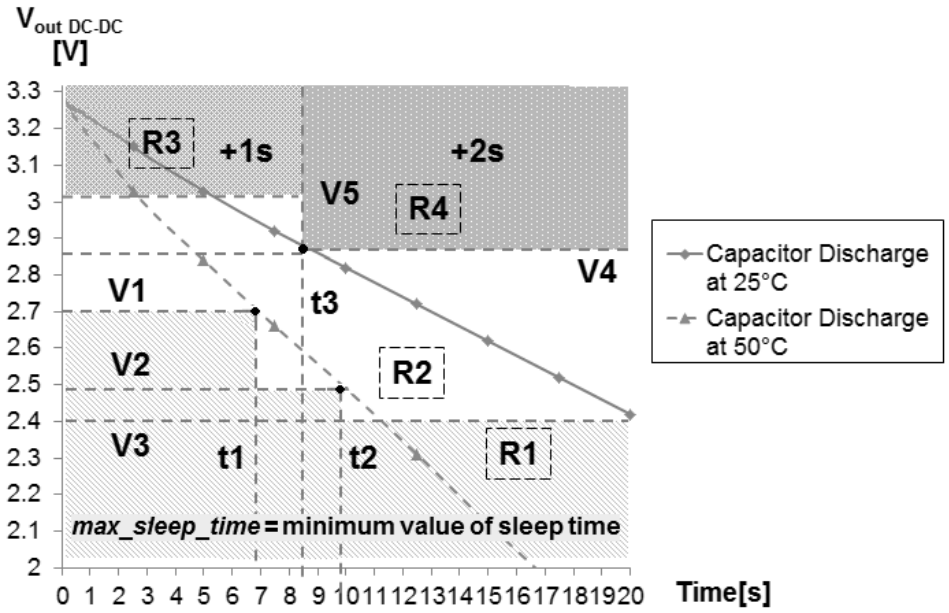

Figure 2.7: D3M algorithm scheme to define the next $max\_sleep\_time(t_{i+1})$ based on the voltage $Vout\_DC\text{-}DC(t_i)$ and the previous $max\_sleep\_time(t_i)$.

max_sleep_time is far enough from its minimum value.

2.5.7 Case study

We applied D3M algorithm to a Wireless Sensor Node designed for structural environmental monitoring (W24TH)(Chapter 5).

The W24TH Node is based on a Jennic JN5148 module [47] equipped with several sensors. The power unit contains two primary batteries, but can be also supplied with a power-harvesting unit.

The module is an ultra-low-power, high-performance wireless microcontroller targeted at ZigBee PRO networking applications. The processor features an enhanced 32-bit RISC processor, a 2.4 GHz IEEE 802.15.4 compliant transceiver, 128 kb of ROM, 128 kb of RAM and analogue and digital peripherals.

Fig. 2.8 shows a simple example of the *Vout_DC-DC* profile between two active phases with the W24TH, which is equipped with the TSP61024 TI DC-DC converter and a *IBC* of $100\mu F$. It also shows five forced wakes-up where at each

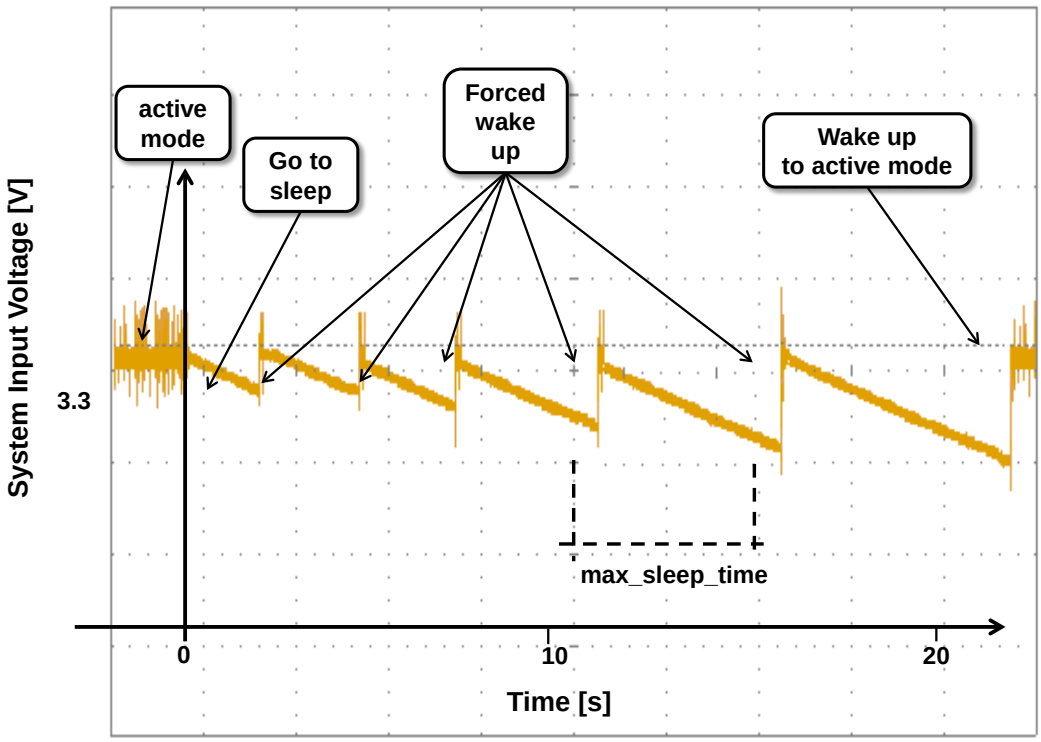

Figure 2.8: Implementation of the power-supply control algorithm with 5 forced wake-up states at 25^oC stationary condition.

wake-up the *IBC* is recharged and *max_sleep_time* is incremented.

Fig. 2.9 shows the start up time during which *max_sleep_time* value increases and then achieves an equilibrium after about *100s* (in steady state conditions at 25^oC) where the *max_sleep_time* is set to *19s.*

Fig. 2.10 shows *max_sleep_time* changing, when the temperature is increasing from 25^oC to 50^oC. During the entire period of time *max_sleep_time* is set to its minimum value with the increase of temperature. Only when the temperature is stable around 50^oC the *max_sleep_time* value remains constant *8s*. The algorithm works in adaptive mode even during the transition from one state to another.

Finally, Fig. 2.11 shows the *max_sleep_time* value for different values of temperature. Notice that *max_sleep_time* raises as the temperature decreases, confirming the adaptability of the D3M algorithm with temperature.

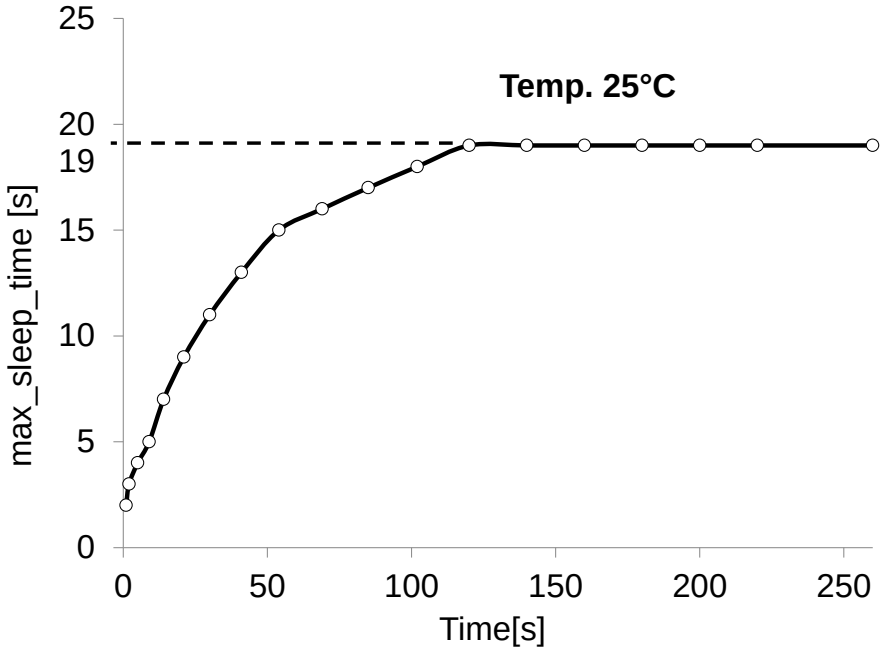

Figure 2.9: max_sleep_time of test node monitored over time with D3M control algorithm (at 25^oC).

2.6 Experimental Results

2.6.1 Experimental Setup

Several experiments were conducted to show that the proposed solution significantly increases the lifetime of WSNs with low-duty cycle activity. We have decided to consider the following DC-DC converters: MCP 1640, TSP61024, LTC 3536 and TSP61097, and two different kinds of IBC: $100\mu F$ and $50\mu F$.

The experiments were performed with twelve wireless sensor nodes that perform the main user's program. These sensor nodes are divided into four groups and each group equips a different DC-DC converter. Performance have been averaged within the same group.

For all the nodes we have used the same kind of battery: Li-Ion battery with a battery capacity $Q = 1Ah$ and a battery constant voltage $E_0 = 3.06V$. The user's duty-cycling period is set to $1min$.

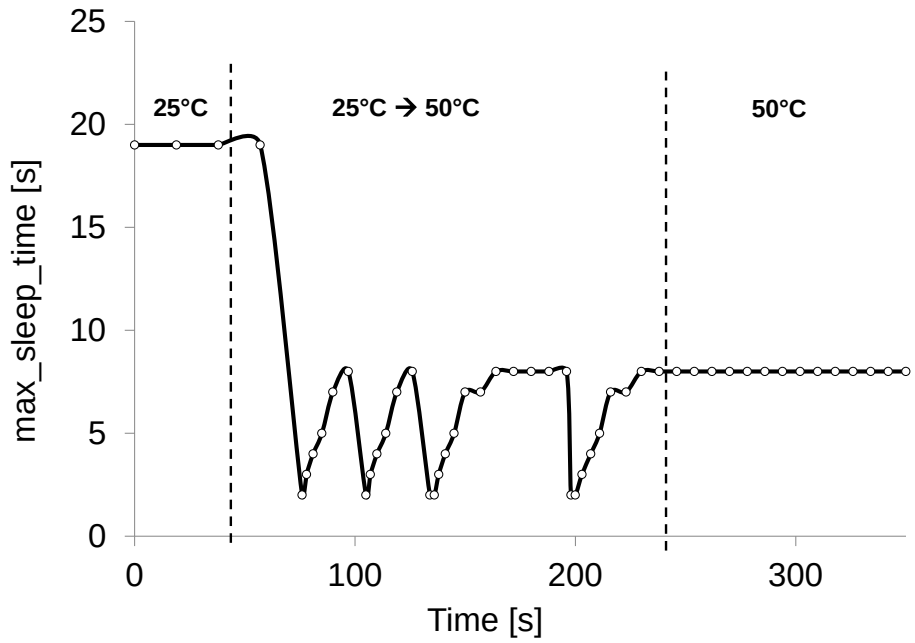

Figure 2.10: *max_sleep_time* during a rapid change of temperature from 25^oC to 50^oC.

2.6.2 Results

In this section we have considered the battery voltage discharge for each group of nodes, which use a different DC-DC converter. In each group, one node has the DC-DC converter always ON while the second and the third ones use the D3M algorithm but with different values of IBC ($100\mu F$ and $50\mu F$). In general, it is possible to observe that the voltage of the battery decreases more gradually with the nodes that use the D3M algorithm compared with the nodes that use the DC-DC converter permanently in the ON state, which confirms that our approach outperforms the standard implementation.

As shown in Fig. 2.12, when the MCP 1640 is used, the discharge time of the nodes that has the DC-DC converter permanently ON is about 911 hours while the nodes with D3M has a lifetime of 1233 hours with $50\mu F$ and 1317 hours with $100\mu F$. This is an improvement of 24% and 31% respectively.

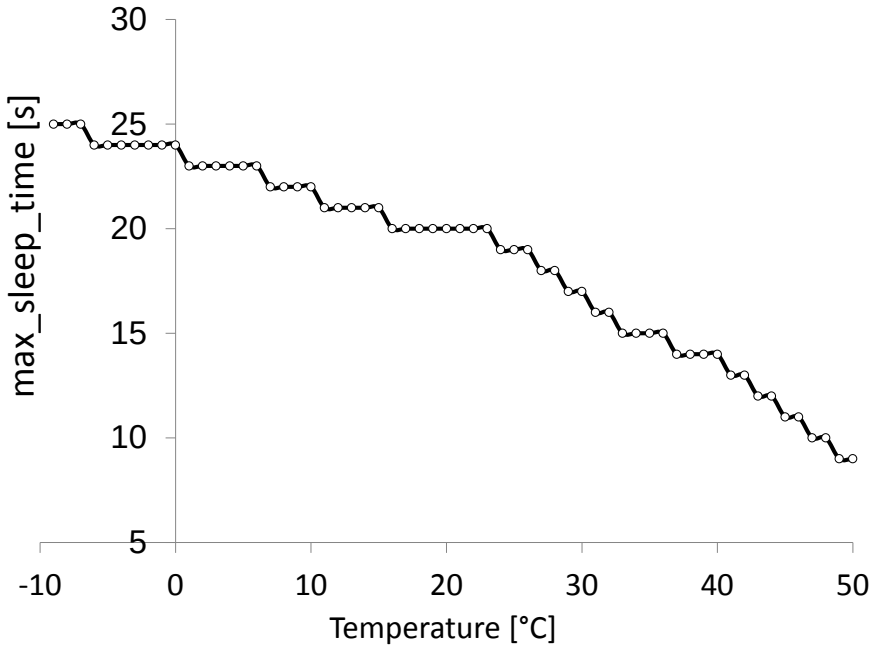

Figure 2.11: *max_sleep_time* as a function of the temperature.

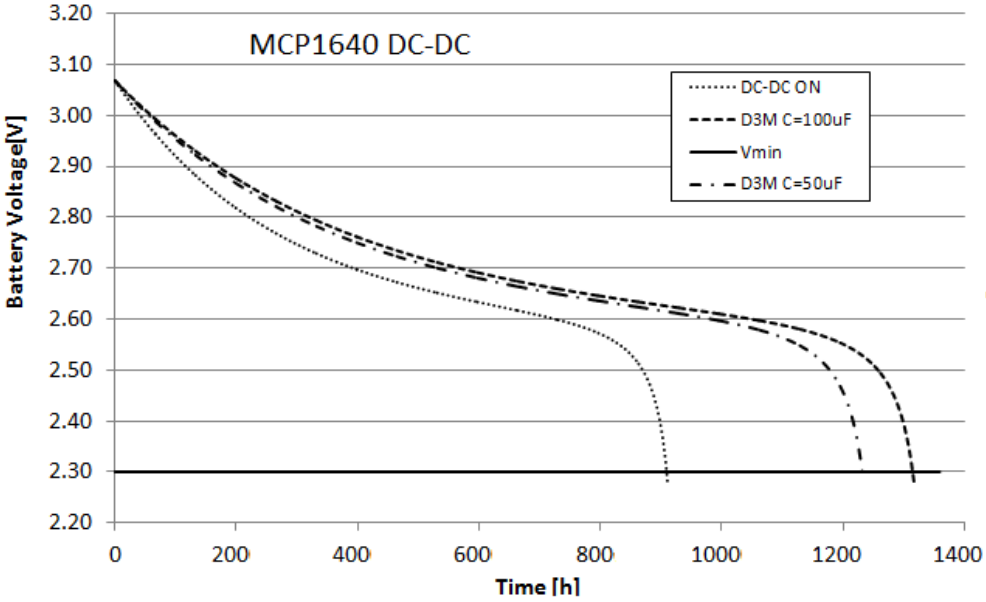

Figure 2.12: Battery voltage discharge for each group of nodes, which use a MCP1640 DC-DC converter.

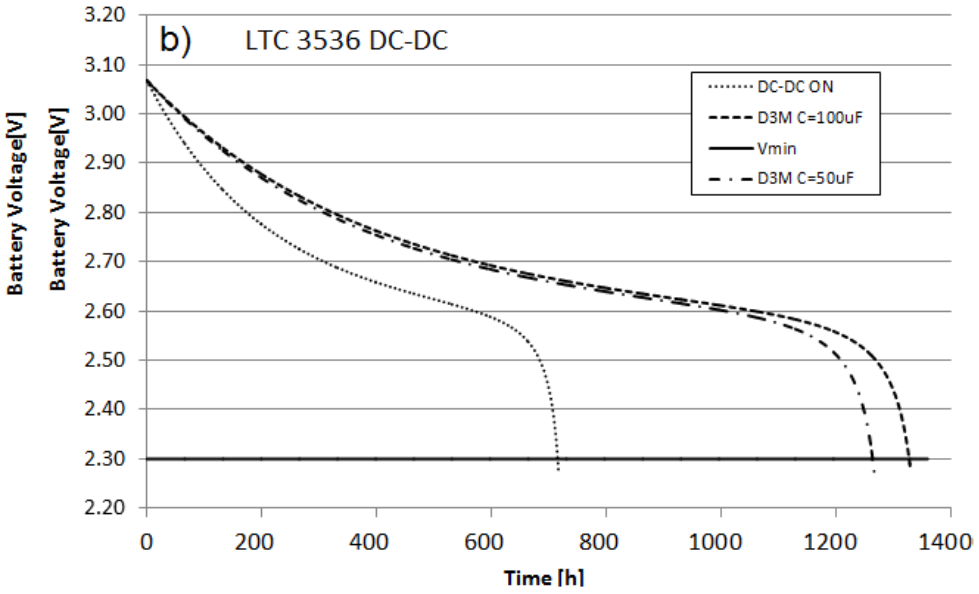

Figure 2.13: Battery voltage discharge for each group of nodes, which use a LTC3536 DC-DC converter.

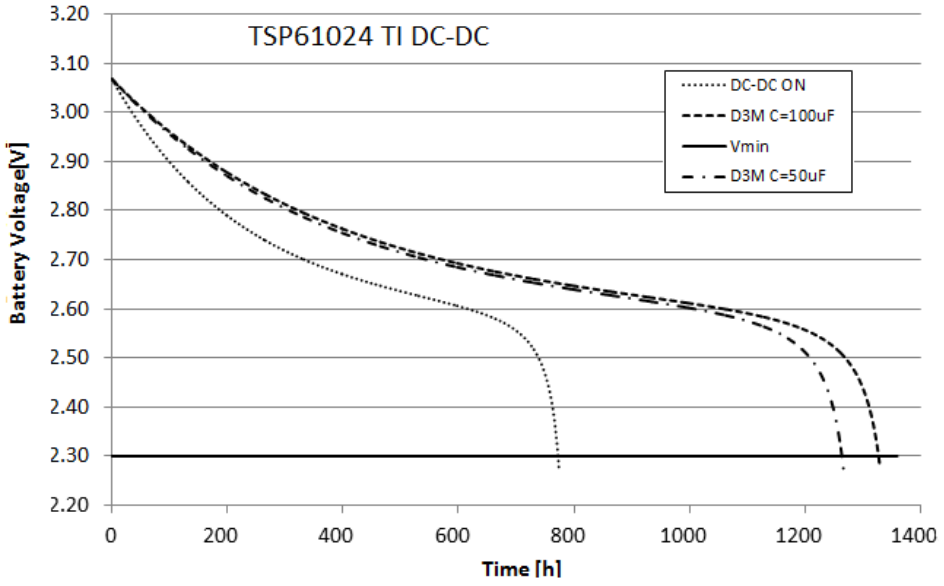

Figure 2.14: Battery voltage discharge for each group of nodes, which use a TSP61024 DC-DC converter.

Similar improvements are registered also using other DC-DC converters. In Fig. 2.13, when the LTC3536 is used, the improvement is 35% and 40%, with

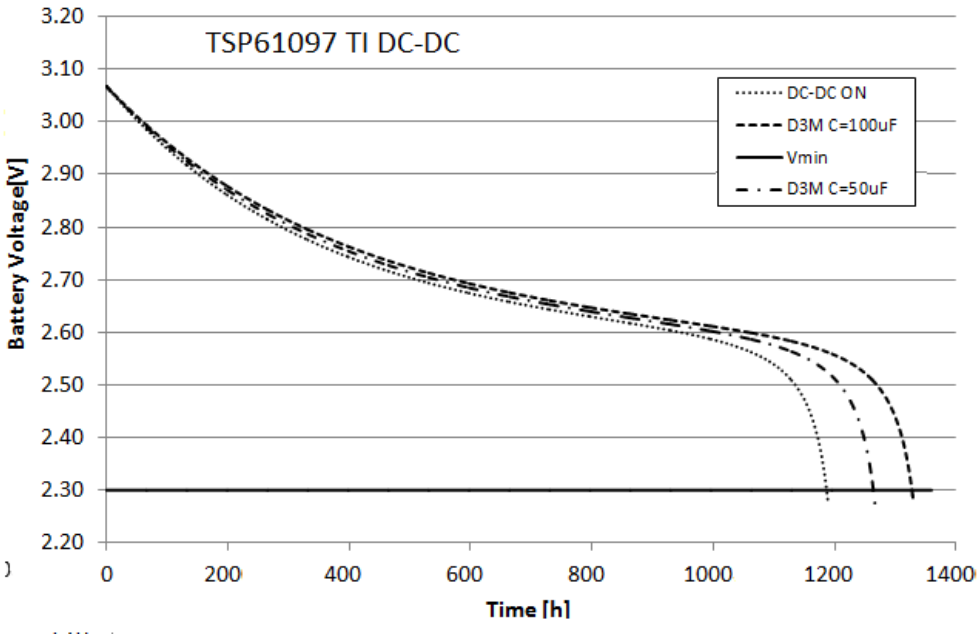

Figure 2.15: Battery voltage discharge for each group of nodes, which use a TSP61097 DC-DC converter.

$50\mu F$ and $100\mu F$, respectively. Also, TSP61024 (Fig. 2.14) shows increments of lifetime of about 36% and 40% .

Interesting information can be extracted from experiments on TSP61097 that has a low quiescent current, where the discharge time of the node that uses the DC-DC converter permanently ON is 1190 hours while the nodes with D3M have respectively a duration of 1266 hours with $50\mu F$ and 1320 hours with $100\mu F$(Fig. 2.15). This is an improvement of 6% and 10% respectively, which is smaller than the former experiments due to the lowest I_Q, but still remarkable.

2.7 Conclusion

In this Chapter a novel technique for extending the lifetime of a WSN node is presented. The main idea is to minimize the consumption of the DC-DC switching converter during sleep mode. This is accomplished through an adaptive algorithm that turns ON and OFF the DC-DC converter to minimize sleep power consumption. The D3M algorithm computes the maximum interval allowed to

operate solely with the *IBC*, taking into account both global leakage and its variations with temperature changes. The proposed solution significantly increases the lifetime of applications with low-duty cycle activity, such as WSNs and portable devices.

Chapter 3

Temperature Compensated Time Synchronisation in Wireless Sensor Networks

Time synchronisation is fundamental in distributed systems such as Wireless Sensor Networks (WSNs) to coordinate activities with multiple nodes. The main aim for WSNs is to maintain the nodes synchronized and, at the same time, to minimize power consumption.

In this Chapter an innovative low-overhead clock synchronisation approach is presented, based on a Temperature Compensation Algorithm (TCA).

Non-uniform and dynamic changes of the temperature are the main causes of clock drift in wireless sensor nodes. The proposed TCA uses a temperature sensor to reduce the effects of environmental temperature changes and then to increase the synchronisation interval.

Using the TCA, the 32 KHz clock achieves an effective clock drift of less than 5 ppm over a wide range of operating temperatures (25 to 62^{o}C), which is a significant improvement compared to the 55 ppm featured without temperature compensation.

3.1 Introduction

Time synchronisation is fundamental in distributed systems for monitoring real-world phenomena such as WSNs. Physical time plays a critical role for coordinating activities performed by multiple wireless sensor nodes and for managing scheduled tasks at single node level. Moreover, time synchronisation is also a key aspect at network level, for power minimisation and bandwidth optimisation [48, 49].

Network protocols, task scheduling and distributed power management require an accurate knowledge of time, locally and globally, to minimise the communication overhead and energy consumption, and maximise the sleep mode time.

Unfortunately, time synchronisation in WSNs is a difficult task compared to other traditional distributed services (e.g. internet services) because of the accuracy and precision required, by also considering the limited energy available for each wireless sensor node [50].

However, a common view of the physical time in the applications with WSNs is a basic requirement in order to have the proper timestamp of phenomena that occur in the physical world. For instance, the times of occurrence of real-world events are often critical for the observer to associate event reports with the originating physical events. Physical time is also crucial for determining properties such as speed or acceleration [51].

In general, traditional synchronisation schemes assume to have a global time-reference (e.g. gateway time-reference) [52, 53]. For each node, WSNs therefore require a way to synchronise local time with the global time. This is obtained by periodically sending a broadcast message. Of course, the specific characteristics of each local oscillator affect the relative clock drift compared to the other local oscillators and consequently, they play a crucial role to determine the maximum period at which the resynchronisation must be performed.

For instance, with our test-bed, using a 32 KHz clock and observing the timestamps between the local node and the gateway, it is possible to notice a drift of +60 ppm, which corresponds to 1 ms of offset every 16.6 s.

In the following Sections we will introduce a new approach for clock synchro-

nisation in a WSNs by considering an an innovative temperature compensation algorithm (TCA). Moreover, we will describe the calibration and the compensation steps and, finally, the obtained results.

3.2 Problem statement

The main idea of the proposed algorithm is to minimise the drift of the local oscillator and then to reduce the rate of the broadcast messages for the synchronisation of each node in the network.

Stable clock sources are commercially available (e. g. timers based on temperature compensated crystal oscillators (TCXO) [54] or GPS with a PPS signal). However, these solutions are too expensive, considering a network of hundreds of nodes. Moreover, they need of a big amount of energy and, sometimes, are limited to be a valid alternative (e.g. GPS does not work indoors).

Frequency stability of a crystal oscillator can be affected by several factors, which generate two different kinds of drift: (i) short-term and dynamic clock drift and (ii) long-term continuous clock drift. Short-term instability is mainly due to both environmental and electrical factors such as variations in temperature and supply voltage. Temperature changes represent the main effect of the clock drift. Long-term instability is caused by several effects such as oscillator ageing. In this way, a compensation of the local oscillator should be periodically performed.

However, a common assumption is that the temperature changes can influence in the same way every local clock in the network over a certain period of time. This assumption is often used to calculate a constant clock drift and then to force a time synchronisation also when it is not strictly necessary.

In the next Section, we will introduce our approach based on a Temperature Compensation Algorithm (TCA), which is useful for dynamically measuring and compensating the clock drift and then for reducing the number of forced synchronisations.

3.3 Temperature Compensation Algorithm

The main idea of the proposed TCA is to measure the temperature for the clock error estimation using the on-board temperature sensor available in many sensor network platforms.

The TCA uses this sensor to autonomously calibrate the local oscillator, remove the effects of environmental temperature changes and then to extend the interval between synchronisations. It is important to underline that TCA does not make any assumption about the network architecture. It is mainly a technique to extend the time between forced clock synchronisations, and it is thus compatible with every kind of network synchronisation protocols.

The TCA consists of two steps: calibration and compensation.

3.3.1 Calibration

We will assume that a slave node receives accurate time measurements from a remote master node (e.g. a gateway) and, at the same time, a slave node can communicate with its master node.

Initially, the slave nodes do not know their current clock error. Thus, it needs to rely on the cooperation of a master node, which has knowledge of the accurate time. The calibration phase is performed without knowing the network architecture and by only using a few nodes as a calibration set. In our test-bed, we have used eight slave nodes with crystal oscillators with nominal frequency fn equal to 32 KHz, which receive a time constant synchronisation beacon (i.e. every 20 seconds) from the master node. All nodes are into a temperature chamber and subjected to an operating temperature range from 25 to 62^o C. After each beacon message, the slave nodes collect their own value of ticks from the real-time clock (RTC) and compute the difference between two beacon events at a constant temperature T.

The values of the RTC counter, for the same beacon interval, change as a function of the temperature changes. As shown in Fig. 3.1 the measured clock drift in ppm presents similar temperature curves for all clocks. The function

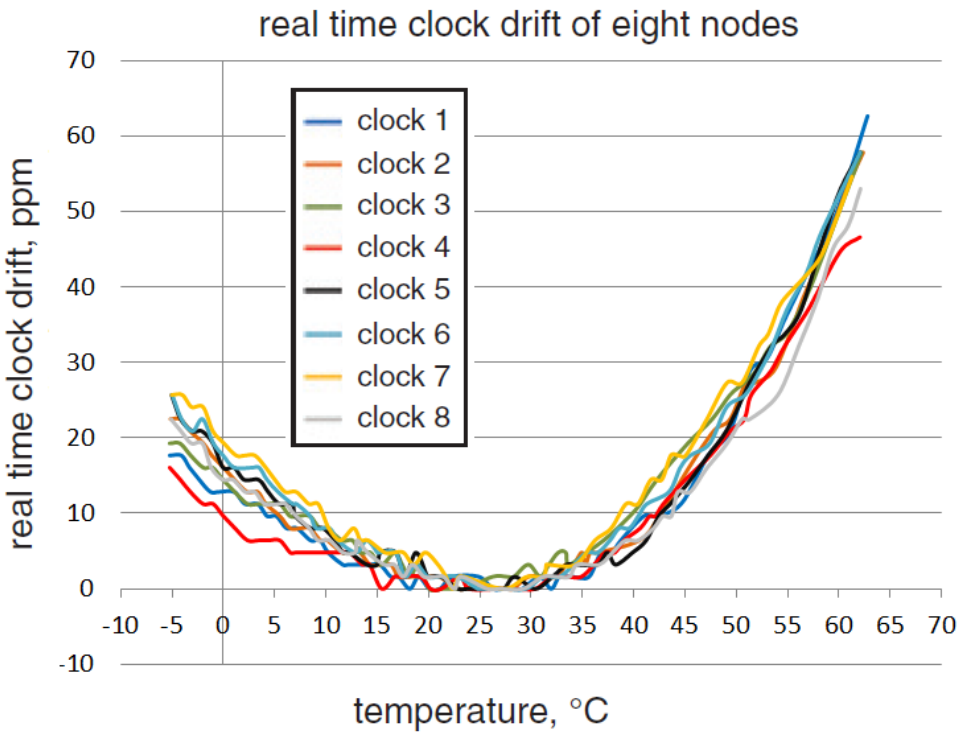

Figure 3.1: Measured clock drift against temperature of eight 32 KHz crystals between two beacon events. All clocks present similar temperature curves.

of the clock drift with the temperature is not linear but it recalls the trend of a parabolic curve. Using this information, it is possible to obtain a curve that contains the average of the mesured drifts, which can be used as the calibration curve, as shown in Fig. 3.2.

Converting this curve into a look-up table simplifies the implementation of the next step, the compensation phase, on an simple microcontroller since no floating point unit has been used.

3.3.2 Compensation

The compensation phase is run-time performed. The slave node regularly measures the environmental temperature. After each measurement, it checks the temperature against the clock error curve (Fig. 3.2) and adjusts its own system clock counter, with the calibration offset at the corresponding temperature.

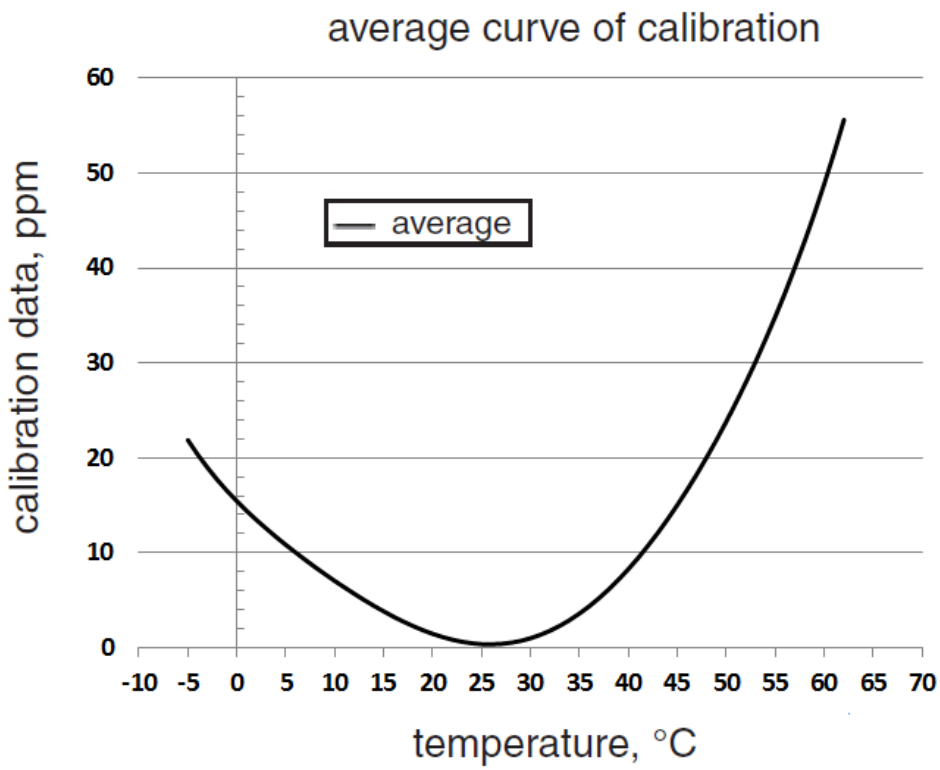

Figure 3.2: During calibration phase, the average curve calibration from obtained drift measurements is generated.

In particular, at every synchronisation period, the slave node changes its clock counter offset as follows:

$$compensated_{offset}(T) = counter_{offset}(T) + clock_{error}(T) \tag{3.1}$$

where $counter_{offset}$ is the difference between the last synchronisation time and the current local time; $compensated_{offset}$ is the result obtained applying the TCA, while the $clock_{error}$ is the new clock error measured using the calibration data, which can be calculated as:

$$clock_{error}(T) = \frac{counter_{offset}(T) calibration_{data}(T)}{(1 - calibration_{data}(T))} \tag{3.2}$$

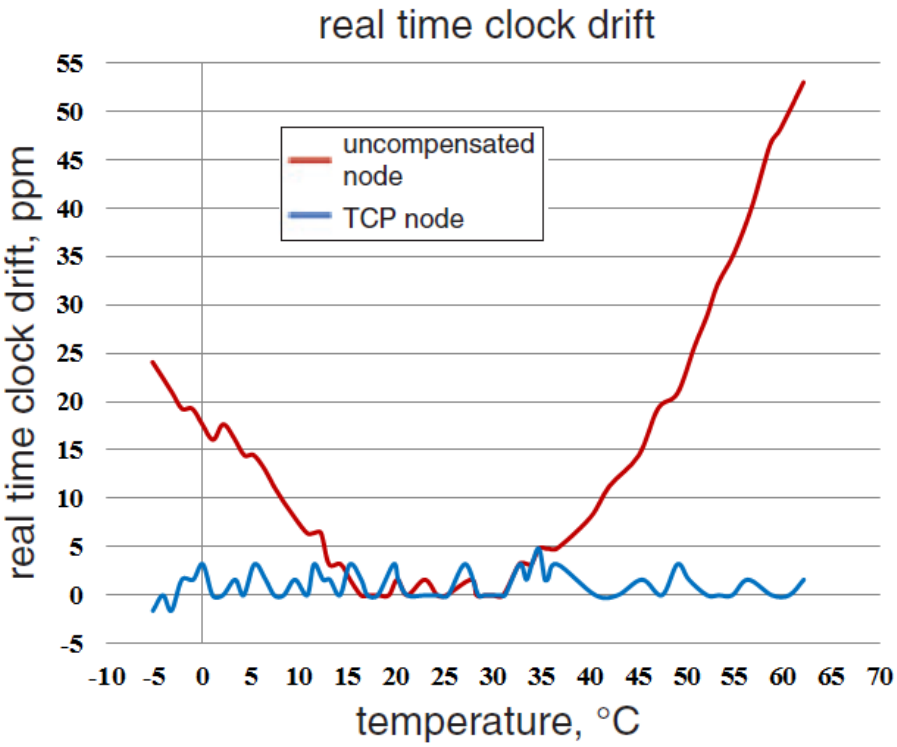

Figure 3.3: Clock drift of two different nodes (uncompensated node and TCA node) subjected to temperature range from 25 to 62^{o}C.

3.4 Results

Fig. 3.3 compares the clock drift of two different nodes (an uncompensated node and a TCA node) subjected to the temperature range from 25 to 62^{o}C. We consider the same synchronisation period of 20 s. In the first case, the local time of the uncompensated node, subjected to 62^{o}C, deviates by about 1.1 ms every 20 s with respect to the master. In the compensated node, the maximum drift is about 100 ms, every 20 s, across the full temperature range.

This means that by using the TCA, the clock drift is less than 5 ppm over the full range of temperatures, which is 10 times less than the drift obtained with the system subjected to 62^{o}C.

Of course, even if the slave node is calibrated with the TCA, the master still needs to send occasional synchronisation beacons due to the effect of this small

drift. These occasional synchronisation beacons ensure that the absolute time error between the master and the slave never increases above a certain threshold. For example, in this case a synchronisation broadcast message every 200 s is sufficient to keep the timestamp of the master node and the timestamp of the slaves locked within 1ms at any operating temperature (25 to 62^{o}C).

3.5 Conclusion

In this Chapter, we have introduced a new time synchronisation approach based on a temperature compensated algorithm (TCA). The main idea of TCA is to measure the temperature during clock error estimation with the on-board temperature sensor. This sensor is then used to calibrate the local oscillator, remove the effects of environmental temperature changes and increase the time between synchronisation intervals. The improvement obtained with this approach is relevant, about an order of magnitude when the system is operating under high temperature (i.e. 62^{o}C). Our approach uses only local processing without requiring any extra network messages.

Chapter 4

Hibernus: Sustaining Computation during Intermittent Supply for Energy-Harvesting Systems

A key challenge to the future of energy-harvesting systems is the discontinuous power supply that is often generated. We propose a new approach, Hibernus, which enables computation to be sustained during intermittent supply. The approach has a low energy and time overhead which is achieved by reactively hibernating: saving system state only once, when power is about to be lost, and then sleeping until the supply recovers. We validate the approach experimentally on a processor with FRAM non-volatile memory, allowing it to reactively hibernate using only energy stored in its decoupling capacitance. When compared to a recently proposed technique, the approach reduces processor time and energy overheads by 76-100% and 49-79% respectively.

4.1 Introduction

Energy-harvesting systems power themselves by extracting energy from the environment [55]. However, the energy provided is often highly temporally dynamic, providing an intermittent supply that is incapable of sustaining computation. This is because processors switch off when the supply drops below their minimum operating voltage and, when power is available again, restart computation from the beginning.

To manage an intermittent supply, one approach is to use a battery or supercapacitor to buffer energy. However, the level of miniaturisation required to realise medical implants [56] or visions of 'smart dust' [57] causes energy storage to be minimised, constraining the computational ability of systems. Recently, a different approach (Mementos [58]) was proposed, which uses the well-known concept of checkpoints [59] placed at compile-time. Mementos saves periodic snapshots of system state to non-volatile memory (NVM), which enable it to return to a previous checkpoint after a power failure. A number of checkpoint placement heuristics are proposed, including at the beginning of every function-call or before any loop. At run-time, when these checkpoints are reached, the supply voltage (V_{CC}) of the processor is inspected using the an analog-to-digital converter (ADC). If it is deemed to be failing ($V_{\mathrm{CC}} <$ a threshold V_{M}), a snapshot of the system state is saved to NVM. This requires regular polling of the supply voltage, and can result in multiple snapshots being saved when the supply voltage is close to the threshold; both introduce time and energy overheads.

This brief proposes *Hibernus*[1], a new approach which automatically saves a snapshot only once (without the need for checkpoint placement heuristics), immediately before power failure, then sleeps. *Hibernus* saves the system's complete volatile memory; this is enabled in part by developments in Ferroelectric RAM (FRAM), a NVM technology that is more efficient than flash, and is now being monolithically integrated into low-power microcontrollers [60]. The speed and efficiency of integrated FRAM means we can react to power loss and save a

[1] In computing, 'hibernation', from the Latin *hībernus*, is the process of saving state to allow power to be removed.

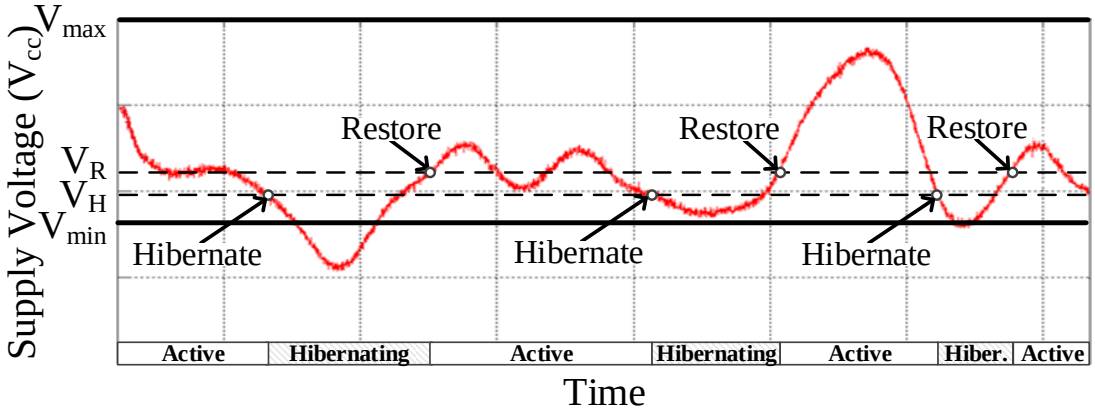

Figure 4.1: Operation of *Hibernus* in response to intermittent supply voltage.

snapshot using only the energy stored in a system's decoupling capacitance.

4.2 Hibernus

The *Hibernus* approach has two states: active and hibernating. It moves between these states when the supply voltage (V_{CC}) passes thresholds (Fig. 4.1). It uses a hardware interrupt to detect when V_{CC} drops below V_H, then prompts a reactive hibernation – saving an immediate snapshot of volatile memory, then entering deep sleep. The snapshot is restored by another interrupt, when the supply voltage rises above V_R. The approach is illustrated in Fig. 4.2 and differs from Mementos, whose checkpoint locations are set in advance. Due to this, our approach is more energy- and time-efficient than existing approaches (experimentally demonstrated in Sec. 4.3), and does not depend on checkpoint placement heuristics.

Hibernus is application-agnostic and transparent to the programmer, because it can reactively hibernate at any time during the execution of an application. Therefore, to save a snapshot of system state, it copies all registers and volatile memory to NVM. The energy consumed by this process, E_σ, depends on the size of the volatile memory and the energy consumption for copying each byte.

$$E_\sigma = n_\alpha E_\alpha + n_\beta E_\beta \tag{4.1}$$

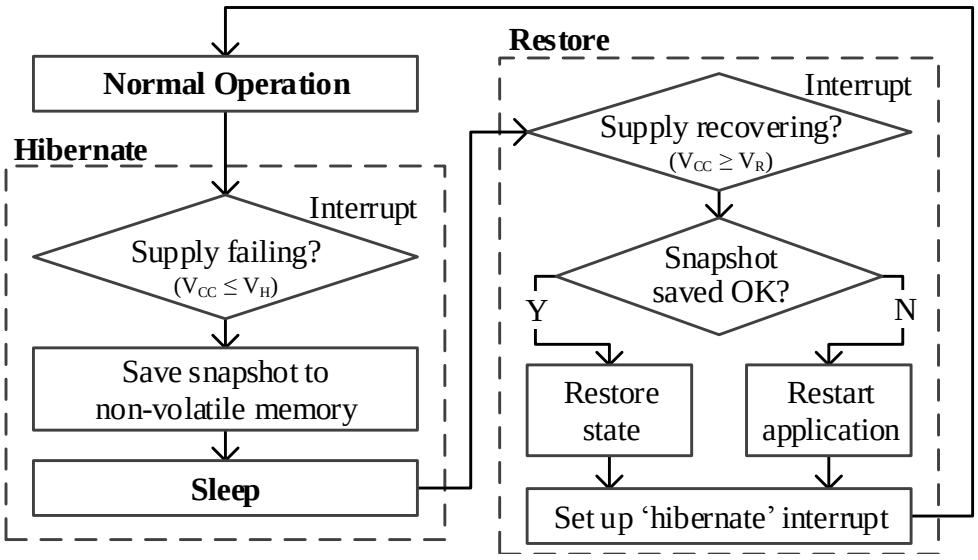

Figure 4.2: Flow-chart illustrating the *Hibernus* approach.

Here, n_α and n_β are the sizes of the RAM and registers (in bytes). E_α and E_β are the energy required to copy each RAM and register byte to NVM (J/byte).

Hibernus requires sufficient NVM to save the contents of all processor registers and RAM. This is the case with modern microcontrollers, e.g. [60]. It also requires enough energy to be stored in the capacitance between the supply rails to save a full snapshot. Energy harvesting systems normally operate across a range of voltages, from $V_{\min}$ to $V_{\max}$. Below $V_{\min}$, processors may operate unpredictably (brown-out), or shut down completely. Given the total capacitance ($\sum C$), the energy E_δ stored between a given voltage V and $V_{\min}$ is:

$$E_\delta = \frac{V^2 - V_{\min}^2}{2} \cdot \sum C \tag{4.2}$$

To ensure stability, V_{H} is set so that $E_\sigma > E_\delta$, to enable complete hibernation (even with a sudden loss of supply). V_{R} is set higher to add hysteresis, allowing the system to restore without taking the V_{cc} below V_{H}, even with sudden loss of supply. For small embedded microcontrollers (with relatively small n_α) using fast-write NVM (therefore relatively low E_α), it is possible to save a snapshot without additional C (using only the system's decoupling capacitance); this is

explored in Sec. 4.3. However, if $E_\delta < E_\sigma$ with $V = V_{\max}$, it will not be possible to guarantee that snapshots can be taken reliably, and extra C must be added.

The total time, T_{hibernus}, to execute a test algorithm with *Hibernus* is given by (4.3), where T_a is the CPU time required to execute the algorithm, n_ι is number of power interruptions (where $V_{\text{CC}} < V_{\min}$) per algorithm execution, T_s is the time required to save a snapshot to NVM, T_r is the time required to restore from NVM memory, and $\overline{T_\lambda}$ is the average time spent sleeping (after a snapshot has been saved but before $V_{\text{cc}} = V_{\min}$, and on power-up when $V_{\min} < V_{\text{CC}} < V_{\text{R}}$). The absolute limit of supply interruption frequency, f_ι, is $1/(T_s + T_r)$.

$$\underbrace{T_{\text{hibernus}}}_{\text{Total execution}} = \overbrace{T_a}^{\text{Algorithm}} + \underbrace{n_\iota}_{\text{No. interruptions}} \left(\overbrace{T_s}^{\text{Save snapshot}} + \underbrace{T_r}_{\text{Restore snapshot}} + \overbrace{\overline{T_\lambda}}^{\text{Sleep}} \right) \tag{4.3}$$

The total time, T_{mementos}, to execute an algorithm with Mementos is given by (4.4), where n_m is the number of checkpoints per complete execution of the algorithm, T_m is the time taken for an ADC reading of V_{CC}, and P_s is the proportion of checkpoints resulting in a snapshot, taking T_s.

$$\underbrace{T_{\text{mementos}}}_{\text{Total execution}} = \overbrace{T_a}^{\text{Algorithm}} + \underbrace{n_\iota}_{\text{No. interruptions}} \left(\overbrace{T_r}^{\text{Restore snapshot}} + \underbrace{\frac{T_a}{2n_m}}_{\text{Backtrack}} \right) + \overbrace{n_m(T_m + P_s T_s)}^{\text{Monitoring and save snapshot}} \tag{4.4}$$

Hence, $T_{\text{hibernus}} < T_{\text{mementos}}$ provided $n_\iota(T_a/2n_m) + n_m T_m + (n_m P_s - n_\iota)T_s > n_\iota \overline{T_\lambda}$; that is, *Hibernus* spends less time sleeping than Mementos spends on backtracks (re-running code that was executed between a snapshot and a power interruption), sampling V_{cc}, and redundant snapshot saves. This is evaluated experimentally in the next section.

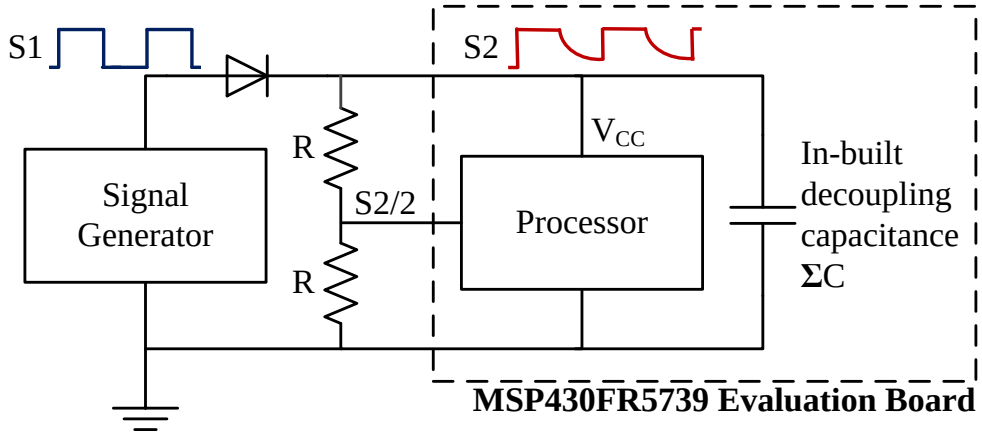

Figure 4.3: The test platform used to experimentally validate *Hibernus*.

4.3 Experimental Validation

Hibernus has been validated with an intermittent power supply and representative workload. Its energy and time overheads have been evaluated, and compared against Mementos.

4.3.1 Implementing Hibernus

While most microcontrollers have flash NVM (and consequently a high E_σ), processors are emerging that incorporate fast, low-power FRAM (and hence have a lower E_σ). The test platform (Fig. 4.3) uses a development board combining a Texas Instruments MSP430 processor [60] with FRAM. This means that its decoupling capacitance alone allows $E_\delta >> E_\sigma$ when $V = V_{\max}$, requiring no additional energy storage (battery or large capacitor) to support *Hibernus*. The approach will work with platforms with flash memory rather than FRAM, but this will significantly reduce the maximum supply interruption frequency and increase the energy overhead, potentially requiring additional capacitance on the supply.

The platform's datasheet parameters were inspected, and identified E_α as 4.2 nJ/byte and E_β as 2.7 nJ/byte, with a total RAM size of 1024 bytes and register size of 524 bytes. The platform operates with a $V_{\max} = 3.6\ V$ and

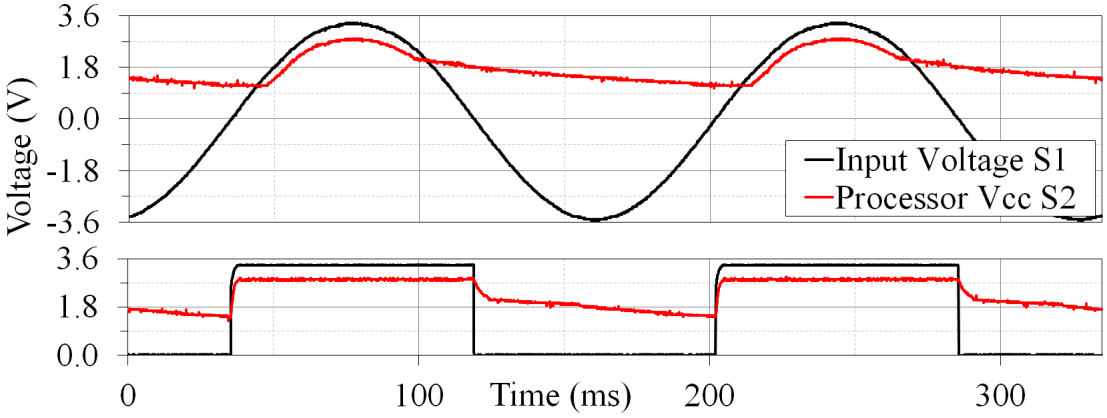

Figure 4.4: Measured behavior of signals *S1* and *S2* (Fig. 4.3) with (a) 6 Hz square-wave input; (b) 6 Hz sinusoidal input.

$V_{\min} = 2.0\ V$. Using (4.1), a complete operation copying all registers and RAM to FRAM consumes 5.7 μJ. The decoupling capacitance on the board totals $\sum C$ = 16 μF. Using (4.2), it was found that this alone is sufficient for *Hibernus* and V_{H} was set to 2.17 V. It was verified experimentally that this and V_{R} = 2.27 V delivered stable operation, even with sudden loss of supply at the beginning of a restore operation. The stability of the system is therefore unaffected by the dynamics of the power source. The test platform's V_{CC} input (*S2*) is connected to the output of a signal generator (*S1*) through a diode, which prevents back-flow of charge to the harvester (Fig. 4.3). The signal generator was selected to mimic a voltage-dominant source such as a typical RFID reader [58]. Traces (Fig. 4.4) with a peak amplitude of 3.6V are presented as examples. The slower decay of *S2* compared to *S1* is due to the input diode; the slow decay on the negative edge illustrates the discharge of the decoupling capacitance by the current drawn by the processor.

Hibernus functionality is contained within the `hibernus.h` library file; application developers need only include this library and call the `initialise()`, `hibernate()` and `restore()` routines, as illustrated in Fig. 4.5. As shown in Fig. 4.2, the algorithm requires that interrupts are generated when V_{cc} passes V_{H} and V_{R}; this is facilitated by comparators and voltage references. The test microcontroller has an on-chip comparator configured with an on-chip variable reference

```
#include "hibernus.h"

int main (void) {
  if (flag) restore(); //restore system state
    else initialise(); //initialise hibernus
  // application code goes here
}

__interrupt void COMP_D_ISR(void) {
  hibernate(); //save system state & sleep
}
```

Figure 4.5: Example code used for evaluation of *Hibernus*.

voltage generator (these are standard features on many microcontrollers), and an external voltage divider ($R = 200$ kΩ) giving $V_{cc}/2$, as inputs. This is set up in the `initialise()` routine. Dependent on whether the system is hibernating or active, the interrupt is set to trigger off either $V_{cc} \leq V_H$ or $V_{cc} \geq V_R$. The handler then calls `hibernate()` or `restore()`.

When `hibernate()` (Fig. 4.2) is called, it first pushes the core registers onto the FRAM memory. It then copies the entire RAM contents (stack segment, local and global variables) into the FRAM, followed by the general registers, and finally the Stack Pointer (SP) and Program Counter (PC). It then sleeps in a low-power mode. The system remains in sleep mode until $V_{CC} > V_R$. The `restore()` routine is then called and the complete previous system state is restored. The system phases the restore of the memory locations to reinstate its operating state reliably. The general registers are restored first, followed by the RAM, and lastly the core registers including the SP and PC. When the PC is restored from the snapshot, the system implicitly transfers to the application and resumes operation.

4.3.2 Experimental Setup

The evaluation test case represents a common long-running task for energy harvesting systems: a Fast Fourier Transform (FFT) analysis of three arrays, each holding 128 8-bit samples of tri-axial accelerometer data. The FFT algorithm was chosen as an illustration: *Hibernus* is application-agnostic and will provide the same functionality to any embedded program, with minimal impact on the application developer (see Fig. 4.5). Supply interruption frequencies f_ι (of 2, 4, 6, 8, 10 Hz, and DC) were chosen to represent the intermittent power output that may be expected from an energy harvester (e.g. micro wind turbine or RFID inductive power transfer). This has allowed *Hibernus'* overheads to be compared against Mementos. Due to the low output impedance of the signal generator, which allows the target voltage to be attained very quickly (figs. 4.3 and 4.4), and low current draw of the microcontroller, $f_\iota > 10$Hz results in the system being continuously powered.

Our implementation of Mementos places static checkpoints after function calls or before loops, referred to as 'function' and 'loop'. ADC (V_{cc}) measurements are taken and compared to a threshold ($V_{\text{m}} = 2.5V$), chosen for each scheme to ensure that a snapshot can be saved at least once before power failure. At each checkpoint, $V_{\text{cc}} < V_{\text{m}}$ indicates imminent power failure, and a snapshot is saved. Mementos consumes energy for multiple checkpoints, both for ADC readings and saving snapshots. In contrast, *Hibernus* consumes energy for a single hibernation per power-outage, plus the quiescent consumption of the voltage reference and comparator.

The power consumption at mid-range between V_{max} and V_{min} of the FFT algorithm (without *Hibernus* or Mementos running), ADC, voltage reference, and comparator were measured as 2.7 mW, 310 μW, 17 μW and 130 μW respectively. These values are used to estimate the energy consumption of the different approaches. For each of the three schemes, and at each frequency f_ι, we evaluated: (1) the number of system restores required to complete the computation of the FFT algorithm, (2) the number of times snapshots were stored, or checkpoints were called, (3) the energy overhead, and (4) the processor time overhead. The

results were averaged over three complete executions of the test program. The overheads are evaluated with reference to the time and energy for the processor to complete the FFT algorithm with a steady supply: without Mementos or *Hibernus*, it completed in 100 ms.

4.3.3 Results

Fig. 4.6(a) shows how many checkpoints were made by *Hibernus* and Mementos during a single execution of the FFT. As can be seen, *Hibernus* reduces the number of times that checkpoints are taken. This can also be seen from Fig. 4.7, which shows when *Hibernus* and Mementos checkpoint (for the case when $f_\iota = 6$ Hz), whereas *Hibernus* snapshots (hibernates) only once per interruption (twice in total), Mementos executes a static number of checkpoints (12 and 27 times), although some are repeated when $V_{\mathrm{CC}} < V_{\mathrm{min}}$ during a snapshot.

Fig. 4.6(b) shows that, at higher f_ι values, *Hibernus* completes execution of the FFT over fewer power interruptions (3, instead of 5). This is because the mean processor time overheads (Fig. 4.6(d)) of *Hibernus* are 80-100% shorter than Mementos (function), and 76-100% shorter than Mementos (loop); this leaves more time to execute the application (also shown in Fig. 4.7, where the arrows denote the total execution time). Furthermore, Fig. 4.6(c) shows that the energy overheads of running *Hibernus* are 65-79% lower than Mementos (function) and 49-76% lower than Mementos (loop).

The benefits of *Hibernus* are most noticeable at $f_\iota = 0$ Hz (i.e. DC, when V_{cc} is uninterrupted), where negligible time and energy overheads are imposed (see Fig. 4.6(c) and (d)), while Mementos still requires the same number of checkpoints. This increases the required processor active time and energy by at least 10% and 11% respectively. Table 4.1 shows experimentally obtained values for the parameters of (4.3) and (4.4). Evaluating these equations support our measured results, and confirm that *Hibernus* spends less time sleeping than Mementos spends on redundant snapshot saves, backtracks, and sampling V_{cc}.

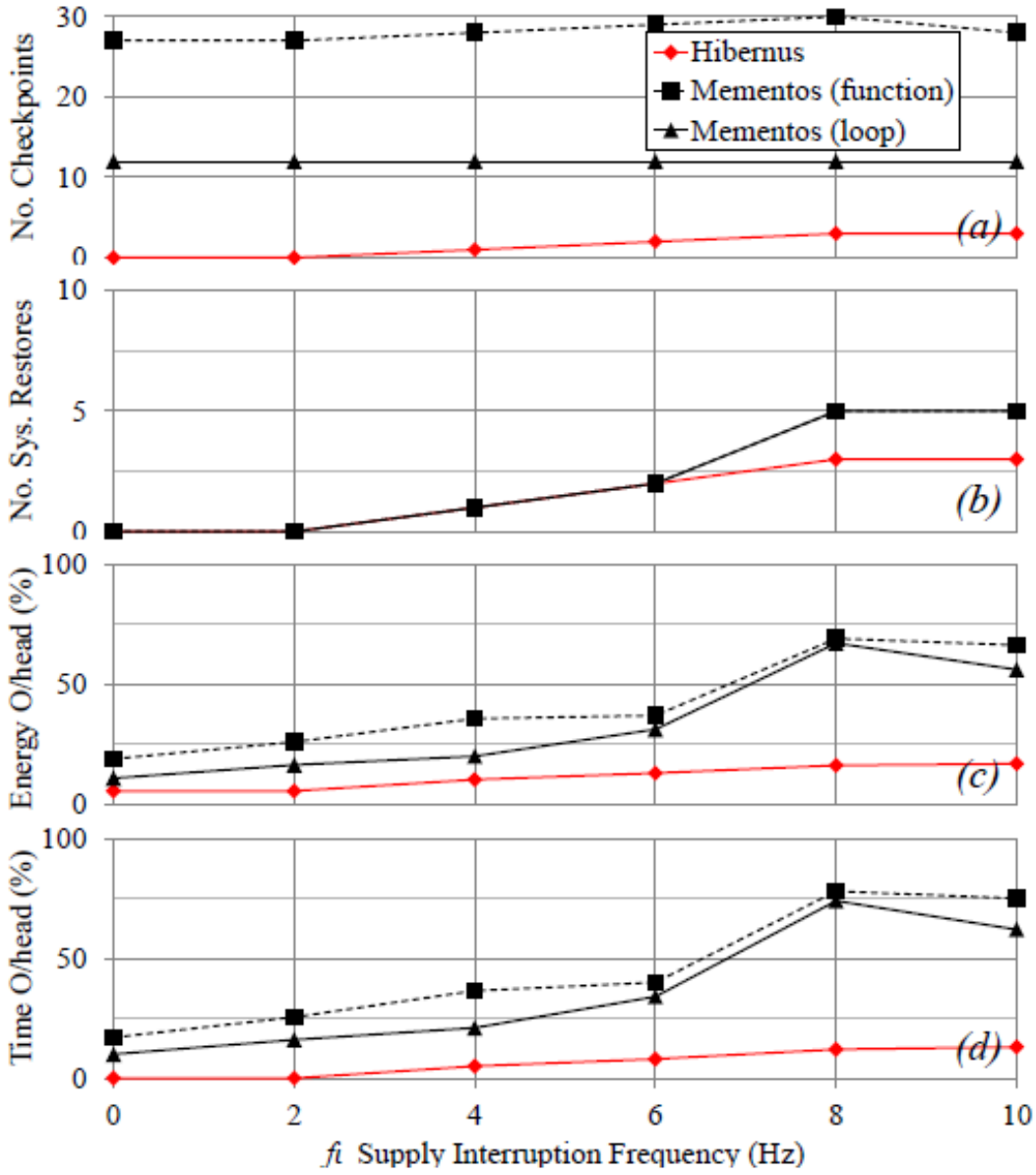

Figure 4.6: Comparison of *Hibernus* against Mementos, showing performance when running the FFT text program (averaged over 3 executions): (a) number of checkpoints/snapshot saves, (b) number of times snapshots were restored, (c) energy overhead, (d) time overhead.

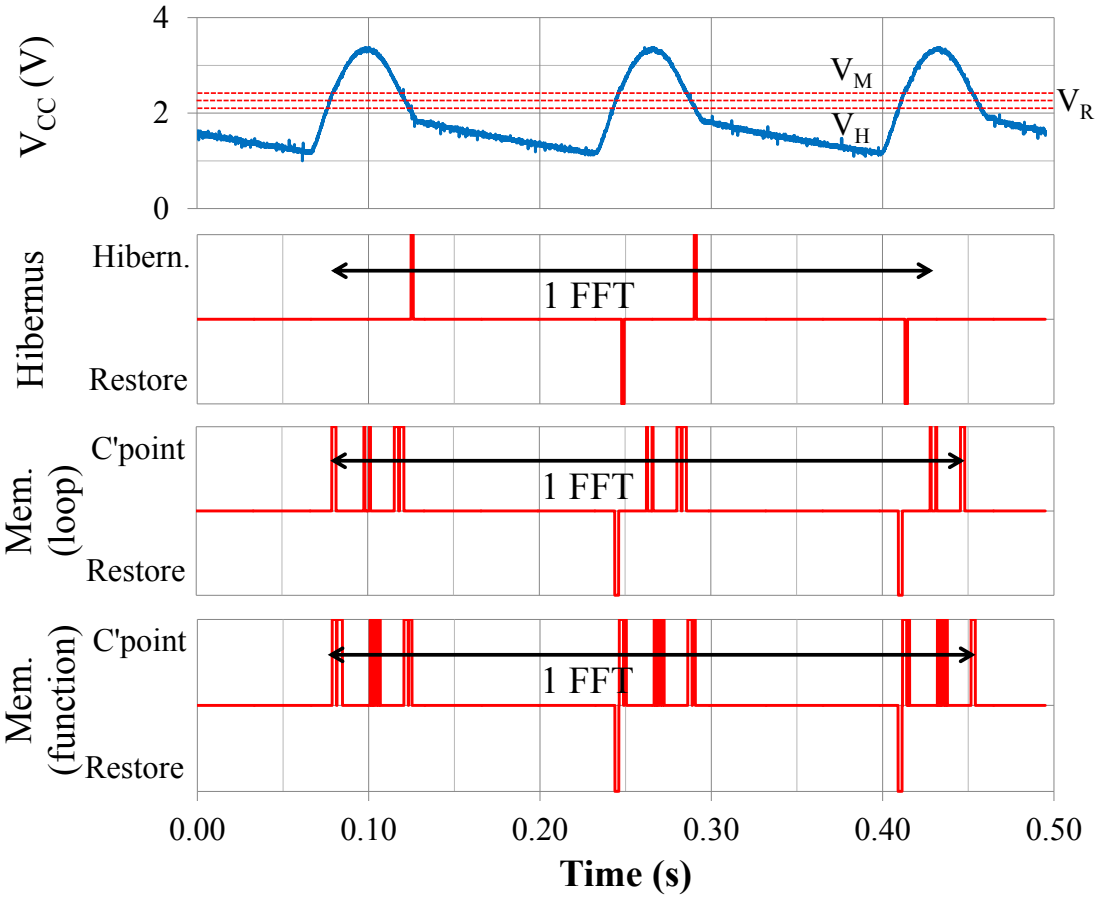

Figure 4.7: Results comparing when *Hibernus* and Mementos hibernate, checkpoint, and restore. Results shown were measured over a complete execution of the test FFT algorithm, powered by a sinusoidal supply with $f_\iota = 6$ Hz.

f_ι	T_a	T_s	T_r	T_m	T_λ	*Hib.*	*Loop*			*Function*		
(Hz)	*(ms)*	*(ms)*	*(ms)*	*(ms)*	*(ms)*	n_ι	n_ι	n_m	P_s	n_ι	n_m	P_s
0	100	2.85	2.2	0.65	-	-	-	12	0.00	-	27	0.00
2	100	2.85	2.2	0.65	17	0	0	12	0.08	0	27	0.11
4	100	2.85	2.2	0.65	9.5	1	1	12	0.25	1	27	0.19
6	100	2.85	2.2	0.65	6.5	2	2	12	0.50	2	27	0.33
8	100	2.85	2.2	0.65	3.8	3	5	12	1.00	5	27	0.70
10	100	2.85	2.2	0.65	2.8	3	5	12	0.83	5	27	0.67

Table 4.1: Experimentally measured parameters (see equations (4.3), (4.4)).

4.4 Conclusions

A new approach for sustaining computation during intermittent supply, *Hibernus*, has been proposed. This allows a system to sustain computation through power outages which are common in energy-harvesting systems. It has a lower energy and time overhead than a recently proposed scheme, as demonstrated experimentally. This contributes to the development of future energy harvesting systems. Our continuing work is investigating performance with real energy harvesters, rather than the voltage-dominant sources evaluated here.

Chapter 5

Monitoring of Historical Buildings using WSNs

Historic buildings are a distinctive and invaluable characteristic of numerous European cities, and living symbols of Europe's rich cultural heritage. Monitoring the structural health and the local climate of historical heritage buildings can be an hard task for civil engineers due to the lack of a pre-existing monitoring model and difficult installation constrains. Wireless Sensor Networks (WSNs) are a valid alternative for monitoring and improving the energy efficiency of historic buildings.

This Chapter presents the experience gathered during an European Project (3ENCULT Project - Efficient Energy for EU Cultural Heritage) related to the design and implementation of an innovative WSNs for monitoring heritage buildings. In more detail, we will introduce a long-term and low-cost distributed environmental monitoring system, which promotes energy-efficient retrofitting in historic buildings.

We have been focused at developing a new hardware and software solution to efficiently satisfy the requirements for long-term monitoring of an historical building, called 'Palazzina della Viola', and located in the centre of Bologna, Italy. The presented system provides real-time feedback for civil engineers, which can retrieve sensed data using remote interfaces.

Based on 7 months of operation, we show that the proposed solution, compared with other standard monitoring systems, is an effective low-cost alternative tool for assessing the environmental monitoring in heritage buildings. The system allows a reliable data transfer and we estimated the lifetime beyond two years.

5.1 Introduction

Historic buildings are often characterized by their extraordinary architecture, design and materials. The conservation of this buildings for future generations is one of the main tasks of the European Union (EU). It is therefore very important to understand the deterioration processes, which affect artworks in museums and historical buildings [61, 62].

Structural and environmental monitoring are fundamental for protecting our heritage from degradation and to obtain more detailed information about the deterioration processes, and real-time monitoring systems represent a valid solution for this purpose.

However, most of the monitoring systems currently deployed are only capable of weather data acquisition and they use basic models for data analysis. Furthermore, most of the commercial systems require cabling, which is neither aesthetically appealing nor applicable in all cases due to the necessity of fastening techniques. This is particularly significant for historical monuments and other cultural heritage.

Wireless Sensor Networks (WSNs) enable a radically different solutions overcoming the above limitations [63, 64]. Historical buildings require periodic observations for assessing their health both during normal operations and during potentially damaging events, such as an earthquake. Moreover, a continuous monitoring of environmental conditions is required for a proper conservation of frescoes, paintings and artworks [65].

In this way, intelligent monitoring of structural health has become an important research topic mainly because of the lack of pre-existing monitoring models and to the constraints associated with the measurement devices.

Today, it is possible to easily obtain prototypes with low-cost manufacturing, and miniaturized smart sensor nodes, which can be easily configured for monitoring purposes. The challenge is however the ability to allow these nodes to operate in a collaborative way over a long period of time without user intervention.

Environmental parameters such as temperature, relative humidity, and light should be as much constant as possible, avoiding abrupt variations and within well-defined ranges suggested by experts. In this context, WSNs can provide pervasive and continuous tracking of the micro-climate in historical buildings, where frescoed walls often refrain the deployment of cables and dangerous conditions should be detected as soon as possible.

This Chapter presents the experience maturated during a 3ENCULT European Project regarding the design and implementation of a WSN for environmental monitoring of heritage buildings. We present the network solution developed to efficiently satisfy the requirements for long-term monitoring of a historical building. We will present an application scenario and the strategies for a rapid, accurate and low-cost intelligent monitoring. The selected hardware allows low-power consumption and long-distance peer-to-peer data transmission. An integrated prototype has been deployed in a 36 wireless sensor nodes test-bed in a 4-storey renaissance building, called 'Palazzina della Viola', and located in the centre of Bologna, Italy.

5.1.1 Palazzina della Viola

A XVI century building it is now an important structure and working area for the University of Bologna of about 1.300 m^2. The area hosts several employees who annually interact with thousands students. The 'Palazzina della Viola' building and some of the frescoes are shown in Figure 5.1. After the refurbishment, post-intervention diagnoses are regularly performed in this building and they are used to evaluate the strategies to improve both user comfort and energy efficiency.

The preservation of the frescoes represents the main concern for these kind of historical buildings. The timely estimation of potential risks to the frescoes requires a real-time monitoring and an appropriate response model, to understand

Figure 5.1: Palazzina della Viola

the structural behavior of this building [66].

5.1.2 Contribution

In this Chapter, we will present our hardware and software solution developed to efficiently monitor each local climate variations in the building and we will discuss about the implementation of a network to guarantee a long-term autonomy to the installation. Specifically, the WSN is composed of wireless sensor nodes (W24TH model), which collect information about air temperature, relative humidity, vibration, air quality and ambient light, and deliver data using multi-hop wireless routing.

The hardware core of each W24TH node in the network is based on NXP JN5148 Microcontroller (MCU) [47]. In addition, the gateway can send e-mails to the building staff if the environmental parameters exceed the adjustable thresholds. A special focus is dedicated to the software system, which manages the wireless sensor nodes. This software is proprietary and adapted especially for long-term, and low-power operation. It consists of a boot-loader function, which is responsible for radio transmission and for the joining of the nodes, and for over-the-air software updates.

On top of the boot-loader a specific application is implemented, which is responsible for the acquisition, conversion and preprocessing of data before transmission.

Deployment details such as the placement of the wireless sensor nodes are then presented. Moreover, we will compare the results obtained with about our WSN and alternative or traditional monitoring instruments.

5.2 Background

The small size of wireless sensor nodes makes WSNs a winning strategy for observing activities and monitoring the environment in buildings that contain artworks and frescoes in which the visual impact of the instrumentations must be limited.

WSNs are usually deployed to acquire both structural and environmental data. However, these two application contexts have different requirements and constraints [67, 68, 69]. In structural monitoring, nodes are mainly placed where the structure is damaged. The main challenge is how to collect, process and deliver the structural and deformation measurements. In general, these measurements are acquired with high sampling rate and high precision, but only for a relatively short-time and periodically repeated.

Conversely, the wireless sensor nodes used in environmental monitoring have to measure long-term critical environmental parameters, which are used to understand the health of artworks and frescoes. Environmental monitoring applications are then designed for low-power and long-term operation.

Many applications have been carried out in recent years such as the 'Villa Regina' [70] case study in Turin and the 'Torre Rognosa' [71] in San Gimignano, Italy. In the first case, an historical Savoy residence, the main aim was to evaluate the reliability of a WSN for protecting and preventing oxidation of old mirrors. The network topology used was simple and the researchers were focused on finding the right position to provide data with high accuracy.

The deployment of San Gimignano was focused on the conservation of the structure, monitoring the parameters which can be considered critical such as temperature, humidity, light and structural information about masonry cracks.

Another notable deployment has been carried out in the last years: the system deployed in Torre Aquila [72], a medieval tower in Trento (Italy), where a cus-

tomized hardware collects efficiently high-volume vibration data and specially-designed sensors acquire the building's deformation. In addition, this system includes a dedicated software services, which provide data collection, data dissemination and time synchronization with low-memory demands.

However, in all presented systems the implementation lacks of the support for time synchronization (Chapter 3) and low-power operations, hampering their use in long-term deployments.

The lifetime of WSNs largely depends on the power consumption of every wireless sensor node and an efficient power management may result in a longer network lifetime (Chapter 2).

Our goal is to reduce consumption both when the node is in active mode by optimizing radio activity through a synchronous power management strategy and when the node is in sleep mode with the presented dynamic power control algorithm.

5.3 Hardware Design

The architectural diagram and the pictures of the wireless sensor node are shown in Fig. 5.2. The node is built on the top of an NXP module, placed on the sensor board, together with several sensors connected to it. The power unit contains two primary batteries, but can be also powered with energy harvesting.

5.3.1 Node Platform

. The core of the sensor node is a NXP JN5148 module, which is an ultra-low-power and high-performance wireless microcontroller, targeted at ZigBee PRO networking applications. The device features an enhanced 32-bit RISC processor, a 2.4 GHz IEEE 802.15.4 compliant transceiver, 128 kB of ROM, 128 kB of RAM and several analogue and digital peripherals.

Compared to other similar platforms (e.g. TelosB [73]), it can reach a better power saving (e.g. more than 35%). Moreover it can be equipped with energy harvesting systems from multiple environmental sources [74, 75, 76, 77].

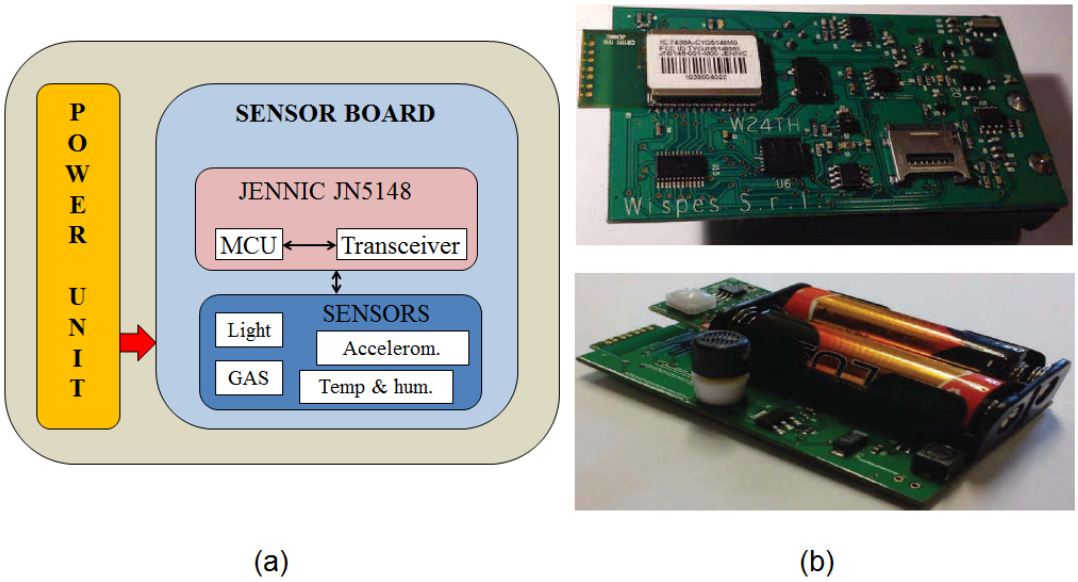

Figure 5.2: Sensor node used for environmental monitoring. (a) Block architecture. (b) Top side and bottom side.

The power consumption of this node is 15 mA for transmission (TX) and 18 mA for reception (RX). The board has several sensors such as a 3-axis accelerometer sensor, temperature and humidity sensor, an ambient light sensor and MOX gas sensor. Each sensor has a specific front-end circuit, which is useful for different environmental monitoring applications. A MicroSD card is also on-board for local back-up, data logging and firmware updating.

Moreover, each node equips a USB battery charger, an external local oscillator and a power management subsystem.

The power management subsystem provides the possibility to switch OFF the whole system, by enabling a consumption of less than 10 uA, when the system is in sleep mode.

5.4 Software Design

Zigbee PRO protocol is considered a standard technology for WSNs. However, the current status of this specification still suffers because of low-flexibility for

different network topologies such as cluster, tree or mesh topologies and it presents several limits when used for kind different applications.

The current IEEE 802.15.4 MAC layer uses two types of channel access mechanisms based on slotted carrier sense multiple access with collision avoidance (CSMA-CA) algorithm and un-slotted CSMA-CA algorithm [78]. The first type is operating in beacon-enabled mode with synchronization, while the second one is operating in a non-beacon enabled mode without synchronization. The non beacon-enabled mode does not provide the time synchronization, while it has the features of high scalability and low complexity. Thus, it can not support the active/sleep scheduling and Guaranteed Time Slot (GTS) mechanism.

On the other side, it is possible to achieve a very low duty-cycle in the beacon-enabled mode with time synchronization, by exploiting the GTS allocation mechanism and using the super-frame structure. Therefore, it is suitable for WSNs applications with stringent energy requirements, to operate in the beacon-enabled mode, but the beacon-enabled mode also has the problem of low scalability, since the super-frame structure of IEEE 802.15.4 MAC is normally operated only in star-based networks.

5.4.1 Network Solution

In the context presented above, we have developed an Energy-efficient Service-Packet-based (ESS) transmission algorithm, which provides a time synchronization by using non beacon-enabled IEEE 802.15.4.

Moreover, this algorithm avoids collisions during the data packets transmission through a Time Division Multiple Access (TDMA) technique where each node in the network transmits information in a given time slot.

The Service-Packet contains several information, including data for time synchronization as well as the sequence of active sensors for all receivers. The transmission of the Service Packet across the network is performed by using a novel approach based on a constructive interference of IEEE 802.15.4 symbols for fast network flooding and implicit time synchronization [80]. This approach considers interference an advantage rather than a problem. Specifically, simultaneous trans-

missions of the same packet (Service Packet) constructively interfere by allowing receivers to decode the packet even in the absence of capture effects.

In this way, it achieves a flooding reliability above the 99% and it approaches the theoretical lower latency bound across different node densities and network sizes. Moreover, this technique provides network-wide time synchronization, since it implicitly synchronizes nodes as the flooding packet propagates through the network.

Using this approach, wireless sensor nodes turn on their radios for the communications over the wireless medium and transmit overheard packets after a certain time delay.

Since the neighbours of a sender receive a packet at the same time, they also start to transmit the packet at the same time. This approach again triggers other nodes to receive and transmit the packet.

Basically, this approach benefits from concurrent transmissions of the same Service Packet by quickly propagating it from the coordinator (source node) to all other wireless sensor nodes in the network. Each node can transmit a finite number of Service Packet by decrementing an internal and local counter. Consequently, each node can infer from the counter how many times a received packet has been relayed.

Moreover, it is possible using the same approach presented above to perform the over-the-air software update. The coordinator collects the information about Link Quality (LQ) from nthe odes and then makes up the virtual topology map of overall network and assigns to each node a specific time slot. In this way, the coordinator defines the right configuration as a trade-off between the network topology and the energy efficiency.

Summarizing, the entire activity of our network is carried out between two Service Packets. Each Service packet is transmitted over the network by exploiting a constructive interference of IEEE 802.15.4 symbols for fast flooding and time synchronization. The coordinator define the network topology and the time slot of each node according to the LQ. Each node transmits through multi-hop radio link solution the data packet to the coordinator in a specific time slot.

5.4.2 Dynamic Power-supply control and TCA Time Synchronization

In this deployment, we have been focused on reducing consumption by keeping the network synchronized with the node in active mode, optimizing the radio activity, by using a synchronous power management strategy presented in the previous subsection and by using the low-overhead and local clock synchronization based on a the presented temperature compensation algorithm (TCA) (Chapter 3).

Moreover, we have been focused on reducing consumption when the node is in sleep mode by implementing a dynamic power-supply control algorithm, which minimizes the use of the DC-DC converter presented in Chapter 2.

The proposed solutions significantly increase the lifetime of this network, achieving in the performed test a lifetime increment of 30%. In this way, the system allows a reliably data transfer and has an estimated lifetime beyond two year.

5.4.3 WSN Coordinator and Web Interface

The coordinator is responsible of two main activities: it has to manage the sensor network by coordinating wirelees sensor nodes, keeping them synchronized, arranging transmissions and reorganizing the network when new nodes enter or fail. On the other side, it is in charge of collecting data from the network and delivering the date and information to a database. The coordinator used in our deployment have the same hardware architecture of the other nodes but it is connected, via UART, to a mini-computer, which permits to access to the Local Area Network. Two different processes run simultaneously on the coordinator: the first process manages the whole network and gather data from the nodes, while the second one connects the coordinator to the database for storing data. The database is a fundamental block of a heritage monitoring system: data need to be properly stored, and the users should be able to retrieve the historical values even after a few months or years, for statical purposes or for scientific aims.

We have decided to use the Catcti front-end for network graphing solution.

Cacti is a complete front-end to RRDTool, which stores information to create graphs with data in a MySQL database. Cacti is usefull to maintain Graphs, Data Sources, and Round Robin Archives in a database and it also handles the data gathering. For instance, in Fig. 5.3 are shown the data relating to acceleration, relative humidity, light and temperature collected in the week from 16/05/2013 to 23/05/2013 from a single node within the 'Palazzina della Viola' building. Of course, the amount of energy for receiving and forwarding is still not negligible. In this way, advanced algorithms can be used to reduce the amount of data through the network. For this purposes, we are considering to use compressive sampling, which is one possible technique for minimising expensive data transmissions [81].

5.5 Deployment

The 'Palazzina della Viola' building contains four floors: the underground that is used for different services, the ground floor and first floor that are occupied by about 40 employees, and, finally, the attic that contains the electric generators.

5.5.1 Node placement

As shown in Fig. 5.4, the network consists of 36 nodes distributed on different building floors. In this way, it is possible to acquire data from the whole building. The sensors are arranged in a static positions, except for 6 sensors, which are located in the large hall and front loggia.

These rooms present both frescoes and are located on the first floor of the building. The 6 nodes can be used as mobile stations in order to carry out specific measurement campaigns.

The sensors position is carefully chosen to detect several variables (light, temperature, humidity and vibration), which are useful for civil engineers to verify several aspects such as: light distribution in different rooms with both natural or artificial lighting or to evaluate the impact on artworks and frescoes; vibration measurements during and after structural and energetic refurbishment and, finally, the changes of the air flow between rooms of different volumes and heights.

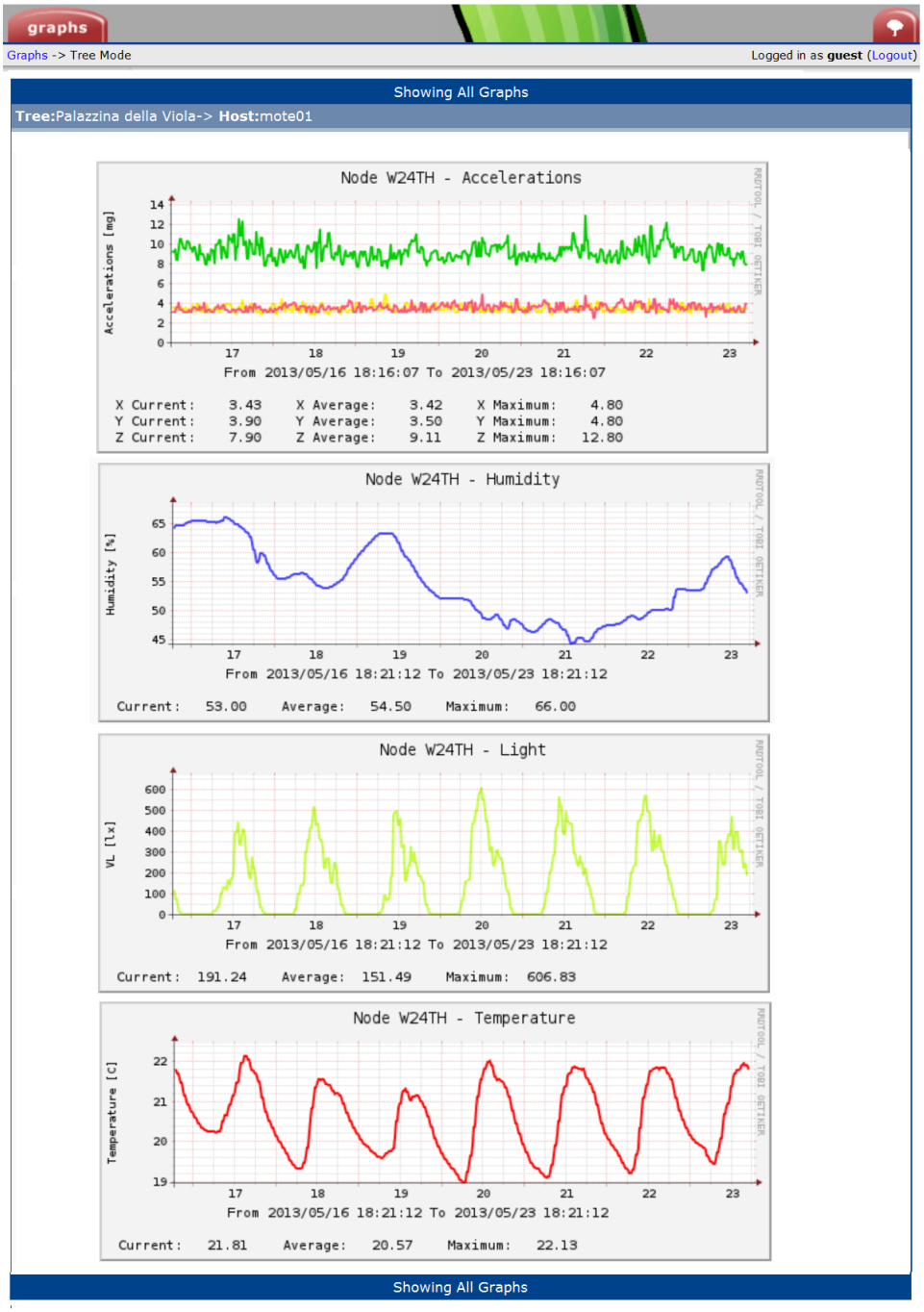

Figure 5.3: Acceleration, humidity, light and Temperature shown through the Graphical User Interface.

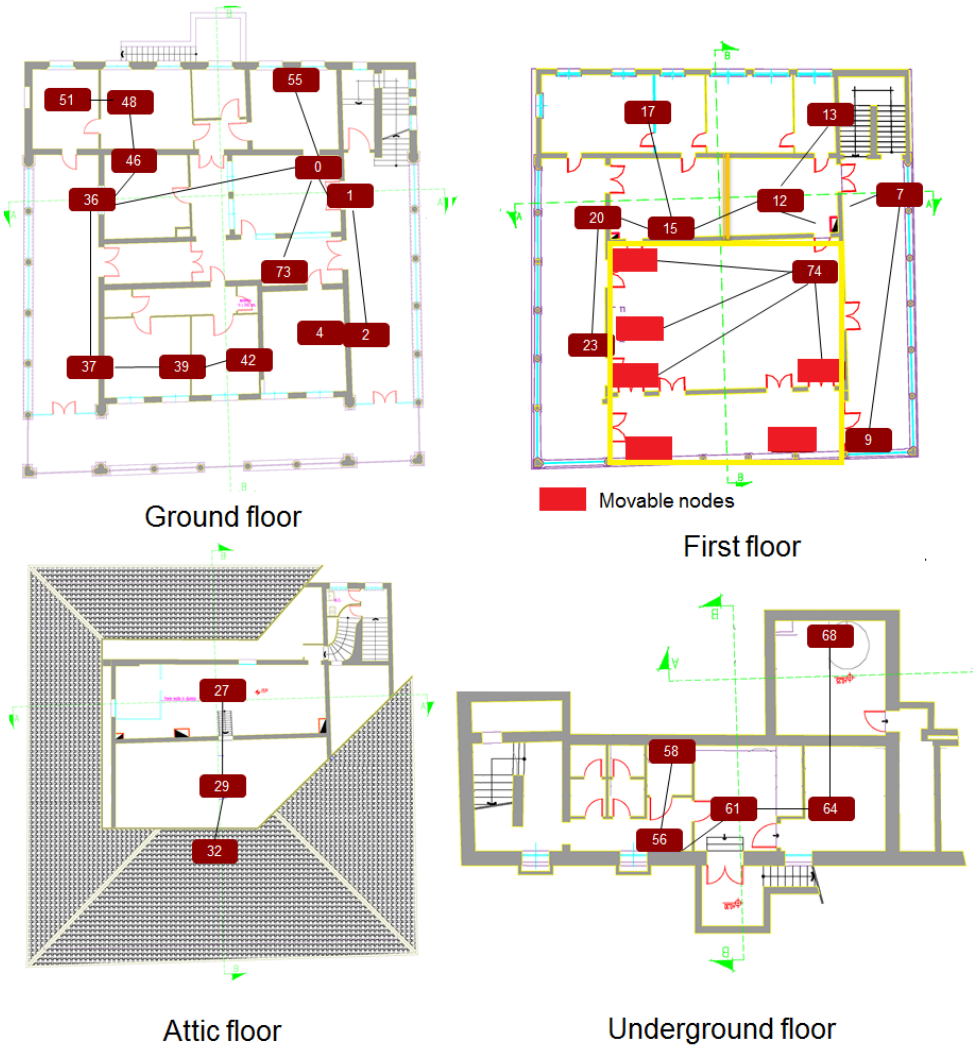

Figure 5.4: Deployment map.

An extensive experimental work was carried out by civil engineers. This work includes several survey campaigns aimed to investigate the environmental and structural conditions of the 'Palazzina della Viola' building. In the following, some examples of methodology survey conducted by civil engineers, using our WSN and, specifically, the dynamic 6 nodes placed on the first floor. This survey is conducted to compare dynamic wireless sensor monitoring in combination or in alternative to traditional climate structural testing. In Fig. 5.5 are shown the 28 fixed points for environmental and structural monitoring the temperature in

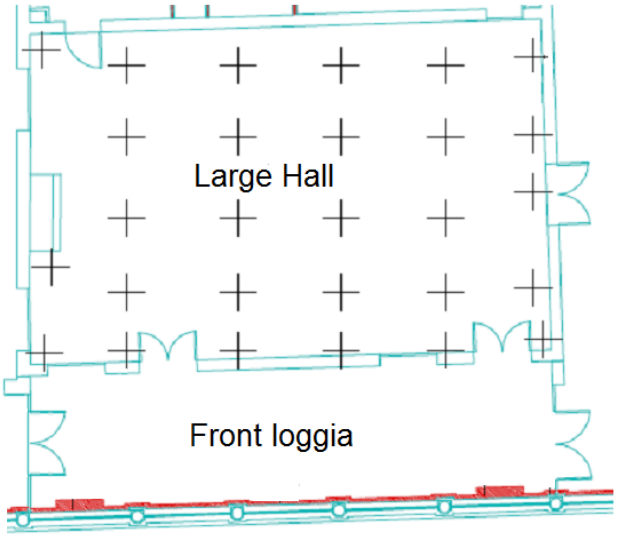

Figure 5.5: 28 Fixed points for temperature monitoring.

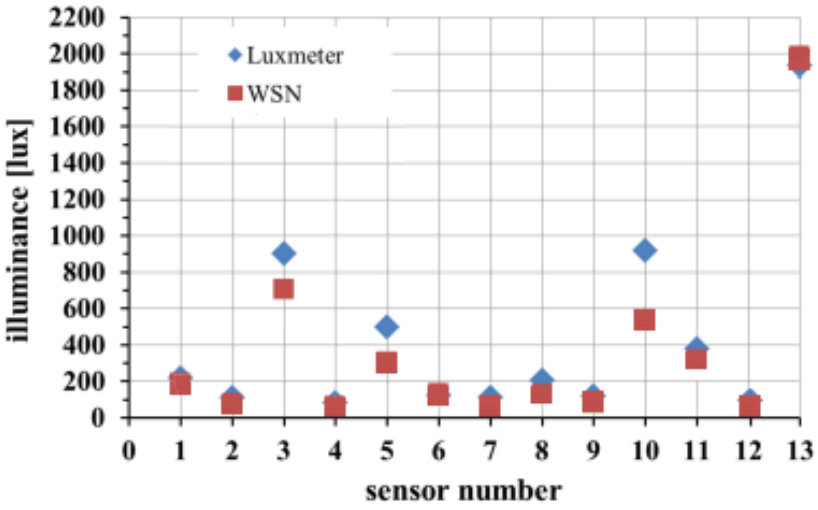

Figure 5.6: Illuminance values measured through both lux-meter and our WSN.

the large hall, using the 6 dynamic node.

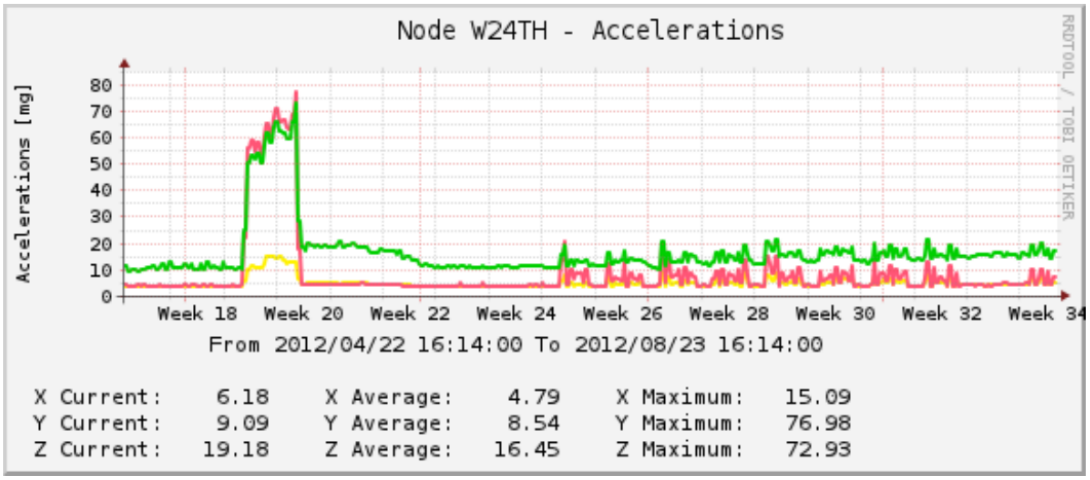

Figure 5.7: Example of acceleration, measured through WSN node, during refurbishment operations.

5.5.1.1 Light distribution.

In Fig. 5.6 is presented the illuminance measures inside the Large Hall room by using both professional lux-meter and 13 WSN nodes. The data are obtained from the dynamic node at the same time of the lux-meter. The obtained results highlight how our nodes, equipped with light sensor, exhibit an average error of 5%. Thus, they can be used in place of a professional lux meter in order to continuously monitoring the daily or seasonal variations of ambient light.

5.5.1.2 Vibration levels testing during refurbishment

The restoration and refurbishment interventions cause structural stress to the building. Moreover, buildings are also undergone to strong vibrations during natural events such as wind gusts, storms and earthquakes. The analysis of vibration level is useful to evaluate the impact on the building and then, to preserve artistic and valuable decorations.

Typically, structural problems such as cracks in masonry walls are monitor through crack meters positioned near the cracks. However, this approach requires several demanding tasks both during the installation of the instrument and during

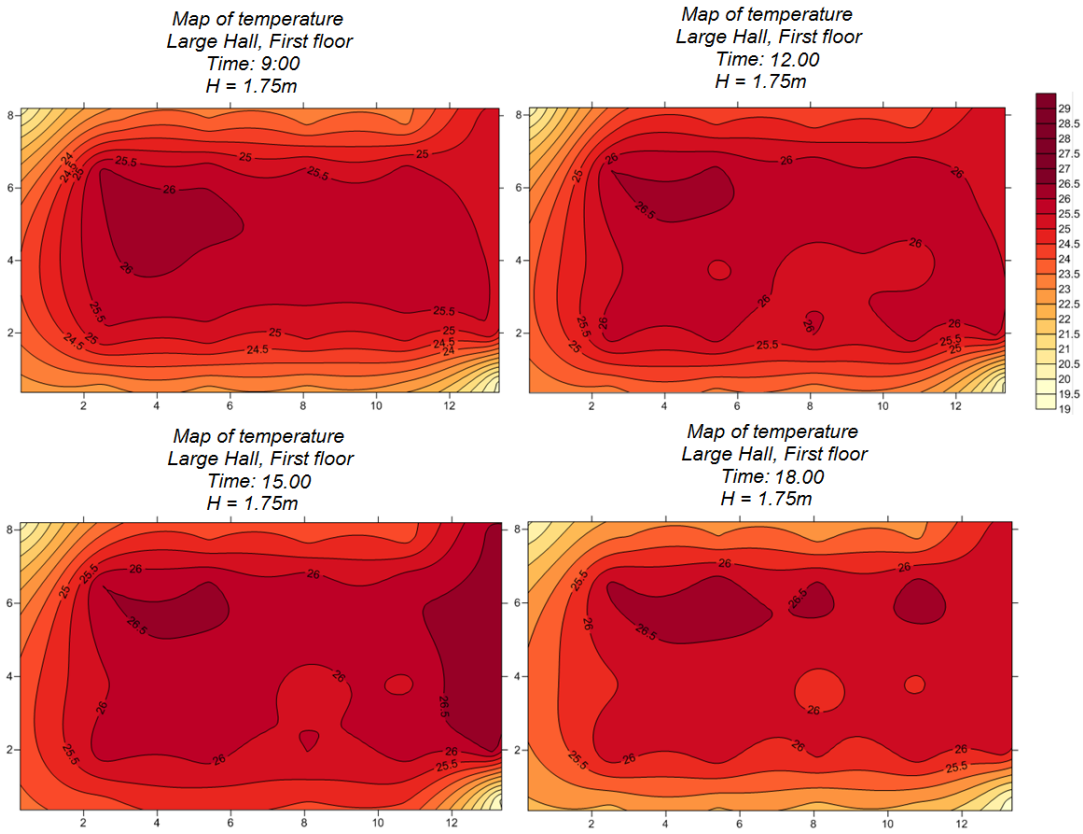

Figure 5.8: Air temperature map at 1.75m height, collected in May 2012 in the Large Hall.

the data readings. Our WSN allows to substitute crack meters by using nodes equipped with accelerometer sensors. In this case the installation is fast and the data are periodically read without any risk to introduce error (i.e. human error) like in the manual measuring.

Furthermore, the accelerometers not need to be placed across the crack because the vibrations can be collected in proximity of each accelerometer. Fig. 5.7 shows an example of vibrations detected during refurbishment operations.

5.5.1.3 Air temperature distribution

The temperature measurements were made to a height of 1.75m from the ground. The civil engineers have compared the temperature values obtained in four dif-

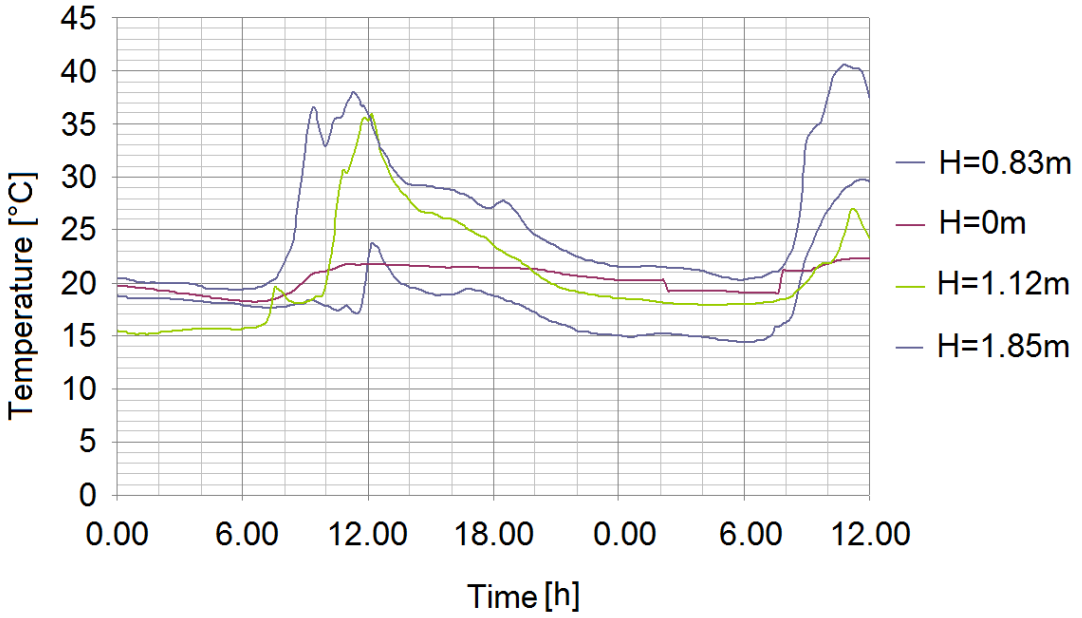

Figure 5.9: Variations of air temperature in a fixed point with different heights in the Front Loggia.

ferent times of day in May 2012. The maps shown in Fig. 5.8 were obtained by moving the 6 nodes in the 28 different positions.

By comparing the results obtained through the nodes of the WSN with a traditional monitoring system (portable instrument), the civil engineers have verified that the results obtained are similar. However, the advantage to use a WSN is that do not require the presence of a technician and a particular measuring instrument for each kind of measurement.

Finally, Fig. 5.8 shows the temperature values obtained over a period of 36 hours with differences in heights compared to ground. In this case, they have used 4 nodes placed at different heights (0, 0.83, 1.12, 1.85 meters) and located near one of the windows of the front loggia. In this way, it is possible to estimate the distribution of temperature at different levels at the same time of the day. As expected, with increasing height, the temperature increases at higher floors confirming a flow of heat from the bottom to the top of the loggia. These discrepancies in the hygro-thermal behaviour of the building obviously affect the comfort of the inhabitants and influence the energy efficiency of this building.

5.6 Conclusion

Continuous monitoring of environmental parameters is crucial for protecting cultural heritage and historical buildings. For this kind of activities, Wireless Sensor Networks represent an alternative to traditional measuring instrumentation. This Chapter describes the development of a technological Wireless Sensor Network tailored to monitoring heritage buildings. The deployment efficiently guarantees long-term monitoring and a high rate of data extracted from an historical building, called 'Palazzina della Viola'. Experimental results show the performance of the preliminary deployment of the network. The proposed WSN includes functionalities for network management and efficient power supply management and provides real-time feedback for the civil engineer. Based on 7 months of operation, we demonstrated that the system is an effective tool for assessing the environmental monitoring in heritage buildings. The system allows a reliably data transfer and has an estimated lifetime beyond two year.

Chapter 6

Low-cost Power Meter for Monitoring Residential and Industrial appliances

The recent research efforts in smart grids and residential power management are focused on pervasive monitoring of power consumption in smart buildings. Real-time monitoring of electric appliances is important to minimize the power wasted and the overall energy cost.

Energy efficiency in smart buildings is mainly oriented to distributed sensor applications, which monitor the power consumption of appliances in industrial, commercial and domestic scenarios. In this context, Wireless Sensor Networks (WSNs) represent a key technology for future smart building applications.

In this Chapter we present an innovative Non-intrusive Wireless Energy Meter(NIWEM) for measuring the current, voltage and power factor developed in collaboration with Telecom Italia s.p.a.

The analysis of current and voltage waveforms is fundamental for diagnostics about power quality. Moreover, it enables Non-intrusive Load Monitoring (NILM), which consists in analysing the voltage and current changes, and recognize the appliances that have been used as well as their individual power consumption from a household's total electricity consumption.

As a key feature, the NIWEM is completely non-invasive and it can self-sustain its operations by harvesting energy from the monitored load. Two primary batteries are only used as a back-up power supply and to guarantee a fast start-up of the system. An active ORing subsystem automatically selects the suitable power source, minimizing the typical power losses of a classic diode configuration.

The node harvests energy when the power consumed by the device under measurement is in the range of 10W÷10 kW, that also corresponds to a range of current of 50mA÷50A, which are directly drawn from the high-voltage line.

Finally, the node features a low-power, 32-bit microcontroller for data processing and a wireless transceiver to send data via the ZigBee PRO standard protocol.

6.1 Introduction

In recent years, the efforts of the scientific community, in the field of electrical energy distribution and management, have moved in two directions, namely Smart Grids and Smart Metering. The driving factor is the constantly increasing demand of energy from industrial, commercial and domestic customers, while the available energy resources are going to be exhausted.

Moreover, an irresponsible usage of the electrical energy and the poor quality of the power transmission line determine waste of energy and low reliability of these distribution systems. All these reasons lead to envision of a new and intelligent way to produce, distribute and use the energy.

The term Smart Grid, coined by [83], refers to the usage of the Information Technology for the power grids of the future, which will integrate the existing power generation systems with large and small scale production of energy from renewable sources.

Concurrently, innovations have been also addressed from the side of consumers. Smart Metering is one of the most important way to promote accurate management of the power resources and to grow a new awareness about the energy cost. For instance, as reported in [84], measuring and profiling of the power

consumption of every appliance helps to reduce waste of energy.

In this context, Wireless Sensor Networks (WSNs) and energy harvesters play a crucial role. Indeed, both Smart Grids and Smart Metering applications require distributed and real-time systems for monitoring the main elements of a power grid and user's appliances [85]. In fact, the next-generation of measurement systems should have a small-form factor and it should be non-invasive, easy-to-install and cost-effective in terms of production and maintenance, because of the large number of expected measuring points.

Since wireless sensor nodes and standalone embedded systems usually are battery powered, energy harvesting capability is becoming a critical requirement to reduce costs of battery replacement. Energy Harvesting technologies have gained increasing interest over the last years and, in particular, for powering embedded systems with the energy obtained from the surrounding environment [86, 87].

In general, a power monitoring system consists of current and voltage sensors because the analysis of such waveforms is important to promote accurate management of resources, to grow new awareness about the cost of energy, to carry out diagnostics about the power quality and to avoid waste of energy. In addition, the use of smart meters that measure and communicate electricity consumption enables the development of new energy efficiency services. Some promising applications involve the disaggregation of individual appliances from a household's total electricity consumption. In particular, smart meters enable Non-intrusive Load Monitoring (NILM) [102, 103]. Smart meters with NILM technology can be also used by utility companies to survey the specific usage of electric power in different scenarios and they are considered a low-cost solution to observe the general state of household's appliances.

In this Chapter we introduce an innovative Non-intrusive Wireless Energy Meter (NIWEM) with self-sustainable capability for smart metering applications.

It embeds two clamp-on Current Transformers (CT): one is used for the measurement of the current consumption and the second one to harvest energy directly from the high-voltage line. The clamp-on transformers are non-invasive sensors because they wrap around the power cable and make the node very easy-

to-install. The voltage is measured using an innovative non-invasive voltage sensor, which exploit coupling-capacitive elements. This new approach does not require any electrical contact to the mains, which makes the measurement much safer. It measures power consumption from 10W up to a maximum amount of 10kW.

The key feature of this sensor node is the energy harvesting subsystem, that scavenges energy from the whole range of measurable currents, making the sensor node fully autonomous. Two primary batteries are only provided as a back-up energy source to avoid unexpected shut-down, when the appliances are not powered and to guarantee fast start-up operations. One of the two power sources is automatically selected using an active ORing system. This active configuration, based on MOSFETs with very low on-state resistance, reduce the voltage drop and the power losses compared to the diode-passive topology.

The data from the current transformer and the voltage sensor are processed by a low-power, 32-bit microcontroller and transmitted using ZigBee PRO standard with Home Automation profile.

In the next two Sections (Section 6.2 and Section 6.3) is presented an overview of the challenges in Smart Metering systems and the state of the art in designing fully autonomous sensor nodes for current metering. The remaining Sections (Section 6.4, Section 6.5, Section 6.6) show a detailed description of the implementation of the proposed sensor node.

6.2 Smart Metering: background

A number of leading energy worldwide companies are making enormous effort to improve energy efficiency, by monitoring energy consumption through smart meters for residential and commercial buildings [88]. The main goal of metering in smart buildings will be to suggest optimal usage schedules for household's appliances for reaching established targets (e.g. to save energy, equalize the demand, or forecast peaks of energy consumption).

Actually, meter manufacturers are going on the market with a differentiated

offer: low-cost metering solutions, which are suitable for large scale distributed monitoring of households, and high-level smart meters, which used for accurate and scientific measurements.

Moreover, manufacturers have to consider the different regulatory requirements of each area as well as the different services required for different markets. For instance, as discussed in [89], the regulations related to automated meter reading impose a specific sampling rate and data transmission.

Smart meters need to acquire a big amount of data, which are stored and processed on-site, by only transmitting few useful information through wireless or wired communication [90]. This increases the cost and the features of each single node.

In general, the presented issues are addressed using integrated System-on-Chip (SoC) solutions, which are configurable and provide a rich set of features tailored for smart metering [91].

Commercial ICs which perform energy measurement are surveyed in [92]. For instance, Microchip MCP3905 supports real power measurement using two ADC channels optimized to perform both current and voltage measurement. A fixed-function DSP block is also on-chip for real power calculation. The output is a pulse signal whose frequency is proportional to the power.

Analog Devices ADE7953 measures voltage and current, and calculates active, reactive, and apparent power, as well as instantaneous RMS values. It provides high-accuracy and the access to the on-chip registers, by using a variety of communication interfaces such as SPI, I2C, and UART.

NXP EM773 energy metering IC is a 32-bit microcontroller (MCU) solution designed specifically for electricity metering applications. This micrcontroller is based on an ARM Cortex-M0 core, which is a low-cost 32-bit MCU and it is designed for 8/16-bit smart metering applications.

Moreover, several MCU manufacturers develop highly-integrated ADCs for multi-phase applications. ADCs on AFE family of Microchip use hardware logic to perform synchronous sampling. For instance, the MCP3903 AFE provides six synchronously ADCs for the three-phase energy measurement. In a similar man-

ner, Atmel 78M6631 contains the hardware (sampling and conversion elements) for implementing a high-precision three-phase measurement.

Another fundamental aspect is the communication technology used for transmitting data in a Home Area Network (HAN) [93]. Depending on the number of smart meters in a HAN, the existing solutions for energy monitoring can be classified into two groups:

- The *distributed approach*: a smart meter is installed in each device of the HAN and information are then transmitted to a central point. Commercially solutions are available as smart plug meters. They measure the power consumption of each appliance on-site and transmit the energy consumption to a central gateway using wireless or wired communication.

- The *centralized approach* [94] is mainly used to monitor a power network, which contains a given number of appliances, by only using one central device. This meter has to estimate the number and type of each load as well as its individual energy consumption and other important parameters, by using a complex analysis of the current and voltage changes (NILM). Of course, this approach requires a priori knowledge about the household appliances and their electrical characteristics, or it needs a complex training phase involving the users are also involved.

Two typologies of networking techniques are usually exploited in a Home Area Network [95]: Power Line Communication and Wireless Communication. In the following, a brief discussion about these two approaches:

6.2.1 Power Line communication (PLC)

PLC [96] uses existing electrical installation to transmit information in a frequency band between 3kHz - 30MHz. PLC is used in smart buildings for monitoring electrical appliances without installing any new structure. The data speed is between 14-45 Mbps for indoor environments and it can reach 224 Mbps for outdoor communication. The mainstream protocols in PLC technology are X-10, LonWorks or KNX.

Moreover, other proprietary standards are also available such as INSTEON and PLC-BUS, but they are not commonly adopted.

The main problem of PLC is the signal attenuation and distortion caused by the interference of the connected electrical devices, which introduce a lack of reliability and security in data transmission.

6.2.1.1 X-10

X-10 is an open standard for PLC that is used for home automation applications such as household smart meter, households appliances control, lighting control, house security and surveillance. It makes use of the existing household electrical wiring to transmit data, by encoding information onto a 120 KHz power carrier, during the zero crossing of the 50 or 60 Hz AC power wave.

X-10 system mainly consists of a module called controller equipped with a transmitter and multiple receivers, which are identified by an address configured using a combination of 16 house codes and 16 unit codes and each data packet contains an identifier (named start code) followed by a house code and a function code.

6.2.1.2 KNX

KNX aims to provide a complete solution for home and building control and it is supported by numerous important manufacturers in the world.

This standard is based upon more than 24 years of experience in the market, amongst others with predecessor systems to KNX: EIB, EHS and BatiBUS. Via the KNX medium to which all bus are connected (twisted pair, radio frequency, power line or IP/Ethernet), devices are able to exchange information. Bus devices can either be sensors or actuators needed for the control of building management equipment. All these functions can be controlled, monitored and signalled via a uniform system without the necessity of an extra control centre.

6.2.1.3 LonWorks

The core of LonWorks technology (Local Operating Network) is the LonTalk protocol, developed by Echelon. The main goal of LonWorks is to make building control systems simple and easy to install, using a platform that offer both hardware (Neuron chips) and software tools (Neuron ANSI C).

The LonTalk is a layered, packet-based, peer-to-peer communication protocol designed to be medium-independent. However, the main used channels are twisted pair and PLC. LonTalk is based on network variables (NVs). The application that runs in each device does not need to know where the input and output NVs come from or go to, because this is the task of the LonWorks firmware. Altogether LonWorks is similar to KNX, but it is used in a wide range of applications and mainly outside to the home and building fields.

6.2.2 Wireless Protocols

A variety of short-distance wireless technologies are emerging to provide flexible networking without considering the complexity and cost of physical wiring in a house.

These technologies work in the Industrial Scientific Medical Bands such us Bluetooth, ZigBee and Z-Wave, especially the 2.4 GHz frequency range. As a proprietary protocol, Z-Wave is not commonly adopted. ZigBee is a low-power wireless communications technology designed for monitoring and control of devices, and it is maintained and published by the ZigBee Alliance. Short-range wireless technologies are tailored to be a low-speed, low-power, low-cost and flexible solution for smart monitoring in a building.

6.3 Energy Harvesting for Smart Metering

Monitoring active and apparent power in smart metering applications is certainly the most important task to promote effective energy polices; therefore recent research efforts are directed to the current sensor nodes and transducers design.

Cai *et al.* in [97] present a prototype of self-sustainable wireless current and voltage meter to monitor the load on the distribution line in Smart Grids. The current sensor is an air coil tested to sense up to 200A of current. The power consumption is high due to the presence of a GPS receiver for time-stamp, starting from 400mW in idle state, it raises to 1300mW during transmission. To achieve autonomous operations, they use two energy harvesters based on cubic shape coil, which can deliver an output power of 744mW with an input current of 170A.

The stick-on wireless sensor node presented in [98] combines current and temperature sensors and it is intended to monitor a set of utilities. This prototype is battery-less equipped with a ZigBee module and a 1F supercapacitor used as back-up source to perform critical operations during power outage. The system exploits an application-tailored flux concentrator for reading and harvesting tasks. A novel boost converter is used to convert and step-up the low AC output voltage of the flux concentrator. The node consumes few tens of microampere in idle state and about 30mA in transmission. It cannot work with primary currents lower than 60A, while operating with a duty cycle of 60s with a primary current below 100A.

In [99], authors have designed and prototyped a very accurate autonomous voltage and current measurement unit which can sense AC voltage in the range 100V÷1000V and AC current in the range 1A÷1000A with an error less than 1% full scale. The supply system consists in two circuits operated in parallel which can harvest energy respectively from measured voltage and current. The operating range of the harvester spans from 5A to much more 350A, nevertheless the most considerable drawback of this solution is the lack of wireless communication.

All the aforementioned works are suitable for grid-level monitoring in which currents are in the order of tens or hundreds of amperes. In contrast to such systems, the IEEE 802.15.4-compliant wireless smart meter presented in [100] features a device-level sensing granularity. In other words it allows to monitor the energy consumption of single appliances with a power consumption up more than 1kW and it can switch-off the appliance under control simply driving a solid-state relay. Even though the system is realized with low power components

Table 6.1: Summary of main electrical features of nodes cited in Sec. 6.3

Reference work	**Primary Current [A]**	**Harvested Power [mW]**	**Power Consumption [mW]**
[97]	≥100	≥270	400 ÷ 1300
[98]	≥60	N.A.	0.4 ÷ 100
[99]	5 ÷ 350	N.A.	N.A.
[100]	≤5	No Harvesting	0.14 ÷ 190
[101]	N.A.	N.A.	N.A.

it does not perform energy harvesting but is powered by mains exploiting a small transformer. The total power consumption spans between the 140μW of the idle state and the 190mW of the radio transmission.

However, the trend is to reach perpetual operation of smart meters. In [101] a battery-free energy harvester is implemented on-chip by using 0.25-μm CMOS process. The harvester convert the AC signal coming from a Rogowski coil by means of an active rectifier and a set of boost converters. Such conversion technique, combined with a switched capacitor sampler, suppresses the total harmonic distortion and improves the power factor making this system good for power measurement. As the system is battery-free, a proper circuit is provided to guarantee the start-up operations when the appliances are powered up. Nevertheless, it does not feature wireless communications or smart operations.

Finally, it is worth to mention that some products are already available on the market. To the best of our knowledge they can perform approximate analysis without any wireless capability and can generate only an alarm when the power consumption of a building rises above a certain threshold.

Table 6.1 summarizes the majority of the wireless sensor meters with energy harvesting capability presented in literature. They are designed to monitor power grids or electrical assets and thus the current under measurement is quite high. Indeed, nodes with lower sensing granularity and used to measure residential appliances are usually powered directly from the main.

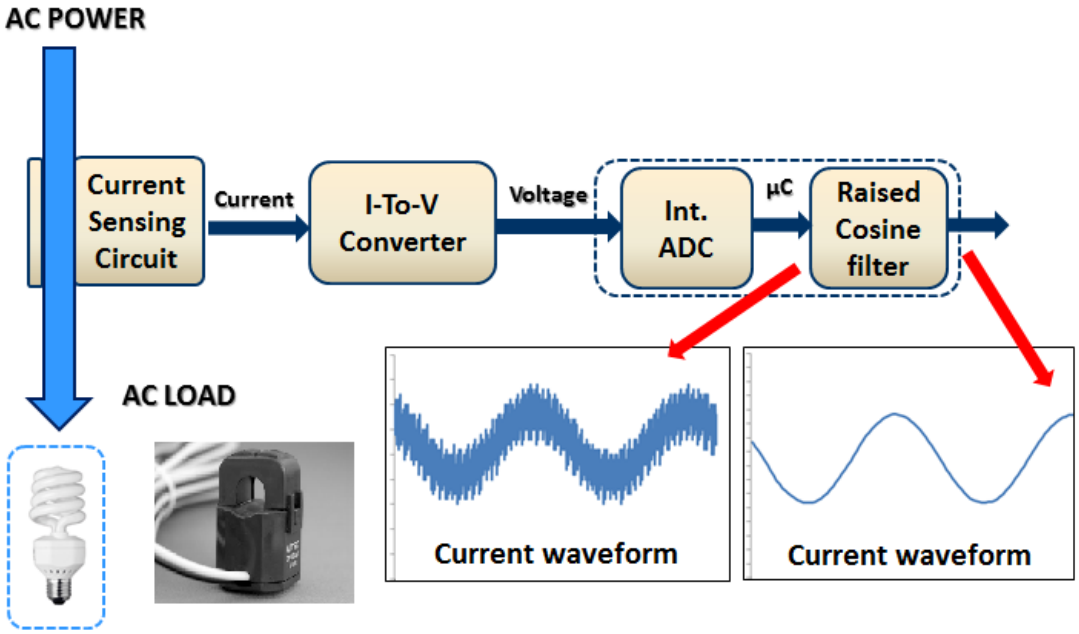

Figure 6.1: Block diagram of the current sensing circuit.

6.4 System Description

Non-intrusive Wireless Energy Meter (NIWEM) exploits two clamp-on current transformers for non-intrusive current measurement and energy harvesting, and an non-invasive coupling-capacitance voltage sensor. NIWEM architecture consists of five main blocks: i) the current sensing section, ii) the voltage sensing section, iii) the active ORing system iv) the energy harvester and finally v) the microcontroller and wireless transceiver.

6.4.1 Current Sensing Section

Fig. 6.1 shows the block diagram for the current measurement. The adopted current transformer features linear performance over a wide range of input currents and it is easy to install because it does not require any interruption or cutting of wires. Moreover it offers galvanic isolation since it decouples the digital circuit from the high-voltage line. The main electrical characteristics of the selected sensor are the number of turns n=3000 and the maximum input current of 60A,

Table 6.2: Values of R_{MEAS}, power and resolution

$\mathbf{R_{MEAS}}$	**Maximum Power**	**Resolution**
560 Ω	1 kW	<1 W
270 Ω	2 kW	1 W
150 Ω	5 kW	2.5 W
80 Ω	10 kW	5 W

which corresponds to a maximum current of 20mA on the secondary side.

In Figure 6.2 we show the schematic of the measurement circuit. The current coming from the inductive coupling is converted to a proportional voltage using a precision resistor R_{MEAS} connected in parallel to the secondary side. The values of current that can be measured strictly depend on the value chosen for R_{MEAS}. The optimal values of this resistance are listed in Table 6.2 with the relative range of measurable power and resolution. These values are calculated with the aim of maximize the span and optimize the accuracy of each power range.

The voltage obtained from the CT conversion is acquired and elaborated by the 32-bit microcontroller. As the 12-bit ADC is single-ended, we introduced a voltage divider formed by R_1 and R_2, which biases the voltage to positive values. The signal V_{REF} is generated by the DAC and it is possible to switch-off the bias and to save the power dissipated by the resistors during the sleep time.

Many residential and industrial appliances are non-linear and they are typically equipped with switching regulators, which generate a harmonic content that is not considered by measuring the simple phase lag φ.

The Power Factor (PF) measures the contribution of both the phase lag φ and the high frequency content of the input current. This harmonic content, as well as the phase lag φ, is regulated by the European Standard EN 60555, which defines the limits and the constraints for appliances and mains. In this context, the analysis of the current and voltage is crucial for measuring PF, which is the ratio between the real power (P) measured in (W) and the apparent power (S) measured in (VA). The PF can get values in the range from 0 to 1 but, in general, it has to be bigger than 0.85. The utility companies supply customers with apparent power but the utility bill is related to the real power. When the

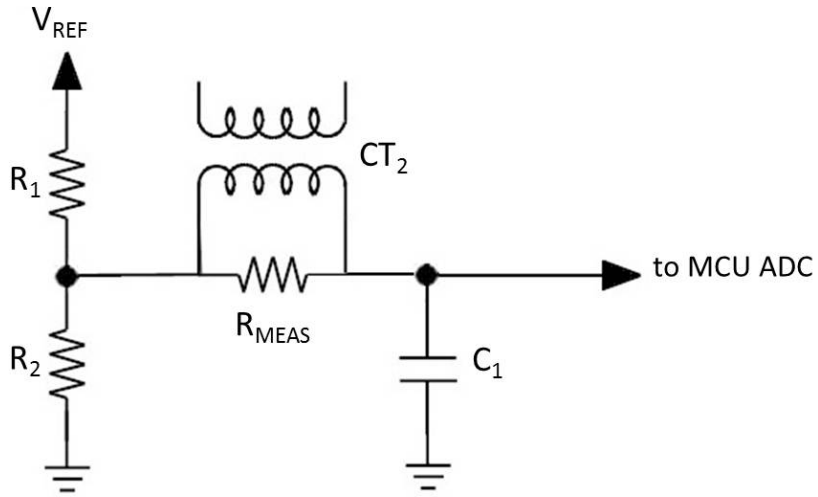

Figure 6.2: Schematic of the current sensing circuit.

PF is lower than 1, the companies need to generate more than the minimum volt-amperes necessary to supply the real power, increasing the costs of the generation and transmission of the energy.

The ADC samples with a frequency of 12.5kHz and the current values are elaborated from the microcontroller. A Raised Cosine Filter (RCF) is implemented to reduce the high-frequency noise. The RCF is a low-pass filter, which is commonly used for pulse shaping in data transmission systems. The frequency response H(f) of a this filter is symmetrical around 0 Hz and it is divided into three parts: it is constant in the pass-band, it sinks in a graceful cosine curve to zero through the transition region and it is zero outside the pass-band. The response of the implemented filter is an approximation to this behaviour. The filter is designed as a Finite Impulse Response filter (FIR) (f=12.5KHz, corner frequency 500Hz, -6dB).

6.4.2 Energy Harvester

The energy harvesting circuit, shown in Figure 6.3, exploits an additional dedicated clamp-on (CT_1) current transformer as energy transducer. The transformer harvests a current of about 5mA when a primary current of 13A is consumed by

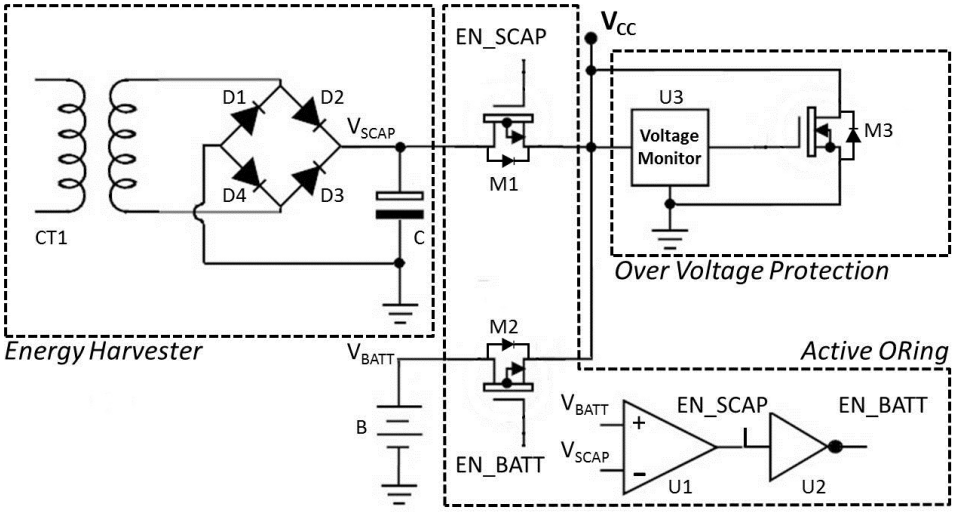

Figure 6.3: Power supply schematic of the wireless current sensor node. A low-loss, low-power active ORing system generates V_{CC} by selecting the suitable source between the backup battery and the energy harvester. An over voltage protection is provided to avoid MCU and radio transceiver damages.

the appliance, while a current of about 700μA is delivered with a primary current of 2A.

The AC to DC converter is a full-wave passive rectifier. It is realized by four Schottky diodes ($D_1 \div D_4$) with very low forward voltage to minimize power losses across the bridge. The energy buffer is a 0.47F electric double layer capacitor (C) with ultra-low internal resistance.

6.4.3 Active ORing

The power supply schematic in Figure 6.3 shows that the V_{CC} signal used to power the WCSN can be derived from two different sources: the energy harvester and two additional AAA batteries (B). These batteries are used as reservoir energy source to guarantee the system start-up. The switching between the energy harvester and the batteries must be automatic, fast and power efficient. For these reasons we implemented it by an active ORing system.Usually, the most simple ORing topology is built with a passive diode for each energy source and the re-

sulting signal is given by the source showing the greatest voltage level decreased by the diode threshold. However, to remove the voltage drop introduced by the diode and to improve the efficiency, we implemented an Active ORing, at the cost of a more complex circuit.

6.4.4 MCU and Wireless Transceiver

A wide range of microcontrollers and radio transceivers are available on the market for a variety of metering applications. Our architecture is based on the JN5148 module from NXP [47], which provides an ultra-low power, high performance wireless microcontroller targeted to WSN applications.

As already described above, this microcontroller features an enhanced 32-bit RISC processor, a 2.4GHz IEEE 802.15.4 compliant radio transceiver, 128kB ROM, 128kB RAM, and a complete set of analogue and digital peripherals such as a 12-bit ADC, a 12-bit DAC and a SPI interface. The key features of the JN5148 module are the very low sleep current, only 2.6μA and the low power consumption of the radio transceiver, namely at 3.0V it draws 15mA during transmission and 17.5mA when receiving.

The smart power meter has to be able to transmit data to an Energy@Home Gateway by using ZigBee PRO protocol with Home Automation profile. The gateway used is named FlexKey and it is one of the most compact Zigbee USB Dongle available on the market today. Due to its RF performance, it enables secure and reliable wireless connectivity between internal and external environment. The Gateway has been designed to be connected to any device equipped with a USB port (ADSL modem, PC, Tablet), to enable to connect in a ZigBee network. In Fig. 6.10, the prototype of the hardware of the smart power meter is shown.

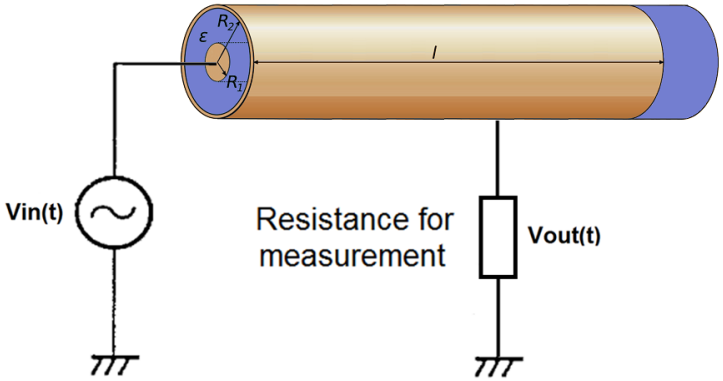

Figure 6.4: Capacitance-decoupling voltage element.

6.5 Non-invasive voltage measurement using capacitive coupling elements

The measurement of current through the magnetic field across a single wire is a well-established technique but there are no non-invasive sensors commercially available for the voltage measurement. The main idea for measuring the voltage with a non-invasive solution is to use capacitive-coupling elements positioned near the electric field generated by the mains. These elements are able to generate a current in response to the voltage variation and they are coupled to the conductive parts of each cable, through the insulation.

As shown in Fig. 6.4, the proposed sensor consists of a conductor body used to cover a part of the insulated surface of each wire in order to create a capacitive coupling between the internal conductive element and the external body. The formed capacitance C can be modelled as a cylindrical conductor of radius $R1$ (distribution line) nested within a larger hollow cylindrical conductor (external body) of radius $R2$. The capacitance of such structure depends on the radius $R1$ and $R2$, the length l of the conductor body and the permittivity ϵ, which varies with the insulation:

$$C = \frac{2\pi l\epsilon}{\ln \frac{R2}{R1}} \tag{6.1}$$

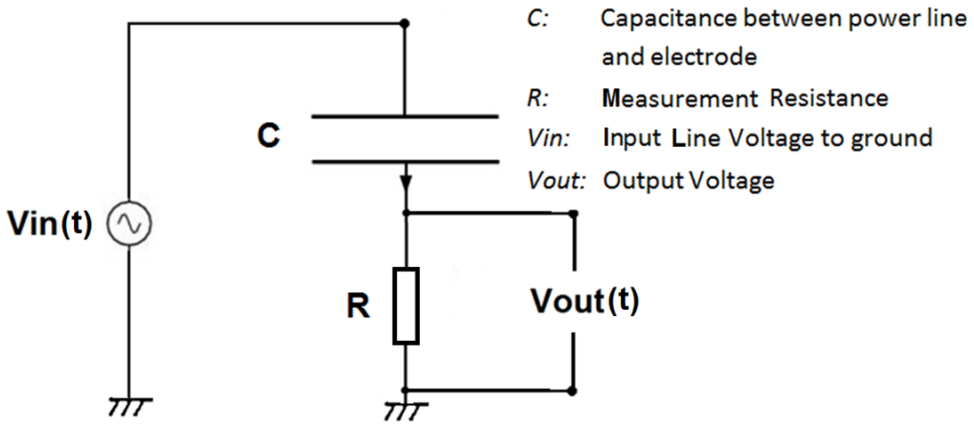

Figure 6.5: Equivalent circuit of the voltage sensor.

The voltage obtained by static induction is the output voltage, which is divided between the inter-electrode capacitance and the resistor connected to ground. The equivalent circuit is shown in Fig. 6.5 where the static capacitance between the distribution line and the electrode is C, the measuring resistance is R, the input voltage to ground is $Vin(t)$ and the output voltage is $Vout(t)$. When the voltage $Vin(t)$ is applied, the current $i(t)$ that flows through the capacitor is given by:

$$i(t) = C\frac{dV_C(t)}{dt} \tag{6.2}$$

If the voltage is sinusoidal with a fixed frequency:

$$\omega = 2\pi f \tag{6.3}$$

the voltage across the capacitor is given by:

$$Vc(t) = V_C \sin \omega t \tag{6.4}$$

where Vc is the amplitude of the voltage across C. The current through the capacitance becomes:

$$i(t) = CV_C\omega \cos \omega t \tag{6.5}$$

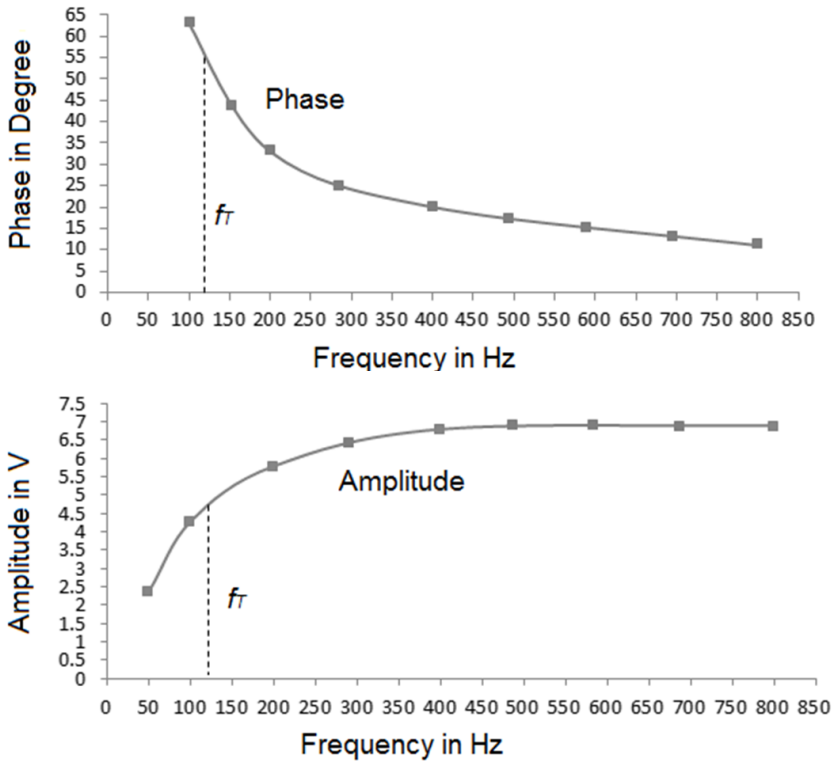

Figure 6.6: Transfert function $H(\omega)$

and the output voltage is defined as:

$$Vout(t) = RCV_C\omega \cos \omega t \tag{6.6}$$

In this way, if C and *Vout(t)* are well known, it is possible to define *Vc(t)*, which means to know the transfer function $H(\omega)$ of the equivalent two-port network that defines the voltage sensor. Unfortunately, C depends of the type of insulating, which can be different for each cable.

In Fig. 6.6 is shown an example of transfer function $H(\omega)$ obtained using a given cable (sec. $10mm^2$) , in a range of frequencies between $50 - 800Hz$. As expected, the $H(\omega)$ function is similar to a simple first-order electronic high-pass filter with a cut-off frequency ft equals to:

$$f_t = \frac{1}{\pi RC} \tag{6.7}$$

Figure 6.7: Prototype of the voltage sensors for different type of cables

The value of R is carefully chosen because, with the value of C, it determines the profile of transfer function and the amplitude and phase of $Vout(t)$, which are respectively attenuated and shifted from the filter.

In Fig. 6.7 is shown the prototype of the voltage sensor and in Fig. 6.8 are shown the block diagram for the voltage measurement and the capacitive-coupling elements. In the electrical distribution systems the voltage is measured between two conductors (e.g. phase P and neutral N). However, these conductors are floating compared to the smart meter if a common reference between them is not available. The differential measurement allows to eliminate the floating component and then to obtain only the useful voltage, eliminating the common reference of the main AC conductors.

One possibility to make the problem of the sensor calibration negligible is to obtain an output voltage Vout(t) in phase with the input voltage Vin(t), integrating each capacitance-coupling element in a differential second-order RC high-pass filter with a frequency f_T much lower than 50Hz 6.9. In this way, it is possible to consider minimal or negligible the effect of the capacitive coupling at

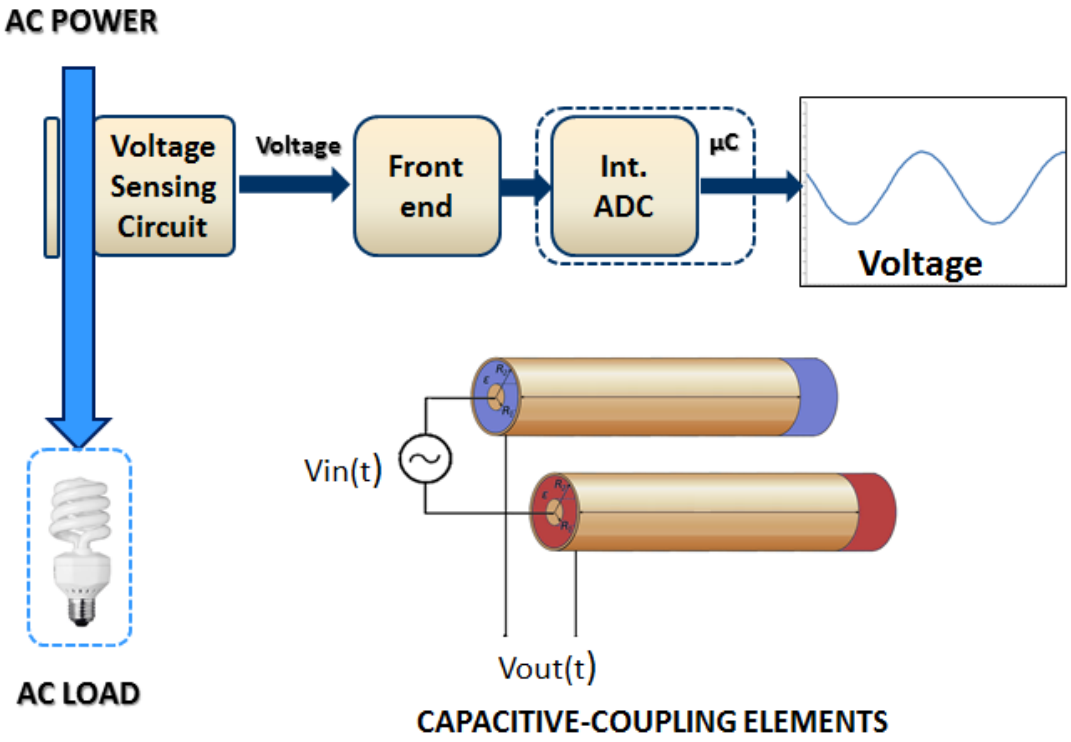

Figure 6.8: Block diagram of the voltage sensing circuit.

50Hz Fig. 6.9. The first stage of the second-order RC passive filter in Fig. 6.9 has been implemented to make negligible the phase shift introduced by the coupling-capacitance, using high-value resistors while the second stage is mainly used to adapt the input signal to the buffer stage, which is used to decouple the front-end circuit to the ADCs.

6.6 Network Protocol and Architecture

The FlexKey USB gateway acts as a ZigBee PRO coordinator, with Home Automation profile, for the smart power meters network. ZigBee is a wireless networking technology developed by the ZigBee Alliance for low-data rate and short-range applications. Home automation is one of the key market areas.

The ZigBee protocol stack is composed of four main layers: the physical (PHY) layer, the medium access control (MAC) layer, the network (NWK) layer, and

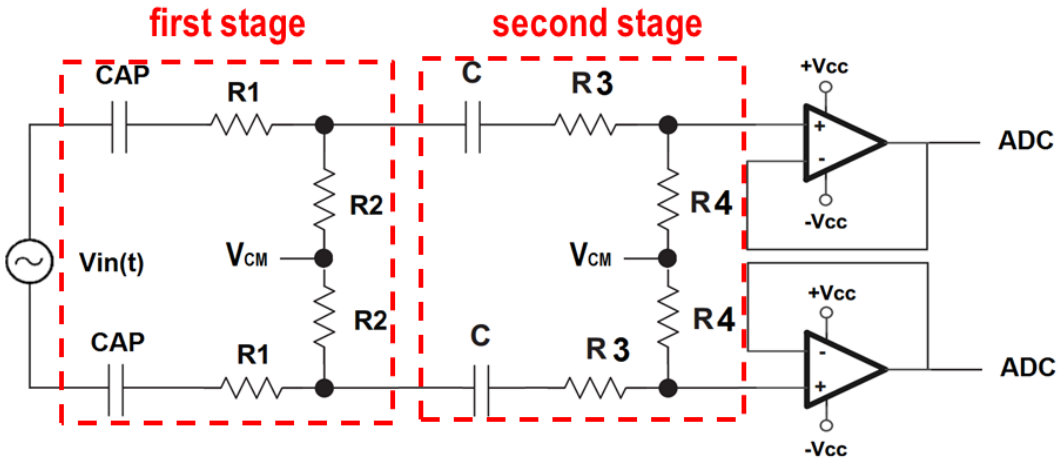

Figure 6.9: Measure of the potential difference through two capacitive-coupling sensors.

the application (APL) layer. In addition, ZigBee provides security functionality across layers. The two lower layers of the ZigBee protocol stack are defined by the IEEE 802.15.4 standard, while the rest of the stack is defined by the ZigBee specification. ZigBee Home Automation is a new profile to create smarter homes that enhance the comfort, convenience, security and energy management for the consumer and it adds several important features that improve the battery life for smart sensors and simplify installation and maintenance for consumers and custom installers. These features have a significant impact on operational and device costs to service providers and quality of service to consumers.

Our ZigBee PRO NIWEM, with Home Automation profile, samples the current and the voltage waveforms and provides the following parameters: RMS current, RSM voltage and power factor. These data are then transmitted through the ZigBee PRO protocol. The total amount of the data is equal to 94 byte and they are sent by using two ZigBee PRO packets. The first packet contains 60 byte of payload, where 40 byte are related to the current waveform and 20 byte are related to the voltage waveform. The second one contains the remaining 20 byte

of the voltage waveform and the RMS current (2 byte), the RMS voltage (2 byte), the voltage across the microcontroller Vcc (2 byte) and, finally, the power factor (4 byte). The use of a multi-packet solution is because payload length can not exceed 60 byte due to the configuration of the network with this specific Gateway. Moreover, we decided to not use the ZigBee PRO automatic fragmentation and to perform a high-level check for the correct reception of the packets.

On the host-side, we have implemented a Java multiplatform software WiStation, which is able to run over every machine (e.g. Windows, Linux, Beaglebone, Raspberry Pi, Android devices) and it acts as a control station. This software communicates with the FlexKey ZigBee PRO gateway through a USB virtual serial port and it allows the end-user to setup, to connect and to configure the ZigBee network. Moreover, it performs packet check and it is able to alert with notification in case of lost packets/nodes. The system displays the information by using HTML/JavaScript pages with a local web server which is embedded into the application. In this way, it is possible to keep the software completely multi-platform and to enable the remote control of the ZigBee network. The main WiStation web data view is shown in Fig. 6.11. This interface can be used by both administrator and end-users for monitoring the voltage and current waveforms, the RMS current and RMS voltage, and, finally, the power factor, the apparent, real and reactive powers.

6.7 Experimental Results

The performance evaluation is focused on the energy harvester and on the sensing circuit. We used a prototype and configuration shown in Fig. 6.12.

6.7.1 Energy harvester

The tests on proposed device started with the energy harvester performance evaluation. We emulated the power consumption (P_{in}) of real appliances by means of a variable power resistor, and then we measured the current in the primary circuit (I_{in}). Next we measure the current delivered by the harvester and charg-

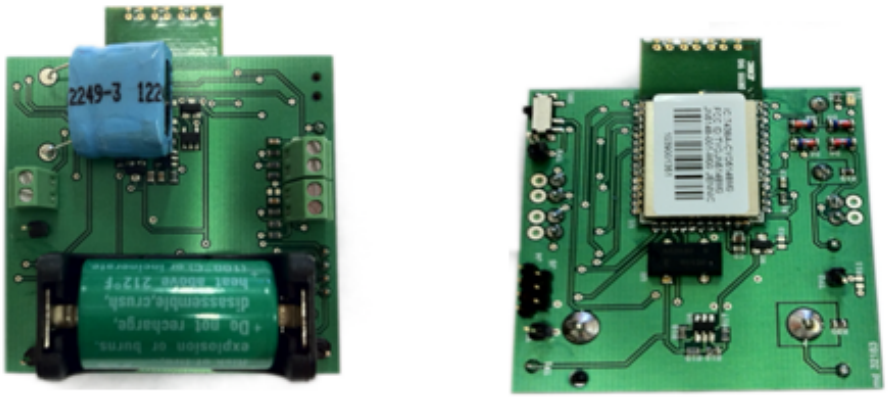

Figure 6.10: Top and bottom view of the hardware prototype used in laboratory test.

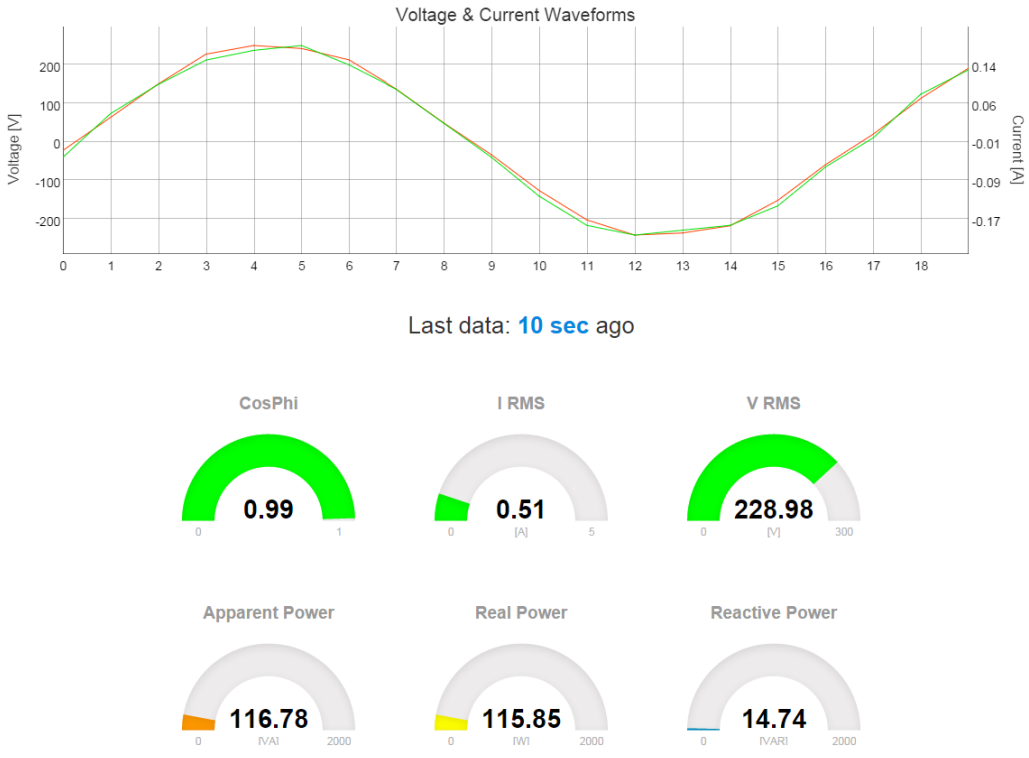

Figure 6.11: Application data view

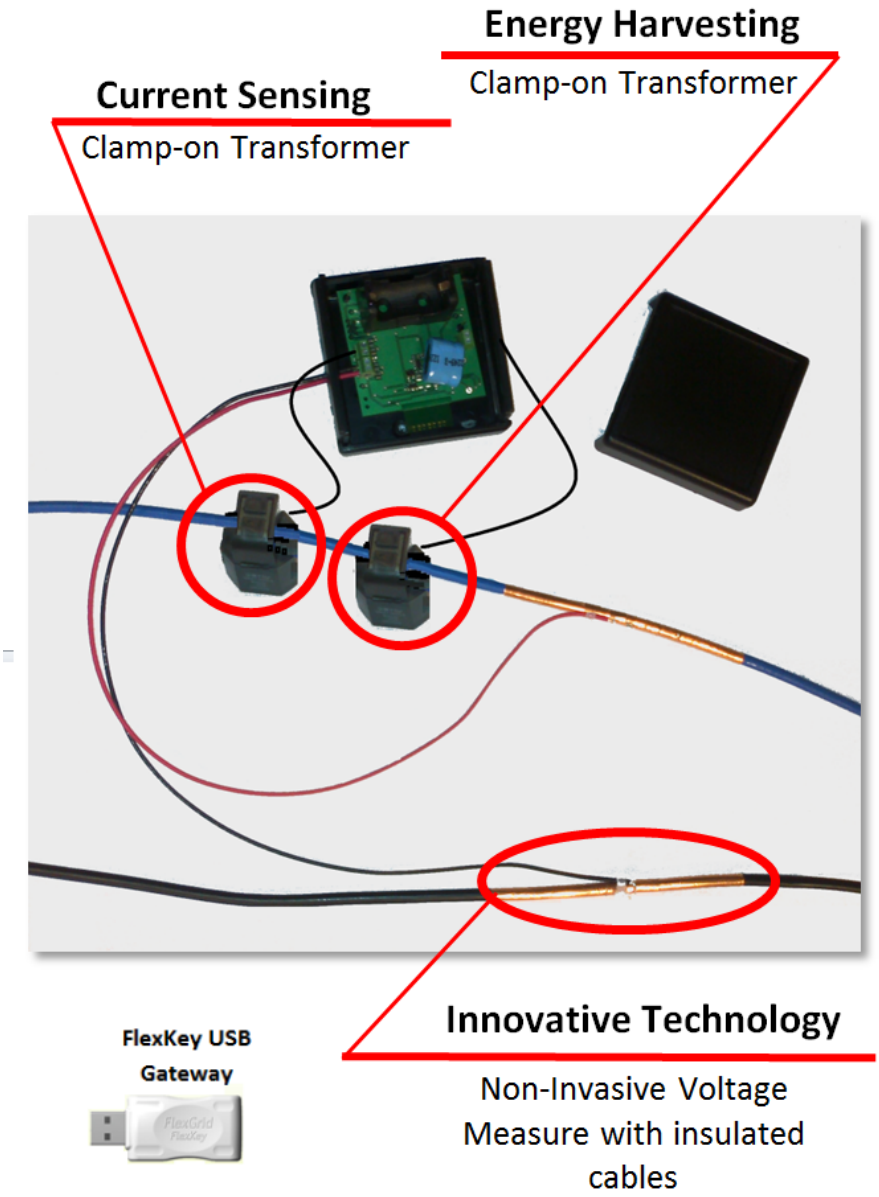

Figure 6.12: Contact-less Smart power meter prototype.

ing the supercapacitor (I_{out}) by connecting the emulated appliances to the energy harvesting circuit. The results are listed in Table 6.3.

The application firmware takes about 200ms for voltage sampling, data filtering and elaboration and radio transmission. Considering V_{CC}=3.0V, in this

Table 6.3: Energy harvester performance for different appliances

Appliance	$\mathbf{P_{in}}$ **[W]**	$\mathbf{I_{in}}$ **[A]**	$\mathbf{I_{out}}$ **[mA]**
Television	70	0.300	0.102
500W lamp	500	1.930	0.642
Oven	2000	8.600	2.856
Dishwasher	2500	10.840	3.610
Washing machine	3000	13.020	4.321

time interval the total power dissipated by the microcontroller and by the active peripherals including the radio transceiver is about 150mW, thus the energy demand is about 30mJ. When the node is inactive (sleep mode), most of the on-board components are switched-off and the meter consumes less than 30μW. Therefore, if the sleep time is properly calculated, the energy harvested during the sleep time balances the amount necessary for a measurement and a packet transmission; in other words a adjusted duty-cycle permits self-sustainable operations on the node. Clearly, shorter sleep intervals necessitate the intervention of the backup batteries to compensate the energy not scavenged by the CT. Moreover, appliances with higher power consumption permit the CT to deliver higher power, hence the sleep interval necessary to harvest enough energy for a measurement is shorter and the duty-cycle could increase. The graph plotted in Figure 6.13 shows the curve of the optimum sleep time as a function of the power dissipation of the appliances. The curve is obtained with experimental data and it shows that any appliance with a specific power consumption, is characterized by a specific duty-cycle which permits to obtain a perpetual measurement activity without the need of batteries.

6.7.2 Accuracy of the measurement circuit

The performance evaluation is related to the error in the current, voltage and power factor measurements. In Table 6.4 is presented a comparison between the current consumption of few appliances measured with both a calibrated current meter (Agilent U1193A) and our wireless energy meter. It is possible to notice that the maximum error of NIWEM is less than 2%.

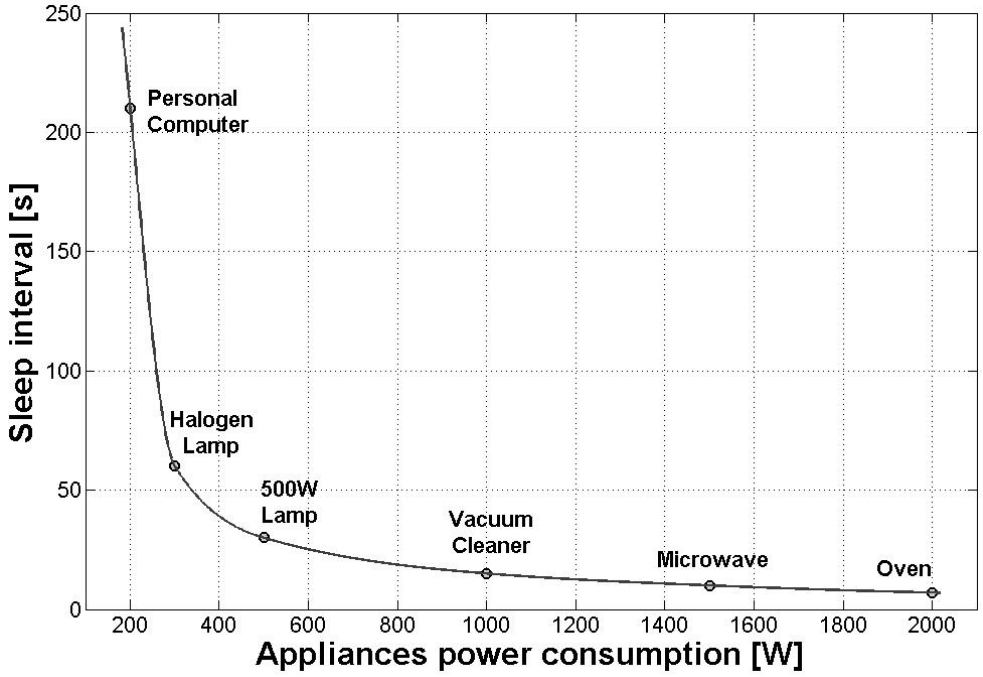

Figure 6.13: Optimized sustainability curve. For a given appliance power consumption the curve returns the minimum sleep time interval to guarantee sustainable operations

Table 6.4: Evaluation of current measurement error

Appliance	**U1193A [A]**	**NIWEM [A]**	**Error [%]**
Personal Computer	0.820	0.828	0.97
Halogen lamp	1.270	1.250	1.6
500W lamp	1.890	1.900	0.53
Vacuum cleaner	3.850	3.820	0.78
Microwave	4.690	4.765	1.6
Oven	7.650	7.580	0.92

Moreover, Table 6.5 shows the measurement of the current, voltage and power factor for three specific loads: a 500W lamp, a resistive-capacitive load and a PC screen. Also in this case, we present a comparison between the consumption of this appliances measured with both a calibrated meter (Agilent U1193A) and our wireless energy meter. It is possible to notice that the values obtained with the presented solution are very close (the error is negligible) to the values obtained using Agilent U1193A.

Table 6.5: Evaluation of voltage, current and power factor measurement

500 W lamp	**Voltage [V]**	**Current [A]**	**Power Factor**
U1193A	224.3	1.956	1.00
NIWEM	227.3	1.960	0.99

Res. - Cap.	**Voltage [V]**	**Current [A]**	**Power Factor**
U1193A	226.5	0.688	0.53
NIWEM	227.1	0.680	0.52

PC Monitor	**Voltage [V]**	**Current [A]**	**Power Factor**
U1193A	225.5	0.170	0.54
NIWEM	227.7	0.173	0.53

6.8 Conclusion

In this Chapter, a new Non-intrusive Wireless Energy Sensor Node to measure the voltage, current and power factor for residential and industrial appliances is presented. As key features, it is no-invasive and it can self-sustain its operations by harvesting energy from the monitored current. It can harvest energy from appliances with a power consumption in the range of 10 W - 10kW. Moreover, this system feature a low-power, 32-bit NXP microcontroller for data processing and a wireless transceiver to send data, via ZigBee PRO standard with Home Automation profile, to a Freescale gateway. Experimental results have confirmed that a complete energy sustainability can be achieved starting monitoring loads of 10W. Finally, the accuracy of this node has been characterized by measuring the current, voltage and power factor values of a set of three appliances where the error, compared to a calibrated instrument, is negligible.

Chapter 7

Conclusions

As extensively discussed in this dissertation, Wireless Sensor Networks (WSNs) are implemented in a wide range of distributed sensing applications and they offer numerous challenges due to their peculiarities. In this dissertation, we have addressed several aspects related to the WSNs, by presenting interesting solutions at different developing levels and describing two real-world WSN applications.

Primarily, we have considered the stringent energy constraints to which sensing nodes are typically subjected, by proposing an innovative and adaptive algorithm, which minimizes the consumption of nodes with energy-hungry sensors in sleep mode, when the power source has to be regulated using DC-DC converters. The proposed solution allows a discontinuous usage of DC-DC converter during sleep time, without any modification of the user's program and without using any external energy buffer. The proposed solution only addresses the aspect related to the nodes in sleep mode, by neglecting the energy efficiency improvement when the node is in active mode. Future works will consider the energy efficiency with the node in both sleep and active mode, extending the proposed solution with innovative power management solutions.

Secondarily, we have addressed the asptect related to the time synchronisation in WSNs, by providing an innovative low-overhead synchronisation, which is based on a Temperature Compensation Algorithm (TCA). Also in this case, this approach can be considered in a larger scenario of time synchronisation, which

also include the knowledge about the network architecture.

Finally, we have considered self-powered WSNs with Energy Harvesting (EH) solution, by presenting a new approach that enables computation to be sustained during intermittent power supply, which is achieved by reactively hibernating: saving system state only once, when power is about to be lost, and then sleeping until the supply recovers. In the future works, we will improve this approach by dynamically setting the hibernation and the restore thresholds as a function of the harvested energy.

In the second part of this dissertation we have considered the discussed approaches (power management, time synchronisation and self-powered solutions) in real-world WSN applications.

The first presented scenario was related to the experience gathered during an European Project (3ENCULT Project - Efficient Energy for EU Cultural Heritage), regarding the design and implementation of an innovative network for monitoring heritage buildings while the second presented scenario was related to project in collaboration with Telecom Italia s.p.a., regarding the design of an innovative smart energy meters for monitoring the usage of household's appliances.

Publications

2012

- **D. Balsamo**, G. Paci, D. Brunelli and L. Benini, "Smart AC Power metering through WSNs and the Cloud," *in poster session of the Fifth European conference on Wireless Sensor Networks*, EWSN 2012, Trento, Italy, 2012.
- D. Brunelli, **D. Balsamo**, G. Paci, and L. Benini, "Temperature compensated time synchronisation in wireless sensor networks," *Electronics Letters*, vol.48, no.16, pp.1026-1028, August 2012.

2013

- **D. Balsamo**, D. Brunelli, D. Porcarelli, and L. Benini, A New Non-invasive Voltage Measurement Method for Wireless Analysis of Electrical Parameters and Power Quality , *SENSORS, 2013 IEEE* , vol., no., pp. 1,4, 3-6 Nov. 2013.
- **D. Balsamo**, G. Paci, L. Benini, and D. Brunelli, "Long term, low cost, passive environmental monitoring of heritage buildings for energy efficiency retrofitting," *Environmental Energy and Structural Monitoring Systems, EESMS 2013 IEEE Workshop on*, pp.1-6, 11-12 Sept. 2013
- D. Brunelli, D. Porcarelli, **D. Balsamo**, and M. Rossi, "Self-powered Wireless Energy Meter," *Proceedings of the 1st International Workshop on Energy Neutral Sensing Systems*, Rome, Italy, ACM, 2013.

- D. Porcarelli, **D. Balsamo**, D. Brunelli, and G. Paci, "Perpetual and low-cost power meter for monitoring residential and industrial appliances," *Design, Automation Test in Europe Conference Exhibition (DATE)*, 2013 , pp. 1155-1160, 18-22 March 2013.

2014

- F. Aderohunmu, **D. Balsamo**, G. Paci, and D. Brunelli, Long Term WSN Monitoring for Energy Efficiency in EU Cultural Heritage Buildings, *Real-World Wireless Sensor Networks Lecture Notes in Electrical Engineering*, vol. 281, pp. 253-261, 2014.

- **D. Balsamo**, D. Brunelli, G. Paci, and L. Benini, "Sleep power minimisation using adaptive duty-cycling of DCDC converters in state-retentive systems," *Circuits, Devices Systems, IET* , vol.8, no.6, pp.478-486, 2014.

2015

- **D. Balsamo**, A.S. Weddell, G.V. Merrett, B.M. Al-Hashimi, D. Brunelli, and L. Benini, "Hibernus: Sustaining Computation during Intermittent Supply for Energy-Harvesting Systems," *Embedded Systems Letters, IEEE*, vol.7, no.1, pp.15-18, March 2015.

- **D. Balsamo**, G. Gallo, D. Brunelli and L. Benini, "Energy Neutral and Non-intrusive Zigbee Power Meter for load monitoring in Smart Buildings," *accepted to 2015 IEEE Sensors Applications Symposium (SAS 2015)*, 13-15 April, 2015.

Bibliography

[1] Li Da Xu *et al.*, "Internet of Things in Industries: A Survey," *Industrial Informatics, IEEE Transactions on*, vol. 10, no. 4, pp. 2233-2243, Nov. 2014 1

[2] D. Puccinelli and M. Haenggi, "Wireless sensor networks: applications and challenges of ubiquitous sensing," *Circuits and Systems Magazine, IEEE*, vol. 5, no. 3, pp. 19-31, 2005 1

[3] R. Senguttuvan *et al.*, "Multidimensional Adaptive Power Management for Low-Power Operation of Wireless Devices," *Circuits and Systems II: Express Briefs, IEEE Transactions on*, vol. 55, no. 9, pp. 867-871, Sept. 2008 13

[4] G. Anastasi *et al.*, "Extending the Lifetime of Wireless Sensor Networks Through Adaptive Sleep," *Industrial Informatics, IEEE Transactions on*, vol. 5, no. 3, pp. 351-365, Aug. 2009 13

[5] J. Heo *et al.*, "EARQ: Energy Aware Routing for Real-Time and Reliable Communication in Wireless Industrial Sensor Networks," *Industrial Informatics, IEEE Transactions on*, vol. 5, no. 1, pp. 3-11, Feb. 2009 13

[6] C. Caione *et al.*, "Distributed Compressive Sampling for Lifetime Optimization in Dense Wireless Sensor Networks," *Industrial Informatics, IEEE Transactions on* , vol. 8, no. 1, pp. 30-40, Feb. 2012 13

[7] G. Qiang *et al.*, "Improving Energy Efficiency in a Wireless Sensor Network by Combining Cooperative MIMO With Data Aggregation," *Vehicular*

Technology, IEEE Transactions on, vol. 59, no. 8, pp. 3956-3965, Oct. 2010 14

[8] J. Ploennigs *et al.*, "Comparative Study of Energy-Efficient Sampling Approaches for Wireless Control Networks," *Industrial Informatics, IEEE Transactions on*, vol. 6, no. 3, pp. 416-424, Aug. 2010 14

[9] V. Raghunathan *et al.*, "Emerging techniques for long lived wireless sensor networks," *Communications Magazine, IEEE*, vol. 44, no. 4, pp. 108 - 114, April 2006 14

[10] R.C. Luo and O. Chen, "Mobile Sensor Node Deployment and Asynchronous Power Management for Wireless Sensor Networks," *Industrial Electronics, IEEE Transactions on*, vol. 59, no. 5, pp. 2377-2385, May 2012 13

[11] C. Moser *et al.*, "Adaptive Power Management for Environmentally Powered Systems," *Computers, IEEE Transactions on*, vol. 59, no. 4, pp. 478-491, April 2010 14

[12] Y. Levron *et al.*, "A Power Management Strategy for Minimization of Energy Storage Reservoirs in Wireless Systems With Energy Harvesting," *Circuits and Systems I: Regular Papers, IEEE Transactions on*, vol. 58, no. 3, pp. 633-643, March 2011 14

[13] C. Jia *et al.*, "Integrated power management circuit for piezoelectronic generator in wireless monitoring system of orthopaedic implants," *Circuits, Devices and Systems IET*, vol. 2, no. 6, pp. 485 - 494, Dec. 2008 14

[14] J.A.R. Azevedo and F.E.S. Santos, F.E.S., "Energy harvesting from wind and water for autonomous wireless sensor nodes," *Circuits, Devices and Systems, IET*, vol. 6, no. 6, pp. 413 - 420, Nov. 2012 14

[15] D. Balsamo *et al.*, "Sleep power minimisation using adaptive duty-cycling of DCDC converters in state-retentive systems," *Circuits, Devices Systems, IET*, vol. 8, no. 6, pp. 478-486, 2014 3

[16] Jean-Marc Berthaud, "Time synchronization over networks using convex closures," *IEEE/ACM Transactions on Networking*, pp. 265-277, 2000 4

[17] D. Balsamo *et al.*, "Hibernus: Sustaining Computation during Intermittent Supply for Energy-Harvesting Systems," *Embedded Systems Letters, IEEE*, vol.7, no.1, pp.15-18, March 2015 5

[18] V. Potdar *et al.*, "Wireless Sensor Networks: A Survey," *Advanced Information Networking and Applications Workshops, 2009. WAINA '09. International Conference on* , pp. 636-641, 2009 1

[19] D. Balsamo *et al.*, "Long term, low cost, passive environmental monitoring of heritage buildings for energy efficiency retrofitting," *Environmental Energy and Structural Monitoring Systems (EESMS), 2013 IEEE Workshop on*, pp. 1-6, 11-12 Sept. 2013 5

[20] F. Aderohunmu *et al.*, "Long Term WSN Monitoring for Energy Efficiency in EU Cultural Heritage Buildings," *Real-World Wireless Sensor Networks Lecture Notes in Electrical Engineering*, vol. 281, pp. 253-261, 2014 5

[21] D. Balsamo *et al.*, "Smart AC Power metering through WSNs and the Cloud," *Poster session of the Fifth European conference on Wireless Sensor Networks, EWSN 2012*, Trento, Italy, 2012 6

[22] D. Balsamo *et al.*, "A new non-invasive voltage measurement method for wireless analysis of electrical parameters and power quality," *SENSORS, 2013 IEEE*, pp.1-4, 3-6 Nov. 2013 6

[23] G.W. Hart, "Non-intrusive appliance load monitoring," *Proceedings of the IEEE*, vol. 80, no. 12, pp. 1870-1891, Dec 1992 6

[24] A. Sinha and A. Chandrakasan, "Dynamic power management in wireless sensor networks," *Design and Test of Computers IEEE*, vol. 18, no. 2, pp. 62-74, Mar/Apr 2001 10

[25] S. Alberts, "Energy-Efficient Algorithms," *Communications of the ACM*, vol. 53, no. 5, May 2010 10

[26] A. Pantazis Nikolaos *et al.*, "Power Control Schemes in Tactical Wireless Sensor Networks," *12th European Wireless Conference - Enabling Technologies for Wireless Multimedia Communications*, April 2006 10

[27] D. Miorandi *et al.*, "Guest editorial: Special section on wireless technologies in factory and industrial automation, Part I," *IEEE Trans. Ind. Informat.*, vol. 3, no. 2, pp. 93-94 , May 2007 10

[28] M. Lemmon, *et al.*, "Overload management in sensor-actuator networks used for spatially-distributed control systems," *Proc. Conf. Embedded Networked Sensor Syst. (SenSys)*, pp. 162-170, Los Angeles, CA, Nov. 2003 10

[29] B. Sinopoli *et al.*, "Distributed control applications within sensor networks," *Proceedings of the IEEE*, vol. 91, no. 8, pp. 1235-1246, Aug. 2003 10

[30] G. Platt *et al.*, "Distributed wireless sensor networks and industrial control systemsA new partnership," *Proc. IEEE Workshop on Embedded Networked Sensors (EmNetS-II)*, pp. 157-158, Apr. 2005 10

[31] F. Salvadori *et al.*, "Monitoring in Industrial Systems Using Wireless Sensor Network With Dynamic Power Management Instrumentation and Measurement," *IEEE Transactions on*, vol. 58, no. 9, pp. 3104-3111, Sept. 2009 10

[32] J. Hu *et al.*, "Increasing sleep-mode efficiency by reducing battery current using a DC-DC converter," *Circuits and Systems (MWSCAS), 53rd IEEE International Midwest Symposium on*, pp. 53-56, Aug. 2010 10

[33] N. A. Pantazis and D.D. Vergados, "A survey on power control issues in wireless sensor networks," *Communications Surveys & Tutorials IEEE*, vol. 9, no. 4, pp. 86-107, Fourth Quarter 2007 10

[34] C. Alippi *et al.*, "Energy management in wireless sensor networks with energy-hungry sensors," *Instrumentation & Measurement Magazine*, IEEE, vol. 12, no. 2, pp. 16-23, April 2009 3, 12

[35] Anastasi *et al.*, "Energy Conservation in Wireless Sensor Networks," *Ad Hoc Networks Journal*, 2009 10

[36] V. Jelicic *et al.*, "Design, characterization and management of a wireless sensor network for smart gas monitoring," *Advances in Sensors and Interfaces (IWASI)*, 2011 4th IEEE International Workshop on, pp. 115-120, June 2011 12

[37] D. Boyle *et al.*, "Energy analysis of industrial sensors in novel wireless SHM systems," *Sensors, 2012 IEEE*, pp. 1-4, Oct. 2012 12

[38] J. Beute, "Fast-prototyping Using the BTnode Platform," *Design, Automation and Test in Europe, 2006 DATE '06*, vol. 1, pp. 1-6, 6-10 March 2006 12

[39] J.L. Hill and D.E. Culler, " Mica: a wireless platform for deeply embedded networks," *Micro IEEE*, vol. 22, no. , pp. 12- 24, Nov/Dec 2002 12

[40] D. Ma *et al.*, "Adaptive on-chip power supply with robust one-cycle control technique," *Proc. ISLPED*, pp. 394-399, Oct 2006 13

[41] W. Yan *et al.*, "Dynamic deadtime controller for synchronous buck DC-DC converters," *Electronics Letters*, vol. 46, no. 2, Jan. 2010 13

[42] B. Yuan and X. Lai, "On-chip current-sensing circuit for DC-DC buck converter," *Electronics Letters*, vol. 45, no. 2, Jan. 2009 13

[43] C. Tao and A.A. Fayed, "A Low-Noise PFM-Controlled Buck Converter for Low-Power Applications," *Circuits and Systems I: Regular Papers, IEEE Transactions on*, vol. 59, no. 12, pp. 3071-3080, Dec. 2012 13

[44] MCP1640: 0.65V Start-up Synchronous Boost Regulator Datasheet http://ww1.microchip.com/downloads/en/DeviceDoc/22234B.pdf 13

[45] Ultralow Quiescent Current DC DC converter for Light Load Applications Datasheet http://cds.linear.com/docs/en/datasheet/3536fa.pdf 13

[46] 96% Efficient Synchronization Boost Converter Datasheet http://www.ti.com/product/tps61024 13

[47] Jennic, Data Sheet: JN5148-001, IEEE 802.15.4 Wireless Microcontroller, 2010 25, 58, 87

[48] J. Elson and D. Estrin, "Time synchronization for wireless sensor networks," *Proc. 15th Int. Parallel and Distributed Processing Symp.,(IPDPS 01)*, IEEE Computer Society, Washington, DC, USA, 2001 34

[49] Q. Gao *et al.*, "Simple algorithm for improving time synchronisation in wireless sensor networks," *Electron. Lett.*, pp. 889 - 891, 2004 34

[50] J. Elson and K. Romer, "Wireless sensor networks: a new regime for time synchronisation," *SIGCOMM Comput. Commun. Rev.*, pp. 149 - 154, 2003 34

[51] W. Ikram *et al.*, "Towards a radio-controlled time synchronised wireless sensor network," *IEEE Conf. on Emerging Technologies and Factory Automation, (ETFA)*, pp. 1 - 4, Sep. 2010 34

[52] J. Van Greunen and J. Rabaey, "Lightweight time synchronisation for sensor networks," *Proc. 2nd ACM Int. Conf. on Wireless Sensor Networks and Applications (WSNA 03)*, pp. 11 - 19, New York, USA, 2003 34

[53] S.M. Lasassme and J.M. Conrad, "Time synchronisation in wireless sensor networks: a survey," *Proc. of IEEE SoutheastCon 2010, Charlotte-Concord*, pp. 242 - 245, NC, USA, March 2010 34

[54] W. Zhou *et al.*, "Comparison among precision temperature compensated crystal oscillators," *Proc. of IEEE Int. Frequency Control Symposium and Exposition*, Vancouver, Canada, August 2005 35

[55] P. D. Mitcheson *et al.*, "Energy Harvesting From Human and Machine Motion for Wireless Electronic Devices," *Proc. IEEE*, vol. 96, no. 9, pp. 1457-1486, Sept. 2008 42

[56] M. R. Mhetre *et al.*, "Micro energy harvesting for biomedical applications: A review," *Proc. ICECT 2011*, vol. 3, pp. 1-5, 8-10 April 2011 42

[57] B. A. Warneke and K. S. J. Pister, "An ultra-low energy microcontroller for Smart Dust wireless sensor networks," *Proc. IEEE ISSCC 2004*, pp. 316-317, vol. 1, Feb. 2004 42

[58] B. Ransford *et al.*, "Mementos: System Support for Long-Running Computation on RFID-Scale Devices," *ASPLOS11*, Newport Beach, CA, USA, Mar. 5-11, 2011 42, 47

[59] P. A. Bernstein *et al.*, "Concurrency Control and Recovery in Database Systems," *Addison-Wesley Longman Publishing*, Boston, USA 1987 42

[60] M. Zwerg *et al.*, "An 82μA/MHz microcontroller with embedded FeRAM for energy-harvesting applications," *Proc. IEEE ISSCC 2011*, pp. 334-336, 20-24 Feb. 2011 42, 44, 46

[61] F. D'Amato *et al.*, "Monitoring heritage buildings and artworks with Wireless Sensor Networks," *Environmental Energy and Structural Monitoring Systems (EESMS), 2012 IEEE Workshop on*, pp. 1- 6, 2012 56

[62] D. Zonta *et al.*, "Managing the historical heritage using distributed technologies,*Int. Journal of Architectural Heritage: Conservation, Analysis, and Restoration*, pp. 200 - 225, 2008 56

[63] P. Gajbhiye and A. Mahajan, "A survey of architecture and node deployment in Wireless Sensor Network," *Applications of Digital Information and Web Technologies, ICADIWT. First International Conference on the*, pp. 426-430, 2008 56

[64] Xiang-dong Jiang *et al.*, "Wireless sensor networks in Structural Health Monitoring based on ZigBee technology," *Anti-counterfeiting, Security, and Identification in Communication, 2009. ASID 2009. 3rd International Conference on*, pp. 449-452, 2009 56

[65] G. Anastasi, G. *et al.*, "WSNs for structural health monitoring of historical buildings," *Human System Interactions, HSI. 2nd Conference on*, pp. 574 579, 2009 56

[66] L.M.P. de Brito *et al.*, "Wireless Sensor Networks Applied to Museums' Environmental Monitoring," *Wireless and Mobile Communications, 2008. ICWMC '08. The Fourth International Conference on*, pp. 364-369, 2008 58

[67] R. Morello *et al.*, "Remote monitoring of building structural integrity by a smart wireless sensor network," *Instrumentation and Measurement Technology Conference (I2MTC), 2010 IEEE*, pp. 1150-1154, 2010 59

[68] GU Changzhan *et al.*,"A wireless smart sensor network based on multi-function interferometric radar sensors for structural health monitoring," *Wireless Sensors and Sensor Networks (WiSNet), IEEE Topical Conference on*, pp. 33-36, 2012 59

[69] Sukun Kim *et al.*,"Health Monitoring of Civil Infrastructures Using Wireless Sensor Networks," *Information Processing in Sensor Networks, 2007. IPSN 2007. 6th International Symposium on*, pp. 254-263, 2007 59

[70] A. Neri *et al.*, "Environmental monitoring of heritage buildings," *Environmental, Energy, and Structural Monitoring Systems, EESMS 2009. IEEE Workshop on*, pp. 93-97, 2009 59

[71] A. Abrardo *et al.*, "Health monitoring of architectural heritage: the case study of San Gimignano," *Environmental Energy and Structural Monitoring Systems (EESMS), 2010 IEEE Workshop on*, pp. 98-102, 2010 59

[72] M. Ceriotti *et al.*, "Monitoring heritage buildings with wireless sensor networks: The Torre Aquila deployment," *Information Processing in Sensor Networks, 2009. IPSN 2009. International Conference on*, pp. 277-288, 2009 59

[73] TelosB, http://www.willow.co.uk/html/telosb_mote_ platform.html, 2012 60

[74] D. Porcarelli *et al.*, "A Multi-Harvester architecture with hybrid storage devices and smart capabilities for low power systems," *Power Electronics, Electrical Drives, Automation and Motion (SPEEDAM), 2012 International Symposium on*, pp. 946-951, 2012 60

[75] D. Dondi *et al.*, "A solar energy harvesting circuit for low power applications," *Sustainable Energy Technologies, 2008. ICSET 2008. IEEE International Conference on*, pp. 945-949, 2008 60

[76] D. Carli *et al.*, "An effective multi-source energy harvester for low power applications," *Design, Automation Test in Europe Conference Exhibition (DATE)*, pp. 1-6, 2011 60

[77] A. S. Weddell *et al.*, "A survey of multi-source energy harvesting systems," *Design, Automation Test in Europe Conference Exhibition (DATE)*, pp. 905-908, 2013 60

[78] C. Buratti and R. Verdone, "Performance Analysis of IEEE 802.15.4 Non Beacon-Enabled Mode," *Vehicular Technology, IEEE Transactions on*, pp. 3480-3493, 2009 62

[79] D. Brunelli *et al.*, "Temperature compensated time synchronisation in wireless sensor networks," *Electronics Letters*, pp. 1026-1028, 2012 4

[80] F. Ferrari *et al.*, "Efficient network flooding and time synchronization with Glossy," *Information Processing in Sensor Networks (IPSN), 10th International Conference on*, pp. 73-84, 2011 62

[81] C. Caione *et al.*, "Distributed Compressive Sampling for Lifetime Optimization in Dense Wireless Sensor Networks," *Industrial Informatics, IEEE Transactions on*, pp. 30-40, 2012 65

[82] D. Porcarelli *et al.*, "Perpetual and low-cost power meter for monitoring residential and industrial appliances," *Design, Automation Test in Europe Conference Exhibition (DATE)*, pp. 1155-1160, 2013 6

[83] S. M. Amin and B. Wollenberg, "Toward a smart grid: power delivery for the 21st century," *IEEE Power and Energy Magazine, 2005*, vol. 3, pp. 3441, Sept - Oct 2005 74

[84] S. Ahmad, "Smart metering and home automation solutions for the next decade," *in Proc. of the international conference on Emerging Trends in Networks and Computer Communications, 2011 (ETNCC 2011)* , pp. 200-204, 22-24 Apr 2011 74

[85] V. Gungor *et al.*, "Opportunities and challenges of wireless wensor networks in smart grid," *IEEE transaction on Industrial Electronics, 2010*, vol. 57, pp. 3557-3564, Oct 2010 75

[86] D. Carli *et al.*,"A high-efficiency wind-flow energy harvester using micro turbine," *in Power Electronics Electrical Drives Automation and Motion (SPEEDAM), 2010 International Symposium on*, June 2010, pp. 778-783 75

[87] D. Brunelli *et al.*, "Photovoltaic scavenging systems: Modeling and optimization," *Microelectronics Journal*, vol. 40, no. 9, pp. 1337-1344, 2008 75

[88] S. Depuru *et al.*, "Smart meters for power grid, challenges, issues, advantages and status," *Power Systems Conference and Exposition (PSCE), 2011 IEEE/PES*, March 2011 76

[89] F. Benzi *et al.*, "Electricity smart meters interfacing the households," *Industrial Electronics, IEEE Transactions on*, vol. 58, no. 10, pp. 4487-4494, Oct. 2011 77

[90] A. Kiani and A. Annaswamy, "The effect of a smart meter on congestion and stability in a power market," *Decision and Control (CDC), 2010 49th IEEE Conference on*, Dec. 2010 77

[91] S. Bruno *et al.*, "Load control through smart-metering on distribution networks," *PowerTech, 2009 IEEE Bucharest*, pp. 1-8, july 2009 77

[92] X. Jiang *et al.*, "Design and implementation of a high-fidelity ac metering network," *Information Processing in Sensor Networks, 2009. IPSN 2009. International Conference on*, pp. 253-264, april 2009 77

[93] M. Huq and S. Islam,"Home area network technology assessment for demand response in smart grid environment," *Universities Power Engineering Conference (AUPEC), 2010 20th Australasian*, Dec. 2010 78

[94] M. Zeifman and K. Roth, "Nonintrusive appliance load monitoring: Review and outlook," *Consumer Electronics, IEEE Transactions on*, vol. 57, no. 1, pp. 76-84, february 2011 78

[95] N.-H. Nguyen *et al.*, "A real-time control using wireless sensor network for intelligent energy management system in buildings," *(EESMS), IEEE Workshop on*, Sept 2010 78

[96] C. Jin and K. T, "Smart home networking: Combining wireless and powerline networking," *Wireless Communications and Mobile Computing Conference (IWCMC), 2011*, pp. 1276-1281, july 2011 78

[97] F. Cai *et al.*, "Self-powered smart meter with synchronized data," *in Proc. of the IEEE Radio and Wireless Symposium (RWS 2012)* , Jan 15-18 2012, pp. 395-398 81, 82

[98] R. Moghe *et al.*, "Design of a lowcost self powered stick-on current and temperature wireless sensor for utility assets," *In Proc. of the IEEE Energy Conversion Congress and Exposition, 2010 (ECCE 2010)*, Sep 12-16 2010, pp. 4453-4460 81, 82

[99] Z. Kolodziejczyk *et al.*, "Novel autonomous voltage and current measurement unit for smart grids," *in Proc. of the Int. Symposium on Power Electronics, Electrical Drives, Automation and Motion, (SPEEDAM 2012)* , Jun 20-22 2012, pp. 780-784 81, 82

[100] A. Reinhardt *et al.*, "Smartmeter.kom: A low-cost wireless sensor for distributed power metering," *in Proc. of the IEEE 36th Conference on Local Computer Networks, 2011 (LCN 2011)* , Oct 4-7 2011, pp. 1032-1039 81, 82

[101] T. C. Huang *et al.*, "A battery-free energy harvesting system with the switch capacitor sampler (scs) technique for high power factor in smart meter applications," *in Proc. of the 19th IEEE/IFIP international conference on VLSI and System-on-Chip, 2011 (VLSI-SoC 2011)* , Oct 3-5 2011, pp. 359-362 82

[102] J. Liang *et al.*, "Load signature study - part 1: Basic concept, structure, and methodology," *Power Delivery, IEEE Transactions on* , vol. 25, no. 2, pp. 551-560, April 2010 75

[103] J. Liang *et al.*, "Load signature study - part 2: Disaggregation framework, simulation, and applications," *Power Delivery, IEEE Transactions on*, vol. 25, no. 2, pp. 561-569, April 2010 75